AD-A097 545 UNITED TECHNOLOGIES RESEARCH CENTER EAST HARTFORD CONN F/G 21/2
NITRIC OXIDE MEASUREMENT STUDY. VOLUME II. PROBE METHODS,(U)
MAY 80 M B COLKET, M F ZABIELSKI DOT-FA77WA-4081
UNCLASSIFIED UTRC/R80-994150-2 AFESC/ESL-TR-80-13 NL

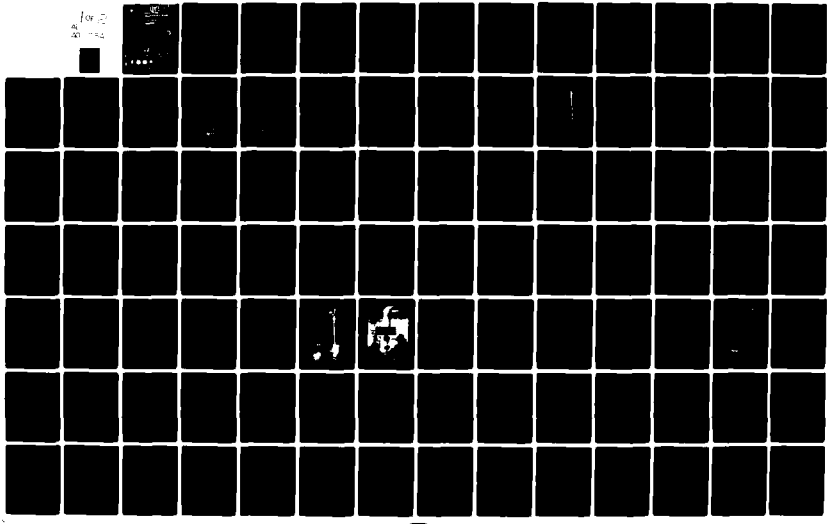

LEVEL II

(13)

B.S.

U.S. Department of Transportation
Federal Aviation Administration

Office of Environment and Energy
Washington, D.C. 20591

(6)

Nitric Oxide Measurement Study: Volume II. Probe Methods,

[redacted]

NH

AD A097545

V3
A097607

DTIC
ELECTE
APR 9 1981
D

(14) UTRC/R80-994150-2, FAA/EE-80-29

(18) AFESC/ESL, NASA

(19) TR-80-13, CR-159862

(15) DOT-FA77WA-4081

(11) MAY 1980

(12) 113

Report Numbers:
FAA-EE-80-29
USAF ESL TR-80-13
NASA CR-159862
USN NAPC-PE-38C
EPA-460/3-80-014

(10) M.B./Colket, III
M.F./Zabielski
L.J./Chiappetta
L.G./Dodge
R.N./Guile
D.J. Seery

DISTRIBUTION STATEMENT A
Approved for public release;
Distribution Unlimited

DTIC FILE COPY

409252

81 4 09 121

This document is disseminated under the joint sponsorship of the Federal Aviation Administration, U.S. Air Force, U.S. Navy, National Aeronautics and Space Administration, and the Environmental Protection Agency in the interest of information exchange. The United States Government assumes no liability for the contents or use thereof.

Technical Report Documentation Page

1. Report No. FAA-EE-80-29	2. Government Accession No. AD-A097545	3. Recipient's Catalog No.
4. Title and Subtitle Nitric Oxide Measurement Study: Probe Methods - Volume II		5. Report Date March 31, 1980
		6. Performing Organization Code
7. Author(s) M. B. Colket, III, M. F. Zabielski, L. J. Chiappetta, L. G. Dodge, R. N. Guile, D. J. Seery		8. Performing Organization Report No. [redacted]-994150-2
9. Performing Organization Name and Address United Technologies Research Center Silver Lane East Hartford, CT 06108		10. Work Unit No. (TRAIS)
		11. Contract or Grant No. DOT FA77WA-4081
12. Sponsoring Agency Name and Address U.S. Department of Transportation Federal Aviation Administration Office of Environment and Energy Washington, DC 20591		13. Type of Report and Period Covered
		14. Sponsoring Agency Code

15. Supplementary Notes Funding for this study was provided by an Interagency Committee. Contributing agencies and report nos. are: DOT-FAA (FAA-EE-80-29); USAF (ESL TR-80-13); NASA (CR-159862); USN (NAPC-PE-38C); and EPA (EPA-460/3-80-014).

16. Abstract

Experimental facilities used in studying the performance of probes and sampling systems for measuring NO are described. A critical review of the literature on probe measurements of NO_x is given with emphasis on reported results indicating that probes may perturb the total concentration of NO_x in a flame. Also, sample line and chemiluminescent analyzer phenomena are reviewed. A model of probe aerodynamics including heat transfer is presented. Kinetics of NO loss are examined and quenching criteria for measuring nitric oxide in flames are given. Sampling probes are described that were designed to preserve NO and are suitable for measurements on small and large combustors. Probes were designed to cool the gases both convectively and aerodynamically. Performance of these probes is compared with model predictions. Concentrations of nitric oxide were measured using several probes for each of three flame environments. The values measured with each probe are compared and related to seed levels of NO. In addition, concentration profiles required to compare probe measurements with optical measurements are provided.

The Nitric Oxide Measurement Study is in three volumes:
Optical Calibration - Volume I;
Probe Methods - Volume II;
Comparison of Optical and Probe Methods - Volume III.

17. Key Words Nitric oxide, probe sampling, chemiluminescent analysis, aerodynamic analysis.	18. Distribution Statement Document is available to public through the National Technical Information Service, Springfield, VA 22161

19. Security Classif. (of this report)	20. Security Classif. (of this page)	21. No. of Pages	22. Price
Unclassified	Unclassified	112	

Form DOT F 1700.7 (8-72) Reproduction of completed page authorized

ACKNOWLEDGMENTS

This contract was administered by the Federal Aviation Administration. Funding for this work was provided by an Interagency Committee representing the Federal Aviation Administration (FAA), Air Force, Navy, National Aeronautics and Space Administration (NASA), and the Environmental Protection Agency (EPA).

The assistance of Mr. D. L. Kocum, Mr. R. P. Smus, Mr. D. D. Santos and Mr. R. L. Poitras during the experimental portions of this study is gratefully acknowledged. The authors also would like to acknowledge the contributions of the following UTRC staff: Mrs. B. B. Johnson and Mr. C. Foley for data reduction and report preparation; and Messrs. P. N. Cheimets, M. E. Maziolek, W. T. Knose, and M. Cwikla for facilities support.

Accession For
NTIS GRA&I ☑
DTIC TAB ☐
Unannounced ☐
Justification
By
Distribution/
Availability Codes
Dist | Avail and/or Special
A

ABSTRACT

Experimental facilities used in studying the performance of probes and sampling systems for measuring NO are described. A critical review of the literature on probe measurements of NO_x is given with emphasis on reported results indicating that probes may perturb the total concentration of NO_x in a flame. Also, sample line and chemiluminescent analyzer phenomena are reviewed. A model of probe aerodynamics including heat transfer is presented. Kinetics of NO loss are examined and quenching criteria for measuring nitric oxide in flames are given. Sampling probes are described that were designed to preserve NO and are suitable for measurements on small and large combustors. Probes were designed to cool the gases both convectively and aerodynamically. Performance of these probes is compared with model predictions. Concentrations of nitric oxide were measured using several probes for each of three flame environments. The values measured with each probe are compared and related to seed levels of NO. In addition, concentration profiles required to compare probe measurements with optical measurements are provided.

TABLE OF CONTENTS

	Page
ACKNOWLEDGEMENTS	i
ABSTRACT	ii
TABLE OF CONTENTS	iii
LIST OF FIGURES	v
LIST OF TABLES	vi
I. INTRODUCTION	I-1
II. EXPERIMENTAL FACILITIES	II-1
A. General	II-1
B. Flat Flame Burner	II-1
C. Test Section for Large Scale Burners	II-3
1. IFRF Burner	II-3
2. FT12 Burner Can	II-8
3. Temperature Measurements	II-8
D. Sampling Systems	II-12
1. Scott Exhaust Analyzer	II-12
a. Pumping Requirements	II-13
2. TECO Analyzer	II-13
E. Mass Flow Measurement	II-14
III. DESIGN OF GAS SAMPLING PROBE	III-1
A. Losses of Nitric Oxide in Sampling System	III-1
1. NO/NO_2 Interconversion	III-2
a. The Bodenstein Reaction	III-4
2. NO_x Reduction in Sampling Probe	III-8
3. Losses in Sampling Line	III-13
4. Response of Chemiluminescence Analyzer	III-14
5. NO_x Converter	III-16
6. Summary	III-17

TABLE OF CONTENTS (Cont'd)

	Page
B. Quenching in Gas Sampling Probe	III-17
1. Kinetics of NO Decomposition	III-20
2. Description of Computer Program for Probe Analysis	III-24
a. Sudden Expansion Losses	III-26
b. Aerodynamic Quench	III-27
C. Design of Probes	III-30
1. Probes for Combustor Measurements	III-30
2. Probes for the Flat Flame Burner	III-35
a. Microprobe	III-42
IV. EXPERIMENTAL RESULTS	IV-1
A. Flat Flame Burner	IV-1
1. Uncooled, Stainless Steel Probe	IV-12
B. IFRF Burner	IV-12
C. FT12 Measurements	IV-20
D. Experimental Verification of Probe Model	IV-25
1. Pressure Profiles for the Reference Probe	IV-25
2. Mass Flow Measurements	IV-28
a. Macroprobe	IV-28
b. Miniprobe	IV-28
c. Microprobe	IV-30
3. Discussion	IV-30
V. RESULTS AND DISCUSSION	V-1
VI. CONCLUSIONS	VI-1
REFERENCES	R-1

LIST OF FIGURES

Fig. No.	Title	Page
II-1.	Top View of Flat Flame Burner and Assembly.	II-2
II-2.	Atmospheric Pressure Combustion Facility.	II-5
II-3.	Swirl Burner Assembly	II-6
II-4.	FT12 Assembly	II-9
II-5.	Pt-Pt/13% Rh Aspirated Thermocouple	II-11
II-6.	Experimental Set-up for Measurements of Mass Flow .	II-15
II-7.	Indicated Reading at Constant Mass Flow and Varying Operating Pressure	II-16
II-8.	Metered Mass Flow Rates vs. Flow Meter Reading. . .	II-17
III-1.	Model for Calculating Sudden Expansion Loss	III-28
III-2.	Drawings of Macroprobes	III-31
III-3.	Reference Probe	III-32
III-4.	Tip of Reference Probe.	III-33
III-5.	Calculated Temperature and Pressure Profiles for Reference Probe	III-34
III-6.	Calculated Cooling Curves for Macroprobes	III-36
III-7.	Drawing of Miniprobe	III-38
III-8.	Stainless Steel Tipped Miniprobe	III-39
III-9.	Calculated Cooling Curves for Miniprobe	III-40
III-10.	Calculated Cooling Curves for Miniprobe at Varying Back Pressure	III-41
IV-1.	Horizontal Temperature Profile over $CH_4/O_2/N_2$ Flat Flame	IV-2
IV-2.	Vertical Temperature Profile over $CH_4/O_2/N_2$ Flat Flame	IV-3
IV-3.	Normalized Nitric Oxide Profiles over $CH_4/O_2/N_2/NO$ Flat Flame	IV-6
IV-4.	Vertical Profiles of Nitric Oxide over Flat Flame Burner.	IV-7
IV-5.	Nitric Oxide Measured vs. Nitric Oxide Seed	IV-10
IV-6.	Temperature Profile Across IFRF Combustor	IV-15
IV-7.	Normalized Nitric Oxide Profiles Across IFRF Combustor	IV-18
IV-8.	Temperature Profiles Downstream of FT12 Combustor .	IV-21
IV-9.	Normalized Nitric Oxide Profiles Across Optical Axis for FT12 Combustor	IV-24
IV-10.	Profiles of Static Pressure for the Reference Probe	IV-26
IV-11.	Relative Mass Flow vs. Back Pressure for Several Probes	IV-29

LIST OF TABLES

Table No.	Title	Page
II-A.	Operating Conditions for the Flat Flame Burner. . .	II-4
II-B.	Operating Conditions for the IFRF Burner.	II-7
II-C.	Operating Conditions for the FT12 Combustor	II-10
III-A.	Flow Conditions in Non-Ideal Sampling System. . . .	III-6
III-B.	Comparison of Calculated and Measured NO and NO_2. .	III-9
III-C.	Reaction Mechanism for NO Decomposition	III-21
III-D.	Estimated Fractions of NO Decomposition	III-23
IV-A.	Mole Percent of Stable Species for Flat Flame Burner	IV-4
IV-B.	Measured Concentration of NO(ppm) Using Uncooled, Stainless Steel Probe over Flat Flame Burner. . .	IV-13
IV-C.	Mole Percent of Stable Species for IFRF Burner. . .	IV-16
IV-D.	Comparison of Nitric Oxide Measurements using the Reference Probe - IFRF Burner	IV-19
IV-E.	Mole Percent of Stable Species for FT12 Combustor .	IV-22
IV-F.	Comparison of Nitric Oxide Measurements using the Reference Probe - FT12 Combustor	IV-25

I. INTRODUCTION

Since Johnston (1971) and Crutzen (1970, 1972) independently suggested that the injection of nitric oxide (NO) into the upper atmosphere could significantly diminish the ozone (O_3) concentration, an accurate knowledge of the amount of NO emitted by jet aircraft has been a serious concern to those involved in environmental studies. This concern intensified when McGregor, Seiber, and Few (1972) reported that NO concentration measured by ultraviolet resonant spectroscopy were factors of 1.5 to 5.0 larger than those measured by extractive probe sampling with subsequent chemiluminescent analysis. These initial measurements were made on a YJ93-GE-3 engine as part of the Climatic Impact Assessment Program (CIAP) which was one of four studies (CIAP, NAS, COMASA, COVOS (see References)) commissioned to determine the possible environmental consequences of high altitude aircraft operation, especially supersonic aircraft. After those studies were initiated, economic factors strongly favored the production and operation of subsonic aircraft. Nevertheless, since the subsonic aircraft fleet is large and does operate as high as the lower stratosphere, interest in the causes of the discrepancies between the two NO measurement methods continued. Few, Bryson, McGregor, and Davis (1975, 1976, 1977) reported a second set of measurements on an experimental jet combustor (AVCO-Lycoming) where the spectroscopically determined NO concentrations were factors of 3.5 to 6.0 higher than those determined by the probe method. In this set of measurements, optical data were obtained not only across the exhaust plume but also in the sample line connecting the probe with the chemiluminescent analyzer. The sample line optical data seemed to agree with the chemiluminescent analyzer data; hence, it was suggested that the discrepancies were due to phenomena occurring in the probe. These results stimulated a third set of measurements involving ultraviolet spectroscopy (Few et al, 1976a, 1976b), infrared gas correlation spectroscopy (D. Gryvnak, 1976a, 1976b) and probe sampling on an Allison T-56 combustor. The measured ratios of the ultraviolet to the probe values typically ranged between 1.5 and 1.9 depending on the data reduction procedure. The ratios of the infrared to the probe values varied between 1.1 to 1.5 also depending on the method of data reduction. In addition to these engine and combustor data, evidence supportive of the accuracy of the ultraviolet spectroscopic method, i.e., calibration data and model predictions, was presented by McGregor, Few, and Litton (1973); Davis, Few, McGregor and Glassman (1976); and Davis, McGregor, and Few (1976). Nevertheless, it was still not possible to make a judgment on the relative accuracy of the spectroscopic and probe methods. The most significant reasons for this were: the complexity of the spectroscopic theory and computer model required to infer concentration from optical transmission; the inadequate treatment of probe use; and the incomplete exhaust temperature and pressure data which are necessary for a valid comparison of the methods. Recently, Oliver et al (1977, 1978) as part of the High Altitude Pollution Program has ranked these discrepancies as a major and a continuing source of uncertainty in atmospheric model predictions.

The purpose of this investigation was to identify and determine the magnitude of the systematic errors associated with both the optical and probe sampling techniques for measuring NO. To accomplish this, the study was divided into three parts. The first was devoted to calibrating the ultraviolet and infrared spectroscopic methods. This entailed developing procedures which could provide known concentrations of NO over a wide range of temperatures and pressures, and also reviewing and correcting the ultraviolet spectroscopic theory used in the engine and combustor measurements cited above. The second part of this study was focused on sample extraction, transfer, and analysis of chemiluminescent instrumentation. The sampling methods were used on three successively more complicated combustion systems starting with a flat flame burner and culminating with a jet combustor. The results are presented in TASK II Report: Probe Methods. In the third part of this study, optical measurements were made on the same three combustion systems operated at the same conditions used for the probe measurements. The results of the optical and probe measurements were compared and are given in TASK III Report: Comparison of Optical and Probe Methods.

This report, i.e., TASK II, is devoted to the important processes in the extractive sampling and measurement of NO from combustion streams. Described are a flat flame burner, swirl combustor, and jet combustor along with their support facilities and operating parameters. Information on the temperature, analytical, and mass flow instrumentation is given. Problems associated with loss of nitric oxide in a sampling system are reviewed and the results of previous investigations are analyzed. Several different probes were used for sampling the flame gases, and their designs were selected using a computer program describing the principal aerodynamic and heat transfer processes encountered in a probe. Direct experimental measurements of the fluid mechanics within probes is presented verifying this model. In addition, temperature and concentration profiles necessary to compare optical and probe measurements are provided. These results are summarized and discussed and major conclusions are given.

II. EXPERIMENTAL FACILITIES

II. A. General

A principal objective of this study is to identify the relative merits of probe and UV optical measurements of NO in the exhaust of aircraft engines. To reach this goal, three combustion systems of varying degrees of complexity were examined. These systems were:

1. $CH_4/O_2/N_2$ flame over a flat flame burner:

   $\phi^* = 0.8, 1.0, 1.2$, P = 1 atm, $m_{TOTAL} \sim 2.75$ g/sec

2. C_3H_8/Air flame in a swirl burner:

   $\phi = 0.8, 1.0, 1.2$, Swirl = 0.63 and 1.25, P = 1 atm, $\dot{m}_{TOTAL} \sim 71$g/sec

3. Jet A/Air flame in a modified FT12 combustor: Idle, Cruise, and Maximum Continuous, P = 1 atm, $\dot{m}_{TOTAL} \sim 470$g/sec.

Physical details and operation of the flat flame burner have been described previously (Dodge, et al., 1979); consequently, only a brief overview will be presented here. For the other two flames, each burner assembly could be installed separately into a single combustor housing with the associated fuel lines and flow controls modified accordingly. This facility and the burner assemblies are described in detail in this chapter. In addition, techniques for temperature measurements with corrections, sample gas transfer and analysis, and mass flow measurements are reviewed. Details of sample probe construction will be discussed in the following chapter since their designs were defined by model predictions.

II. B. Flat Flame Burner

The flat flame burner is made of sintered copper and has two zones: the main zone (containing the main flame seeded with nitric oxide) with dimensions of 17.5 x 9.2 cm or 161 cm^2 and the (unseeded) buffer zone with an area of 76 cm^2. A methane flame was burned above the buffer flame to provide a hot zone in the wings of the flame. The burner was enclosed by a stainless steel shroud/chimney with optical ports to separate windows (quartz or salt) from the flame. The ports were purged with nitrogen at room temperature to reduce the local nitric oxide concentrations within these ports. A top view of the burner is shown in Figure II-1. Temperatures were measured using a butt-welded, Ir/60% Ir-40% Rh thermocouple coated with a mixture of Yttrium and Berylium oxides.

* The stoichiometry, ϕ, is defined to be $(f/a)/(f/a)_{\phi=1}$ where ϕ=1 when the fuel (f) and air (a) are at the stoichiometric ratio.

FIG. II-1

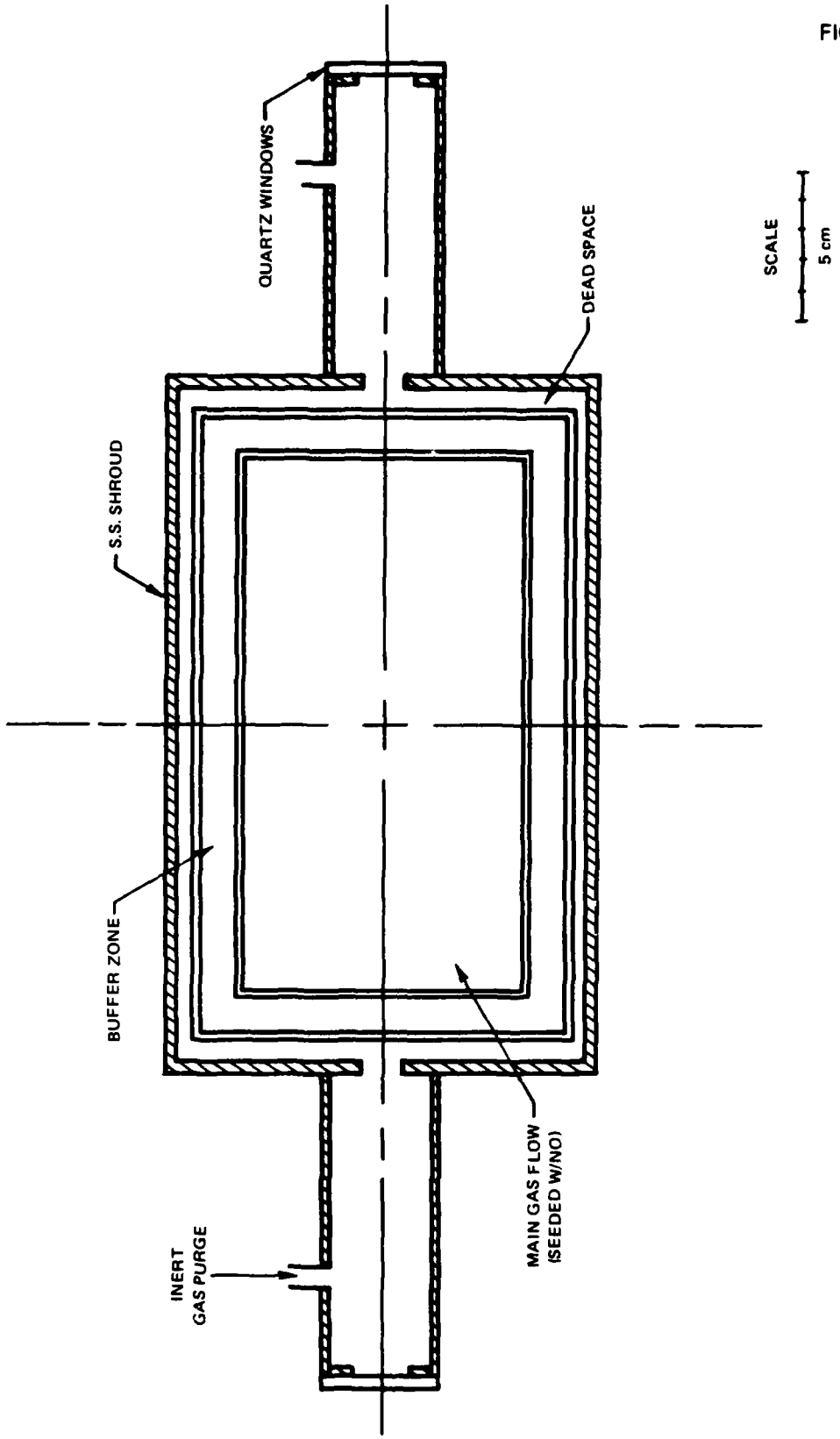

TOP VIEW OF FLAT FLAME BURNER AND ASSEMBLY

79-04-54-3

The diameter of the bead and coating was approximately 90 microns (0.0035 inches). Gases were individually metered using critical flow orifices. Separate mixes of gases (N_2, O_2, CH_4, NO, H_2, Ar) were blended for the main and buffer flows. Details of these facilities are provided in the Task I Report (Dodge, et al, 1979). The flames examined in this program are listed in Table II-A.

II. C. Test Section for Large Scale Burners

The combustor test section used for the swirl burner and FT12 combustor is shown schematically in Fig. II-2. It consists of a water-cooled, double-walled chamber 50 cm in diameter (i.d.) and 150 cm long. Four (4) rows of eight (8) viewing ports are provided in the combustor section at 90° intervals. It was constructed at UTRC specifically to investigate flame phenomena with various optical and probing techniques. The two burner systems were designed to fit inside the burner housing. One is a swirl burner and is a scaled down verison of the burners designed at the International Flame Research Foundation (IFRF). The second is a modified FT12 burner and shroud. The optical axis used for subsequent optical measurements was the center of the third window from the far right in Fig. II-2. All probes (sample and thermocouple) were designed to translate across this axis.

II. C. 1 IFRF Burner

The IFRF burner assembly, as shown in Fig. II-3, is a model of those burners described by Beér and Chigier (1972) and consists of a central fuel nozzle and an annular air supply. A movable vane block arrangement provides variable air swirl intensity from a swirl number of 0 to 2.5; in this case, the swirl number is defined as the ratio of the tangential to the axial momentum divided by the radius of the exit quarl. The swirl number was calculated using the appropriate equations in the text by Beér and Chigier (1972) and, as they demonstrate, experimental and theoretical values agree fairly well for this type of burner. An axially adjustable, 19 mm diameter, fuel feed tube can be equipped with various pressure atomizing of air-assisted fuel spray nozzles.

This swirl burner has been tested previously during internal programs at UTRC and has been used recently to study the combustion of a coal/oil slurry (Vranos, et al, 1979). In the present program, gaseous propane was used for fuel and a nozzle was constructed to inject the fuel radially into the swirling air flow. Six stable operating conditions were selected for these tests and provide three stoichiometries and two swirls. Input conditions are listed in Table II-B. The optical axis and the probe tips were located 87.5 cm downstream of the quarl exit.

The two swirl levels used in these tests (0.63 and 1.25) were selected by performing a series of tests on flame stability. At lower swirl numbers, the propane flame was relatively long and unstable and was not considered to be suitable for this series of tests. Beér and Chigier argued that below a swirl number of 0.6 axial pressure gradients are insufficient to cause internal

TABLE II-A

OPERATING CONDITIONS FOR THE FLAT FLAME BURNER*

Test Condition	B1	B2	B3
$\dot{m}_{N_2}$ (g/sec)	2.15	2.20	2.07
$\dot{m}_{O_2}$ (g/sec)	0.512	0.466	0.494
$\dot{m}_{CH_4}$ (g/sec)	0.103	0.116	0.149
T_{inlet} (K)	285	285	285
P (psia)	14.7	14.7	14.7
ϕ	0.8	1.0	1.2

*Without Seed

FIG. II-2

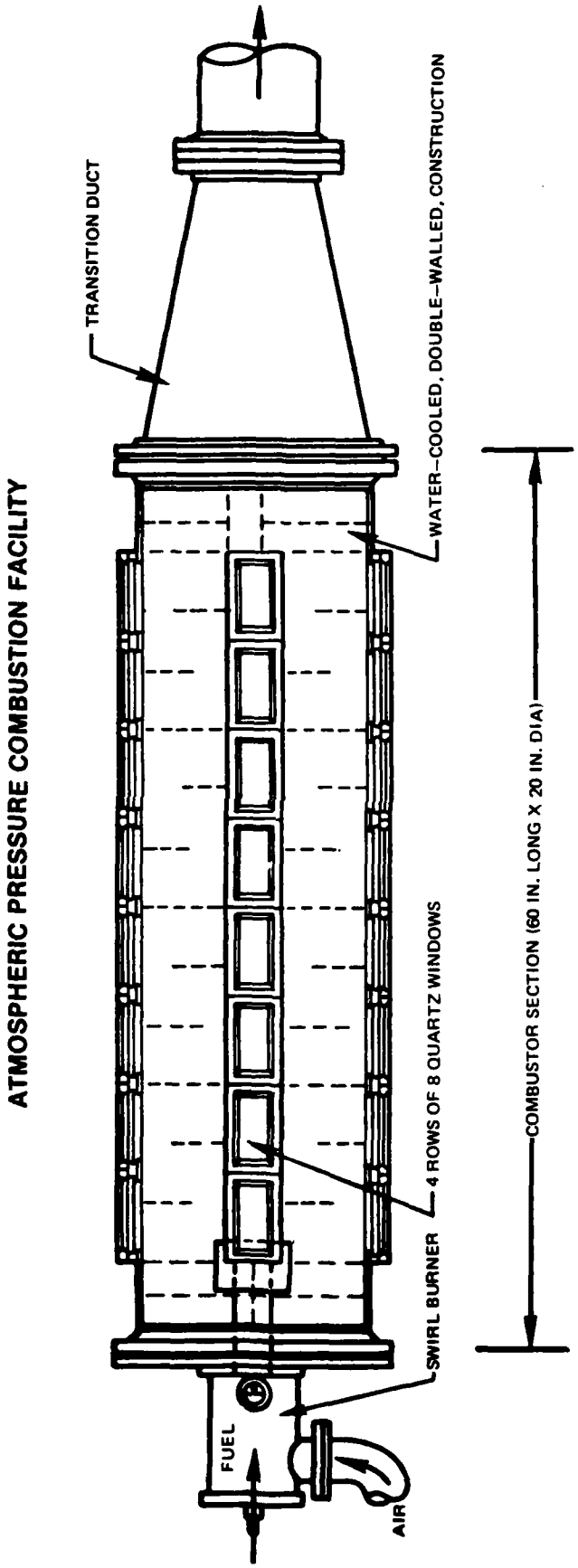

ATMOSPHERIC PRESSURE COMBUSTION FACILITY

79-06-11-5

SWIRL BURNER ASSEMBLY

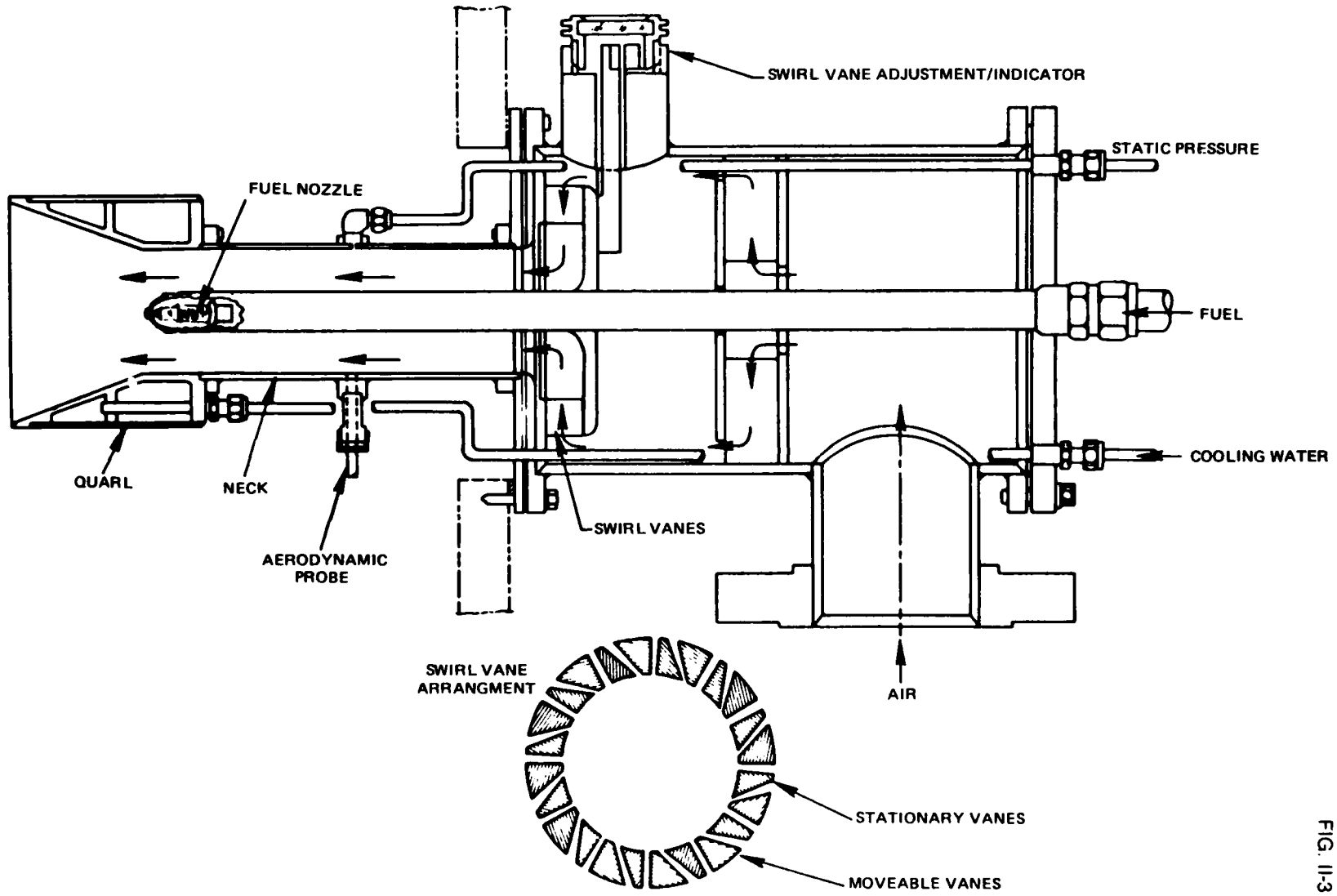

FIG. II-3

79-06-11-4

TABLE II-B

OPERATING CONDITIONS FOR THE IFRF BURNER

Test Condition	1, 4+	2, 5+	3, 6+
$\dot{m}_{air}$ (g/sec)	66.7	66.7	66.7
P (psia)	14.7	14.7	14.7
T_{inlet} (K)	290	290	290
$\dot{m}^{*}_{fuel}$ (g/sec)	3.40	4.26	5.11
ϕ	0.8	1.0	1.2

* Gaseous propane

\+ Swirl number (see definition in text) was 0.63 for test conditions 1-3 and 1.25 for test conditions 4-6.

recirculation; however, at higher swirl intensities a recirculating zone in the central portion of the jet is required to support a strong adverse pressure gradient along the axis. Since recirculation zones tend to stabilize the flame and increase the intensity of reaction, the ability to achieve stable flame conditions only above swirl numbers of 0.6 in this research program is in agreement with Beér and Chigier's analysis.

II. C. 2 FT12 Burner Can

A modified FT12 combustor can used in this program was 29.5 cm in length (11.5 cm shorter than the original can) and 13.0 cm in diameter. It was altered to make all air addition holes symmetric. This can was welded at its exit to a shroud and was placed in the test section with the swirl burner removed. As shown in Fig. II-4, a flow straightener was placed in the burner housing upstream of the combustor can and appropriate fuel lines and cable for spark ignition were fed through the housing. A standard fuel nozzle for the FT12 (Pratt & Whitney Part No. 525959) was used in this series of tests.

Three flight conditions, i.e. idle, cruise, and maximum continuous, were simulated. A simulation was necessary since the test section could only sustain a maximum pressure of four atmospheres, while the cruise and maximum continuous flight conditions required pressure above 6 atmospheres.

In addition, since gas sampling and accurate definition and examination of the optical path is simplified by operating at one atmosphere, all experiments were performed at one atmosphere. Simulated flight conditions at this lower operating pressure, were calculated by equating Mach numbers. This is a common test procedure and is useful in simulating equivalent fluid flow patterns and heat transfer. In this case, the mass flow rate was reduced appropriately to maintain the chamber pressure at one atmosphere and the inlet temperature was identical to the flight conditions. The simulated flight conditions are listed in Table II-C. The optical and probe axis was 78 cm downstream from the exit of the FT12 burner can.

II. C. 3 Temperature Measurements

Exhaust temperatures from the IFRF and FT12 combustors were made using a water-cooled, double shielded, aspirated thermocouple probe with a bead made of Pt/Pt-13%Rh. The probe was manufactured by Aero Research Instrument Co. (Part Number T-1006-6 (25) R) according to specifications described by Glawe, et al. (1956) but was modified (by water cooling and material substitution) to increase the temperature range to above 1370 K (2000°F). . photograph of this probe is shown in Fig. II-5. Radiation and conduction corrections were made according to equations supplied by the manufacturer. For the measurements made in this study (P = 1 atm, Mach no. << 1), these equations can be written

$$T_{gas}\ (K) = T_{thermocouple}\ (K) + \Delta\ T_{RC}$$

FT12 ASSEMBLY

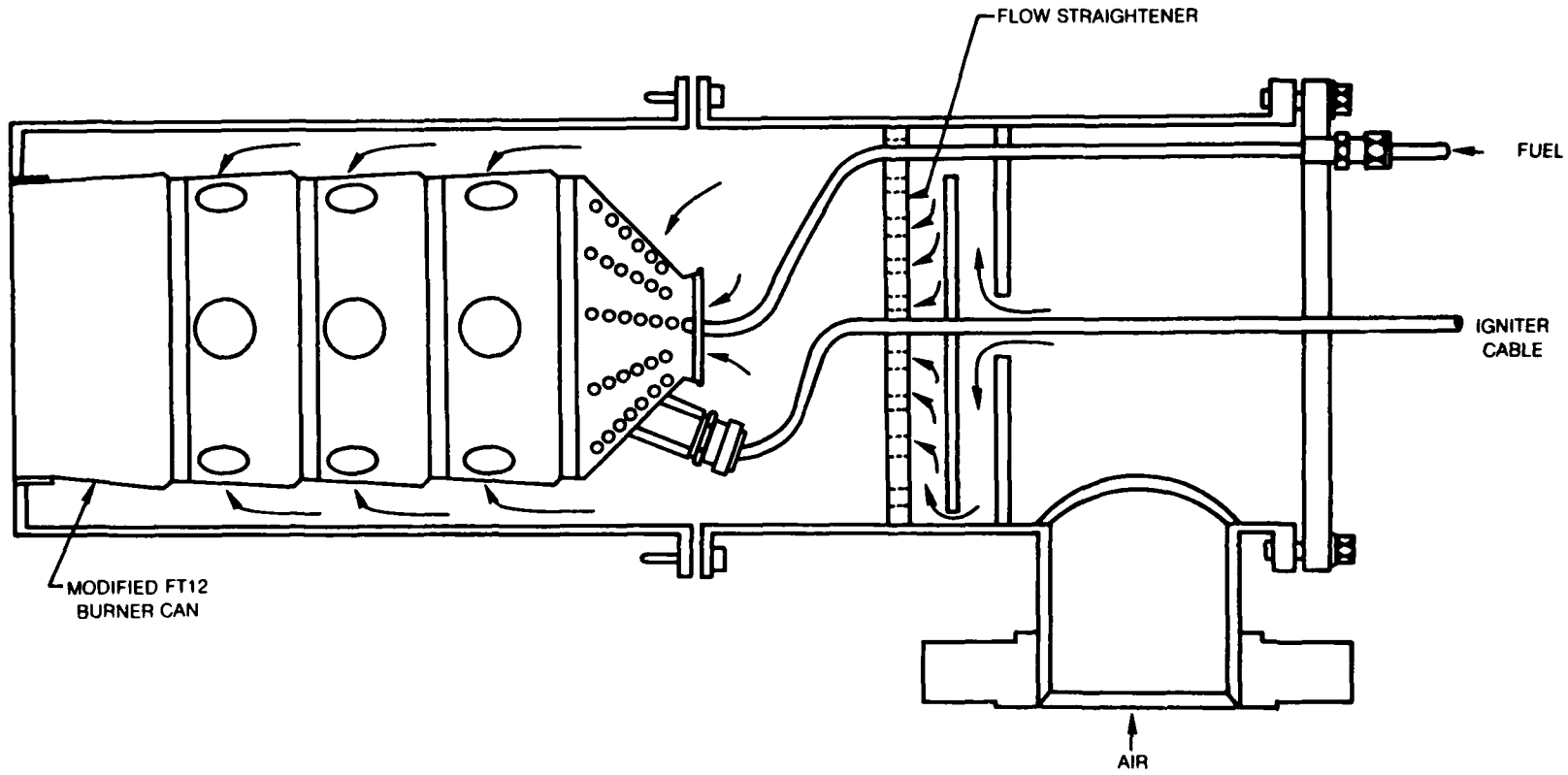

~1/3 ACTUAL SIZE

FIG. II-4

79-10-85-16

TABLE II-C

OPERATING CONDITIONS FOR THE FT12 COMBUSTOR

	Idle	Cruise	Maximum Continuous
m_{air} (g/sec)	485	463	454
P (psia)	14.7	14.7	14.7
T_{inlet} (K)	335	515	524
$\dot{m}$ *$_{fuel}$ (g/sec)	5.15	6.62	6.92
f/a	.0106	.0143	.0152

*Jet A

Pt-Pt/13% Rh ASPIRATED THERMOCOUPLE

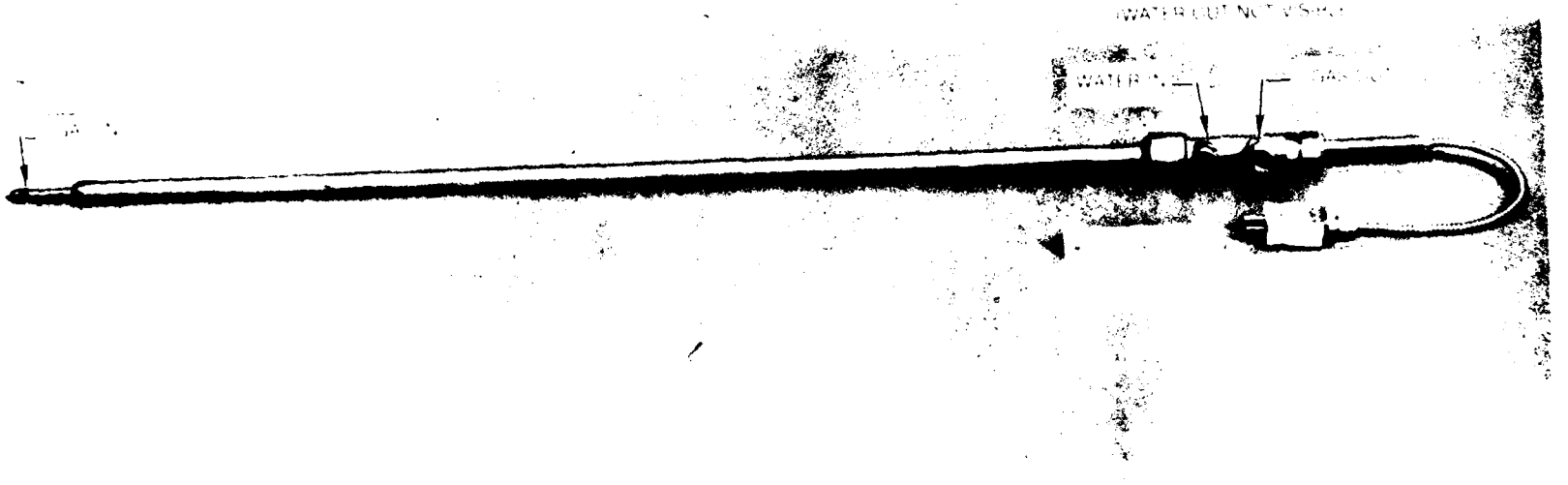

FIG. II-5

79-10-85-7

where the radiation and conduction correction, ΔT_{RC}, is given by

$$\Delta T_{RC} = \frac{0.55\ C_1}{\sqrt{M}}\ (K)$$

$$C_1\ (K) - 0.00917\ T_{thermocouple}\ (K) - 7.136$$

and M is the Mach number. For the FT12, no correction was made since ΔT_{RC} was negligible (< 10 K). For the IFRF burner, corrections were typically on the order of 50 K. Additional description on the operation of aspirated probes is given by Land and Barber (1954).

II. D. Sampling Systems

Two instrumentation systems were used for measuring the products of combustion. The first is the Scott Exhaust Analyzer used in the Task I of this program and the second is a chemiluminescence analyzer made by Thermo Electron Corporation (TECO). The Scott system was used during the initial tests with the flat flame burner to obtain concentrations of the major species. The Scott system was thereafter dedicated to the larger scale combustor tests and the TECO instrument was used for subsequent measurements of NO/NO_x over the flat flame burner. The Scott system was dedicated to the combustor measurements for two reasons. First of all, it was impractical to move this system between facilities and secondly it was determined that the Scott package (under the conditions of the flat flame tests) did not satisfy the Federal requirements for total instrument response time and could not be easily modified to meet those requirements.

II. D. 1 Scott Exhaust Analyzer

The Scott Model 119 Exhaust Analyzer provides for the simultaneous analysis of CO, CO_2, NO or NO_2, O_2 and total hydrocarbons (THC). The analyzer is an integrated system, with flow controls for sample, zero and calibration gases conveniently located on the control panel. The incoming gas sample passes through a refrigeration condenser ($\sim$ 275K), to remove residual water vapor. As the sample passes from the condenser, it is filtered to remove particulate matter. The system is comprised of five different analytical instruments. Beckman Model 315B Non-Dispersive Infrared (NDIR) Analyzers are used to measure the CO and CO_2 concentrations in the gas sample. Concentration ranges available on the CO analyzer were from 0-200 ppm to 0-15% on several scales. Concentration ranges available on the CO_2 analyzer were 0-4% and 0-16%. The accuracy of the NDIR analyzers is nominally $\pm$ 1% of full scale. A Scott Model 125 Chemiluminescence Analyzer is used to measure the NO and NO_2 concentrations in the gas sample. Concentration ranges available with this instrument were from 0-1 ppm to 0-10,000 ppm on several scales, with a nominal $\pm$ 1% of full scale accuracy. The thermal converter used in the chemiluminescent

analyzer was stainless steel, and was operated at a temperature of approximately 1000 K. A Scott Model 150 Paramagnetic Analyzer is used to measure the O_2 concentration in the gas sample. Concentration ranges available with this instrument were from 0-1% to 0-25% on several scales, with a nominal accuracy of ± 1% of full scale. A Scott Model 116 Total Hydrocarbon Analyzer is used to measure the hydrocarbon concentration in the gas sample. This analyzer utilizes an unheated flame ionization detection system to provide for measurement of hydrocarbons (as methane) in concentration ranges from 0-1 ppm to 0-10%, with a nominal accuracy of ± 1% of full scale. Output signals from the various analyzers are displayed on chart recorders and a digital display.

The sample line was teflon-lined aluminum. The typical operating temperature was 380 K. When sampling from the large combustors, water was removed from the sample by two traps cooled to 3° C. The first was located 6 ft. beyond the probe exit and the second was housed in the Scott analyzer.

II. D. 1a Pumping Requirements

Two problems specific to this sampling/probe system were encountered. First of all, the orifice diameter of the macroprobes (2mm) was sufficiently large that a separate vacuum pump (17.5 cfm) was required to reduce the back pressure of the probe to the very low values (~ 1/10th of an atmosphere) required in this program. This vacuum pump was attached directly to the probe via a line one inch (2.54 cm) in internal diameter and three feet (90 cm) long. The second requirement was that, at the reduced pressures, the pumping capacity of the sampling system must be sufficient to deliver flow to the analytical instrumentation. To accomplish this task, a MB-301 pump and two MB-118 pumps (metal bellows) were assembled in a series/parallel arrangement. These pumps were in addition to the two MB-118 pumps in the Scott analyzer and the vacuum pump associated with the CLA. As discussed in Section IV. D. 1, even with this pumping capacity the deliverable flow was marginal at the lowest of probe back pressures.

II. D. 2 TECO Analyzer

The Thermo Electron Corporation (TECO) Model 10AR Chemiluminescent NO/NO_x analyzer was used for the reported data for the flat flame burner. This instrument has a stated minimum detectable concentration of 50 ppb and a maximum limit of 10,000 ppm. Linearity within any of its eight operating ranges is given as ± 1%. A TECO Model 300 Molybedenum NO_x Converter was used for the NO_2 determinations. Sample was delivered to this analyzer at atmospheric pressure by a metal bellows pumps (Metal Bellows MB-118). The sample line was 12 ft of treated teflon line (Technical Heaters, Inc.). The back pressure of the probe was continuously monitored using a Matheson test gauge (0-760 mm, absolute).

II. E. Mass Flow Measurements

The purpose for measuring mass flow rates through the sampling probes was to provide data for comparison with model predictions. Using the experimental arrangement depicted in Fig. II-6, flow rates through probes of three orifice diameters (75, 635, and 2000 microns) were measured at varying external temperatures and probe back pressures. To prevent water condensations, heating tape was used between the probe and exit of the mass flow meter. The Hasting meters which were used for these mass flow measurements, operate by siphoning a small but constant fraction of the gas flow and passing it over a series of heated thermocouples. Cooling of the thermocouples due to the gas flow is measured by the meter and is primarily a function of the mass flow and the specific heat of the gas. According to the manufacturer, mass flow calibrations made for one gas can be related to another gas or mixture of gases by the ratio of specific heats.

To accommodate the wide range in mass flow due to changes in orifice size ($\dot{m} \sim d^2_{orifice}$) and temperature ($\dot{m} \sim 1/\sqrt{T}$), three low pressure drop, Hastings mass flow meters (ALU-100, ALU-5K, ALU-20K) were used. Full scale on these Hastings meters were 100, 5000, and 20,000 sccm (.00191, 0.0953, and 0.382 g/sec of nitrogen, respectively). The reported accuracy is $\pm$ 1% of full scale. In addition, these units each have pressure drops of less than 0.13 torr at an operating pressure of 760 torr (1 atm) and less than 1 torr at 30 torr. The transducers were installed in the lines according to the manufacturer's recommendations. The assembled plumbing with meter was checked for leaks by pressurizing to 100 psig.

To verify their operation two tests were made. First, a constant mass flow of nitrogen was passed through the transducer while the operating pressure of the transducer was varied by adjusting the valve between the transducer and a vacuum pump. At each constant mass flow, the meters produced a constant reading (typically $\pm$ 0.5%) independent of the operating pressure. In agreement with the specifications, pressure measurements up and downstream from the transducer indicated a small pressure drop (< 3 torr). Throughout the pressure range investigated (100-760 torr), the range of mass flows were supplied using critical flow orifices upstream of the transducers. Typical data are presented in Fig. II-7.

The second test was a check on the linearity and the calibration of these units. The experimental set-up was identical to the check for constancy of indicated reading with varying pressure and constant mass flow. Experimental data are shown in Fig. II-8. Although the linearity appears to be quite good (other than a small deviation with the ALU-5K meter), a noticeable discrepancy with the calibration was found for the ALU-100 ($\sim$ 7%) and ALU-20K ($\sim$ 10%) meters. For these tests, the calibrations obtained at UTRC were used. Less than 1% change was observed for the mass flow measurements shown in Fig. II-8 when the lines were heated to 60° C.

EXPERIMENTAL SET-UP FOR MEASUREMENTS OF MASS FLOW

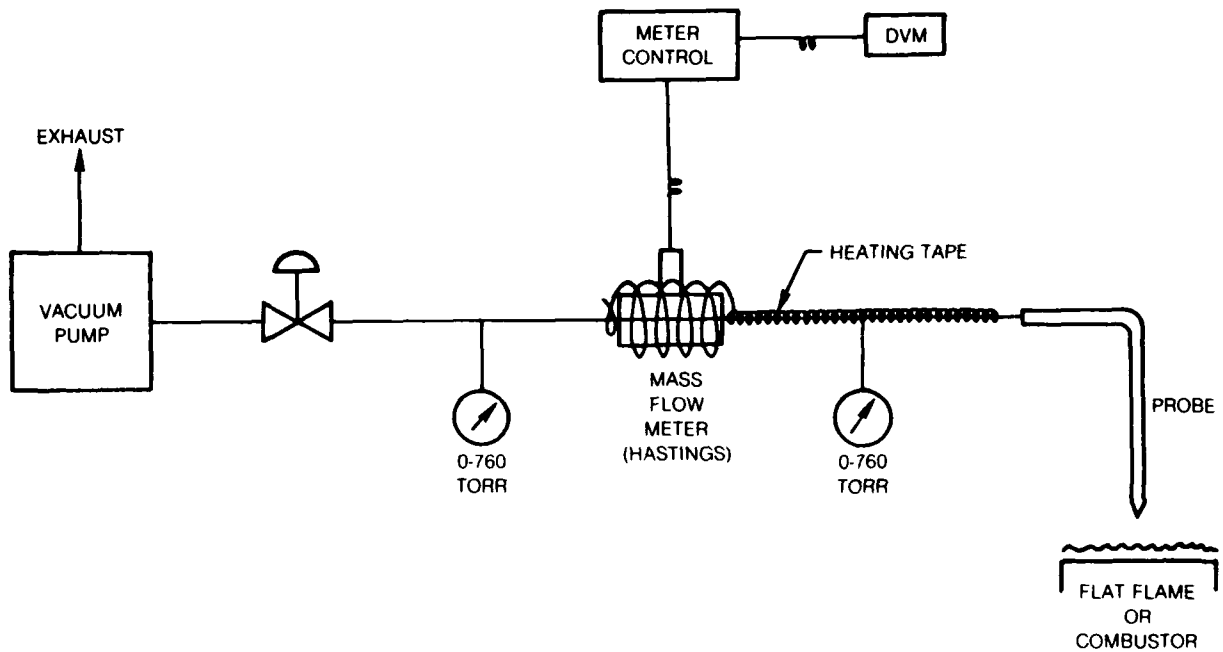

FIG. II-6

79-10-85-8

INDICATED READING AT CONSTANT MASS FLOW AND VARYING OPERATING PRESSURE

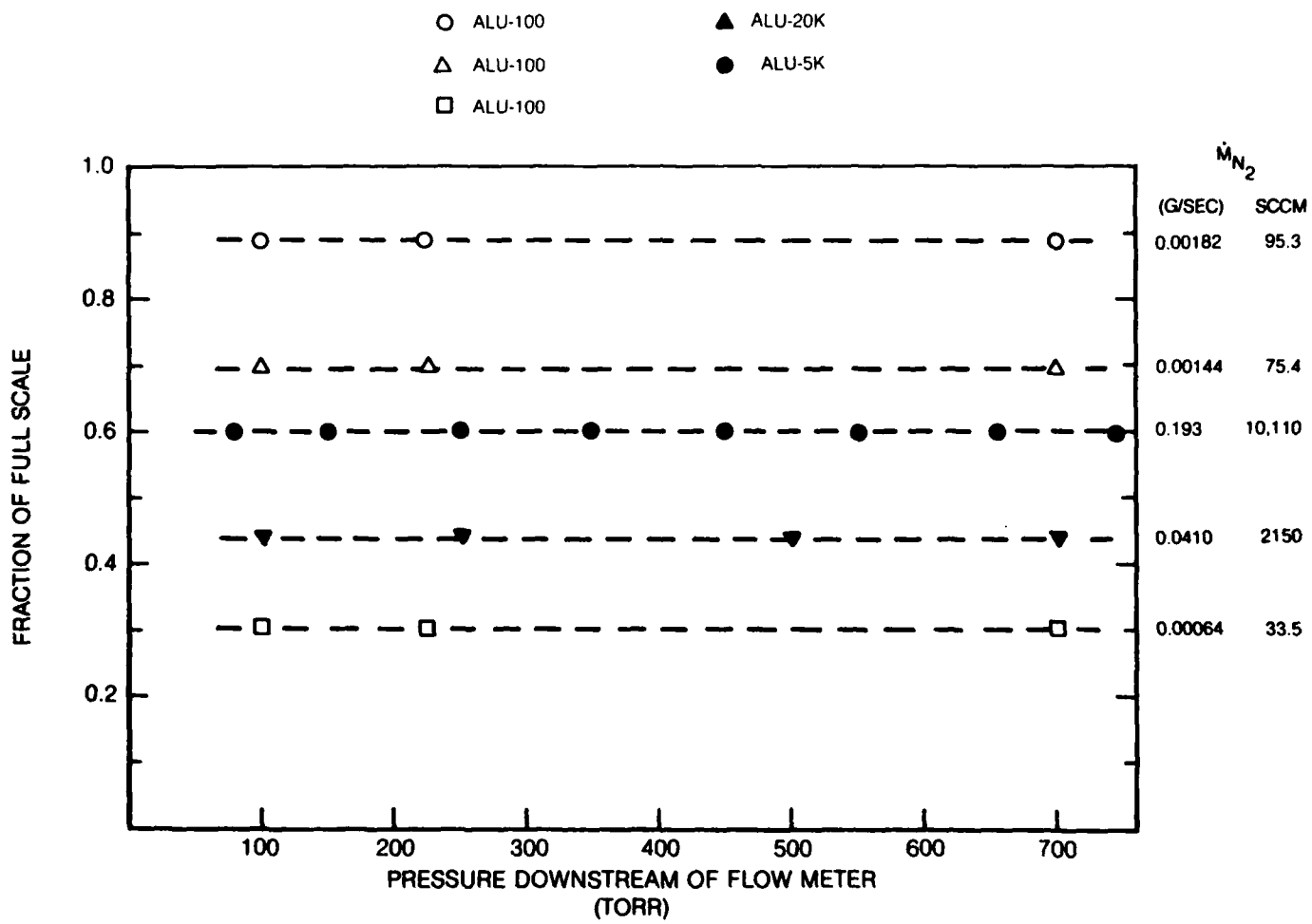

FIG. II-7

FIG. II-8

METERED MASS FLOW RATES VS. FLOW METER READING

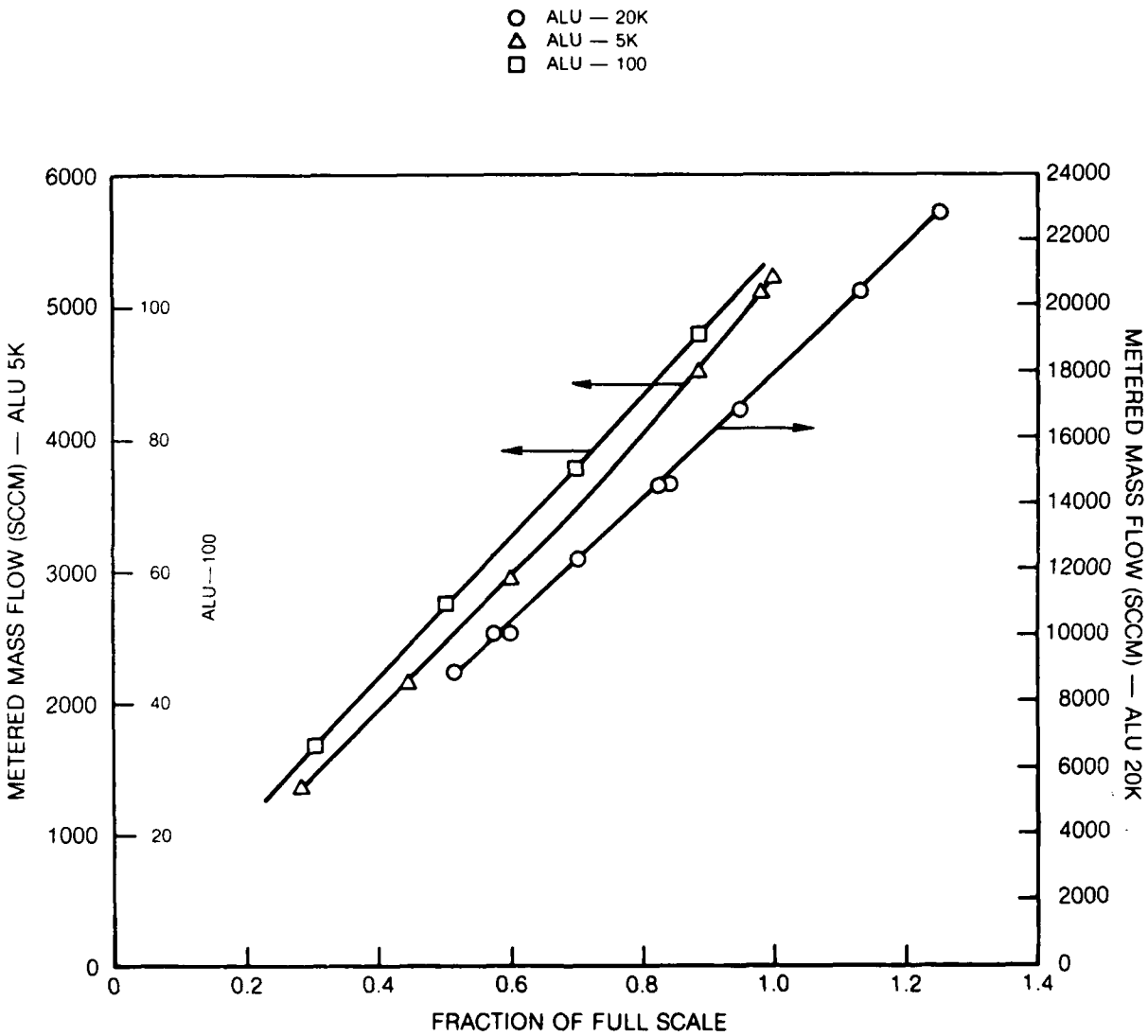

79-10-85-10

III. DESIGN OF GAS SAMPLING PROBES

III.A. Losses of Nitric Oxide in Sampling System

Although this report focuses on probe measurements of nitric oxide and associated probe phenomena, it is clear that a gas sample probe (and the corresponding extraction of a gas sample from a flame environment) is only one part of a sampling system. Since any portion of this multistep process (from gas sampling to species analysis) could cause errors, it is worthwhile to review this process. Typically, the individual steps include:

1. Extraction of the sample from the flame environment without perturbations external to the probe due to local temperature changes or catalysis (due to the presence of a probe).

2. Quenching of the flame gases inside the probe by rapid temperature and, usually, pressure reduction without the occurrence of hetero- or homogeneous kinetics.

3. Removal from the flame environment and transfer of the sample to the instrumentation without condensation or reactions on walls.

4. Water removal using, for example, an ice trap to minimize condensation and/or interference in the detectors yet without condensing or absorbing other species of interest.

5. Filtering of the gas sample for particulates.

6. Pressure recovery using a non-interfering pump to produce gas samples at pressures required by the detector(s).

7. Analysis of the sample for the species of interest with known or calculable corrections for the presence of interfering species.

In specific cases, certain items such as the water trap, filter, or pump may not be necessary due to combustor conditions, instrumentation, and required pressures; while in other systems, additional facilities, such as a storage capability, may be needed.

In regard to the sampling and analysis of nitric oxide (NO) or total nitrogen oxides (NO and NO_2), nearly all of the above steps have been suspected and examined as a source of sample perturbation. For this report, problems associated with sampling both NO and NO_2 are important due to the known interconversion between these species. Although many authors have discussed selected problems associated with the measurement of nitrogen oxides,

perhaps the most comprehensive reviews have been written by Cernansky (1976) and Tuttle, et al. (1973). Complications with measurements of nitric oxides such as those mentioned in these reports and with measurements of other gaseous emissions led the Federal government to write regulations (according to recommendations by the Society of Automotive Engineers (E-31 Committee)) for the gas sampling and measurement of aircraft emissions (Federal Register, 1973 and 1976). In spite of these efforts, many uncertainties in the measurements of nitrogen oxides remain. Primarily, these uncertainties include:

1. Interconversion between nitric oxide and nitrogen dioxide within the sampling probe or sampling line.

2. Chemical reactions within the probe that reduce nitrogen oxides to molecular nitrogen or other nitrogeneous species.

3. Sampling line losses of NO_x (i.e., NO and NO_2).

4. Improper calibration or corrections for a chemiluminescent detector for the presence of species other than nitrogen (the usual diluent in calibration gases).

5. Low efficiency for the $NO_2 \rightarrow NO$ converter or complete reduction of nitrogen oxides to molecular nitrogen or other nitrogeneous species in the absence of oxygen.

Experimenters can also observe apparent losses of nitric oxide due to a variety of experimental problems, including unconditioned sample lines, small leaks, and even under unusual operating conditions (e.g., flow rate through probe is less than that required by the analytic instruments) reverse flow through a bypass valve that may dilute the gas sample. The above items are discussed in detail in the following sections.

III.A.1 NO/NO_2 Interconversion

Prior to the early seventies, it was believed that very little nitrogen dioxide was formed during combustion processes and that nitric oxide made up nearly all of the emissions of nitrogen oxides. Since that time, however, many experimenters (e.g. Anon, 1971; Schefer, et. al., 1973; Merryman and Levy, 1974; Allen, 1975; Kramlich and Malte, 1978; Amin, 1977; Cernansky and Singh, 1979; Johnson, et. al., 1979, and Clark and Mellor, 1980) have probed various combustion systems for nitrogen oxides and have found large NO_2/NO ratios. Throughout this decade the source(s) of this measured NO_2 has been questioned. Although the flame, probe, and the sampling line have each been suspected as its source, it is apparent now that each system must be analyzed separately. In a gas turbine combustor, for example, nitric oxide formed in the primary zone may be converted to NO_2 by relatively cold air entering from the dilution holes (Chen et. al., 1979). Alternatively, as the

gases in a probe are cooled to approximately 1000K, flame radicals are quenched and may be converted to the hydroperoxyl radical (HO_2) which can oxidize nitric oxide via the reaction

$$NO + HO_2 \rightarrow NO_2 + OH \qquad \text{(III-1)}$$

Kinetic analyses by Johnson, et. al. (1979) and Kramlich and Malte (1978) for cooled probes indicate that this reaction is of prime importance in the conversion of NO to NO_2. The reaction

$$NO + O + M \rightarrow NO_2 + M \qquad \text{(III-2)}$$

although considered, is relatively unimportant due to the short lifetime of atomic oxygen. In fact, the model by Johnson, et. al. predicts that if all the NO_X begins as NO_2, some will be converted to NO. In general, they conclude that for these flames (producing small quantities of NO_X, $\sim$ 10 ppm), no relationship exists between the measured NO/NO_2 ratio and the actual ratio in the flame.

Schefer, et. al., (1973) observed the unusual result that cooled probes (quartz and stainless steel) indicated virtually no nitric oxide but several ppm of NO_2 in an opposed jet combustor (premixed, propane) and with uncooled probes the nitrogen oxides were composed nearly entirely of NO. Since the probes were placed in the reaction zone and sampled only partially burned gases, the authors argued that within the uncooled probes exothermic reactions continued, thereby heating the surfaces to feed the catalytic conversion of NO_2 to NO (similar to NO_X convertors used with CLA). They concluded, therefore, that the very high $NO_2/(NO + NO_2)$ ratios (nearly 1) obtained with the cooled probes are realistic measurements. Based on the recent studies by Johnson, et. al. (1979) and Kramlich and Malte (1978), it seems more reasonable that Reaction (III-1) is at least partly responsible for conversion of NO to NO_2 in the cooled probes, especially in light of the presence of oxygen and unburned fragmented hydrocarbons which are known to produce the HO_2 radical during decomposition. Any NO_2 similarly formed in the uncooled probes would undoubtedly be reconverted to NO on the hot surfaces.

Other experimenters have considered the NO_2 to NO conversion (based on the same principle as a catalytic NO_X converter) to be important for uncooled stainless-steel probes. Benson, Samuelsen, and Peck (1976) and Benson and Samuelsen (1976, 1977), for example, have examined a similar phenomena in simulated (heated) probes and in the presence of carbon monoxide, hydrogen, and unburned hydrocarbons. Their work cannot be directly applied to probe behavior since no (overall) kinetics were derived from their work and, more importantly, the residence time ($\sim$ one second) in the simulated probes was much longer than expected residence times in an uncooled probe. This data is much more descriptive of the behavior of catalytic converters.

In the case of either the NO to NO_2 oxidation via Reaction (III-1) or the surface reduction of NO_2 to NO, neither mechanism can be used for quantitative predictions at the present time due to the inability to describe accurately and simultaneously the fluid dynamics, heat transfer, and chemical kinetics (both hetero- and homogeneous) occurring within a probe. (Note: The present study contributes substantially to the understanding of the fluid mechanics and heat transfer for a certain class of sampling probes. Section III.B.2)

Another possible mechanism for conversion of NO to NO_2 is the reaction

$$NO + NO + O_2 \rightarrow 2NO_2 \qquad \text{(III-3)}$$

that may occur in the sample transfer lines or in the instrument lines leading to the reaction or measurement chamber. Although Cornelius and Wade (1970) have concluded that this reaction was unimportant in their system, it should be noted that each sampling system should be examined since this reaction is a strong function of the nitric oxide concentration and the total pressure. For systems with low concentrations of nitric oxide (< 250 ppm), low oxygen concentration, or low sampling line pressures and residence times, this reaction is undoubtedly insignificant; however, for systems with large NO concentrations due to seed NO or fuel nitrogen, with high oxygen concentrations, or with high sampling line pressures even in only part of the system, this reaction may convert substantial fractions of the nitric oxide to nitrogen dioxide. Although this phenomena was observed in the first phase of this program (Dodge, et. al., 1979), complete details of this conversion were not reported. Since this reaction is also of interest in this part of the program, further details of these measurements have been given in the following section.

Since the rate constant for Reaction III-3 is well known, the contribution of this reaction can be estimated once initial NO and O_2 concentrations are identified, and pressures and residence times throughout the sampling system are measured.

III.A.1a The Bodenstein Reaction

The reaction

$$NO + NO + O_2 \rightarrow 2NO_2 \qquad \text{(III-3)}$$

under certain conditions may contribute to conversion of NO to NO_2 in a sampling system. It is undoubtedly not a three-body (or termolecular) reaction but rather represents a sequence which either forms the dimer,

$$NO + NO \rightleftarrows (NO)_2 \qquad \text{(III-4)}$$

$$(NO)_2 + O_2 \rightarrow 2NO_2 \qquad \text{(III-5)}$$

or one that forms the nitrate

$$NO + O_2 \rightleftarrows NO_3 \qquad \text{(III-6)}$$

$$NO_3 + NO \rightarrow 2NO_2 \qquad \text{(III-7)}$$

Although this has been discussed by many authors (see review by Baulch, et. al., (1970)) the actual route is not resolved. Nevertheless, this reaction has been examined by many experimenters and its rate constant is known better than +50%, $k_{III-3} = 1.2 \times 10^9 \exp(+523/T)$ $cc^2/mole^2$-sec (Baulch, et. al., 1970; Hillard and Wheeler, 1977) when the reaction rate is defined as in Equation III-8.

The rate of loss of NO with respect to time due to this reaction can be written

$$\frac{d[NO]}{dt} = -2k_{III-3}\,[NO]^2\,[O_2] \qquad \text{(III-8)}$$

where brackets, [ ], represent concentration of the molecule in moles/cc. According to this equation, the rate of the Bodenstein reaction is dependent on the square of nitric oxide concentration and the first power of the oxygen concentration. Since number densities are directly proportional to pressure, this reaction rate is also indirectly dependent on the total pressure to the third power.

This reaction then becomes quite important in sampling systems where either high concentrations of nitric oxide or oxygen exist, high pressures exist, or long residence times occur. Alternatively, their opposites will tend to disfavor Reaction III-3. Specifically, this reaction may be of importance when NO or fuel nitrogen is added to the flame and when high sample line pressures exist, even for short line lengths.

During the course of the Task I investigation (Dodge, et. al., 1979) high concentrations of NO were added to a $H_2/O_2/Ar$ flat flame so that infrared optical measurements could be made. Simultaneous probe measurements were also made during these tests. For the particular sampling conditions used in these experiments, Reaction III-3 was found to contribute significantly to the conversion of NO to NO_2. The results can best be understood by examining the complete sampling system. In Table III-A, a review of different components of the sample system from the probe tip to the reaction chamber in the CLA is given. Estimates of lengths of line, local pressure, residence times, and temperatures are provided. This sampling system is only part of the complete

TABLE III-A

FLOW CONDITIONS IN NON-IDEAL SAMPLING SYSTEM

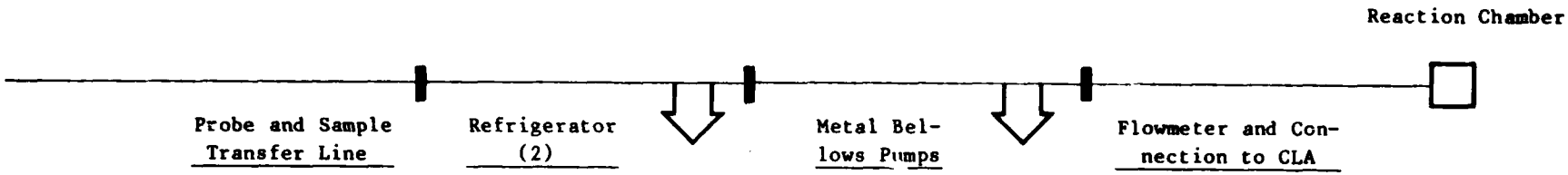

	Probe and Sample Transfer Line	Refrigerator (2)	Metal Bellows Pumps	Flowmeter and Connection to CLA
Distance cm (feet)	550 (18)	1070 (35)	460 (15)	470 (15.5)
Pressure torr (atm)	350 (0.46)	350 (0.46)	785 (1.03)	760 (1.0)
Estimated Residence Time (sec)	1.6	4.2	3.7	3.7
Temperature (°C)	110	0	20	20

Conditions for $T_{flame} \sim 1600$ K

SCOTT Instrument system in which the gas can be transferred to any of five analytical instruments. In a more compact system containing only a CLA, it is expected that line lengths and therefore residence times will be noticeably shorter. For the estimates provided in Table III-A, the individual residence times were based on total residence times and estimated mass flow, temperature, cross-sectional area, etc. in each section. The total residence time was measured as the time betweeen the moment when NO is first visually observed after a toggle valve is opened to add seed NO to the flame (i.e., when the flame turns a greenish-gray color) and the moment when the indicated nitric oxide concentration begins to rise rapidly. The pressures at various locations in the sampling system were obtained by placing several pressure gauges along the sample lines. The sampling system was operated to meet the Federal Requirements for a sampling system with the following exceptions. First of all, the sample line was held at 110 °C rather than the required 150 °C since, in this case, the sampled gas consisted of H_2/O_2 combustion products and condensation of hydrocarbon fragments was not of concern. Secondly, the total response time of the analytical system (from probe tip to 15% response at the detector as defined by the Federal Register) was approximately 18 seconds vs. the required time of less than nine seconds. For sampling over the flat flame burner with the SCOTT instrument package, this time could not be greatly reduced at the flame temperatures of these measurements ($\sim$ 1600 K). Logical modifications for decreasing the residence time include increasing the mass flow (and consequently bypass ratio) or reducing line lengths, however, neither of these approaches were feasible. The orifice diameter for the probe ($\sim$ 0.035") limited the mass flow and was already considered to be large for the flat flame burner. In addition, line modifications would have also reduced the capabilities of this package of analytical instruments. Consequently, the SCOTT system was not used for nitric oxide measurements in the Task II study of the flat flame burner. In the case of the Task I study, it should be pointed out that at lower gas temperatures where much of the study was performed, the mass flow through the probe increased ($\dot{m} \sim 1/\sqrt{T}$) and the residence times were closer to the federal requirements. In addition, data obtained using the CLA in the SCOTT instrument package over a range of operating conditions and with the above probe (water-cooled, quartz, 0.035" orifice diameter) agreed well with data taken, for similar experimental conditions, using a mass spectrometer and a water-cooled, quartz microprobe ($\sim$ 0.004" orifice diameter). The inability to meet the federal requirements described here does not invalidate the following analysis, although it is expected that under similar flame conditions and with a proper sampling system the conversion problem will not be quite as severe as presented here.

To estimate the amount of NO remaining after a period of time (t_i) in a given section, i, at constant temperature, pressure, and $[O_2]$, Equation III-8 may be integrated to obtain

$$\frac{1}{[NO]_i} = 2k_{III-3}[O_2]\ t_i + \frac{1}{[NO]_o} \qquad \text{(III-9)}$$

where $[NO]_o$ is the nitric oxide concentration before passing through the ith section of the sampling line and $[NO]_i$ is the concentration at the end of this section. By summing Equation III-9 for each section (accounting for pressure variations appropriately) and assuming that the measured NO_x estimates the original nitric oxide concentration at the probe tip, the final value of NO just prior to the CLA may be calculated. These values were estimated for several experimental seed levels of NO at various flame conditions. Calculated and experimental values of NO and NO_2 are reported in Table III-B. Good relative agreement is found between the calculated and measured values of NO_2 (see ratios) although the calculated value is approximately a factor two higher than the measured value. This factor of two difference is not due to an error in the rate constant but is probably due to inaccurate estimates of the flow parameters in the sampling system and/or loss of NO_2 in the system. In any case, the similarities in the trends and magnitudes of conversion between the calculated and measured values of NO_2, provides good evidence that Reaction III-3 is responsible for the conversion of NO to NO_2 in this sampling system.

III.A.2 NO_x Reduction in Sampling Probe

For uncooled stainless-steel probes sampling fuel-rich flames there exists much evidence that nitrogen oxides can be reduced (probably to molecular nitrogen) within the probe. This phenomena is not unexpected since it is the same as that observed when attempting to use a stainless-steel catalytic converter to convert NO_2 to NO in the presence of fuel-rich gases. Reduction by stainless-steel probes has been observed by Halstead, et. al. (1972) who compared an uncooled quartz-lined probe with an uncooled stainless-steel lined probe and by others (England, et. al., 1973; Cernansky and Singh, 1979; and this work). This problem is easily eliminated or at least drastically reduced by using cooled probes for sampling fuel-rich flames.

Under stoichiometric or fuel-lean conditions very little evidence exists that indicates probes significantly alter total concentrations of nitrogen oxides. England, et. al (1973) have observed some dependence of NO concentration with changes in probe type; total NO_x, however, is not reported in this report and some of the differences may be due to interconversion between NO and NO_2. In addition, the only major differences are noted between the cooled and uncooled probes. Few, McGregor, and coworkers (1972, 1975, 1976, and 1977) have compared UV optical measurements of NO to probe measurements and have concluded that the probe measurements are up to a factor of six lower than the optical measurements. These conclusions are, however, subject to question due

TABLE III-B

COMPARISON OF CALCULATED AND MEASURED NO AND NO_2

Calculated O_2 %	Measured NO_x (ppm)	Measured NO (ppm)	Measured NO_2[2] (ppm)	Calculated[1] NO (ppm)	Calculated[1] NO_2 (ppm)	Calc/Meas. NO_2
5.0	4891	4727	164	4550	341	2.08
5.0	7266	6833	433	6539	727	1.68
5.0	7114	6715	399	6416	698	1.75
7.9	3312	3189	123	3080	232	1.89
7.9	4533	4272	261	4110	423	1.62

[1]Estimated concentration at CLA assuming the initial NO concentration at the probe tip is equal to the measured NO_x

[2]Measured NO_x minus measured NO

to errors in the calibration procedures and theoretical model (Dodge, et. al., 1979). Cernansky and Singh (1978) have observed some differences in total NO_x for a variety of probes sampling fuel-lean, stoichiometric and fuel-rich flat flames; however the differences are typically small (< 15%).

Recently, Clark and Mellor (1980) have compared NO and NO_x measurements using several different probes in a model gas turbine combustor. They report some rather large differences between measurements of NO using blunt and tapered tip probes (as much as a factor of three); however, measurements of total NO_x indicate relatively small scatter (~20%) which is typical of the day to day variations in their combustor and/or analysis system. It should be noted that this agreement is achieved despite high measurements of hydrocarbons (>4%) that indicate the probe is sampling within the reactive flame zone.

Optical and probe measurements have been compared at other laboratories and in general good agreement is found. Meinel and Krauss (1978) have made in situ measurements of NO in both H_2/air and C_3H_8/air laminar premixed flames using a UV resonant lamp. In lean flames, agreement between the probe and optics is excellent, i.e., within several percent. For rich flames, the optics produce values which are not greater than the probe values but are approximately 20 to 25 percent lower. Falcone, et al. (1979) have made optical measurement using an infrared, tunable diode laser. For a lean flat flame, $\emptyset = 0.67$, the optical measurements are about 20 percent higher than the probe values; however, they conclude that the primary uncertainties are associated with the laser system since the probe measurements agree well with the seed values of NO.

Bilger and Beck (1975) have made probe measurements on a turbulent diffusion, hydrogen/air flame and compared these measurements to those of previous work on the same or similar system. The measurements of the major species, i.e., H_2, H_2O, O_2, in general agreed quite well with only a small axial shift observable. The NO measurements, however, differed quite noticeably with the more recent results (using a probe with a slender nose) suggesting peak NO concentrations as much as 30 to 35 percent higher than earlier measurements with a probe having a blunt nose profile. In addition, they compare data where substantially different NO profiles between the small and large probes are observed with the small probe producing the highest NO. A substantial shift was also observed in the major species. For the large probe, the NO profiles were dependent on the flow rate, but no difference in the major species were observed. In these tests, it is not too surprising that different probes produce different results since the length of the turbulent flame is on the same order as the probe diameter. For example, the flame length is approximately 5 to 6 mm and the blunt-nosed probe has a diameter of 6 mm very near to its orifice. This large probe certainly must be considered a poor design for probing the reaction zone of such a flame. The slender nosed probe is a better design with an initial diameter greater than 1.2 mm but even this probe quickly tapers back to 4 mm diameter. The differences in the profiles (both NO and major species) may be due to the presence of a large heat sink, i.e., the probe, or possible

stagnation zones in front of these probes. The difference between the NO profiles obtained using the large probe at various flow rates may be due to the phenomena stated above or to NO/NO_2 interconversion within the probe. NO_2 was measured only for the smaller probe and in that case was found to be negligible. Bilger and Beck also conclude that the slender nosed probe provides a more realistic measurement of nitric oxide.

Bryson and Few (1978) at Arnold Research Organization (ARO) have observed relatively large differences ($\sim$ 50%) in total nitrogen oxides between a tubular probe and either a 'quick-quench' or dilution probe (the latter two agree). Since this discrepancy is rather large, it is worthwhile to investigate the ARO study in detail to see if this report identifies areas that require further research.

Quite clearly, there are several significant conditions of the Bryson and Few study that are different from other reports. First of all, in their study supersonic exhaust from an AVCO-Lycoming engine is sampled. In all other papers that report measurements using different probes, subsonic flows are examined. Secondly, three distinct, water-cooled probes were compared: a tubular inlet probe, a 'quick-quench' probe, and a dilution probe. In addition, the stainless-steel tubular probe was constructed to accept inserts of copper or fused silica. Alternatively, other studies primarily examined effects due only to changes in surface material. (Some papers, e.g., England, et al. (1973), do test some modifications to probe design but in general these changes are minor relative to the design variations found in the ARO study). In regard to the design variations, it should be noted that the tubular probe which produced the relatively high NO_x measurements also had a very large opening (0.77 cm i.d. vs 0.12 and 0.127 for the other two probes) and was operated with a sample line pressure much larger than the latter two probes. The ratios of sample line to combustor pressure were typically 0.9 for the tubular probe and less than 0.5 for the other probes. Undoubtedly the pumps used for the 'quick quench' and dilution probe were insufficient to choke the tubular probe. Under choked conditions (not well defined for a constant area tube where the flow should friction choke at the exit rather than at the entrance), the probe would draw approximately 40 times the flow of the smaller probes. Based on the above analysis, it seems likely that the different NO_x measurements between a tubular probe and either a 'quick-quench' or dilution probe may be associated with differences in sampling pressure and flow rate through the probe and/or the existence of a stagnation zone in front of the probes.

A stagnation zone, for example, in front of these fairly blunt probes in a supersonic stream could perturb the gas samples. For air at a Mach number of 1.15, for example, a stagnation of the flow results in a 25% rise in temperature. For the tubular inlet probe, the problem may be the most severe. First of all, the gas decelerates to a very low Mach number at the entrance (estimated to be less than 0.1) and consequently stagnation temperatures must be

approached even in the absence of an external stagnation zone. Secondly, the rate of cooling is undoubtedly much slower in this probe than in the other two since the sample tube is quite large (producing a low surface to volume ratio for heat transfer) and since the pressure and mass flow through this tube are significantly larger. The problem should be less important when sampling exhaust gas at lower temperatures because the magnitude of the temperature rise is less and since kinetics are slower at lower temperatures. In Bryson and Few's study, essentially no difference between the probes was found for the NO measurements at the lowest stoichiometries which produce exhaust temperatures approximately 600 K less than the other tests.

Sample line leaks from either the atmosphere or from a purge system may also affect relative readings when a probe and/or pumping system create large differences in sample line pressures and flow rates. Consider a case with a small leak across a purge valve. If the sample line pressure is only slightly less than the purge pressure and the mass flow through the sample line is large, the leak would be unchoked and, if small, would dilute the sample minimally. However, when the sample line pressure reduces to below 50% of the purge pressure and simultaneously the sample flow rate decreases (such as by reducing the probe orifice diameter) then the importance of the leak may increase substantially. Based on the data presented by Bryson and Few, the above phenomena could explain some of the differences between the tubular inlet and the other two probes. This effect, however, is not believed to be the cause of the discrepancies since at low power levels NO measurements did not vary with probe type. It is more likely that the increase in temperature (and pressure) due to shock recovery and subsonic diffusion created the sampling problems encountered by Bryson and Few.

Another aspect of the study by Bryson and Few is that, for the dilution probes, wide scatter was observed. The authors comment that part of the scatter may be due to estimation of the dilution ratio which was calculated via two techniques. A factor not considered in their study is that a change in the diluent or carrier will change the response of a chemiluminescent detector. The response is not only a function of the quenching efficiency of a third body as pointed out by Matthews, et al. (1977) but also dependent on the viscosity of the sampled gas for standard commercial units (Folsom and Courtney, 1979 and Dodge, et al., 1979a). Although this phenomena is discussed in greater detail in Section III.A.4, it can be estimated based on data from Folsom and Courtney that the NO_x measurements made when diluting with argon should be increased by approximately 10 percent depending on the diluent ratio. No data were found for the case of a helium carrier, but since the viscosity of helium and nitrogen are similar and if helium is less efficient than nitrogen for the reaction

$$NO_2^* + M \rightarrow NO_2 + M \qquad \text{(III-10)}$$

which competes with

$$NO_2^* \rightarrow NO_2 + h\nu \qquad \text{(III-11)}$$

then one would expect that the data obtained with a diluent of helium should be reduced by several percent. We estimate that these corrections should reduce the uncertainty for data obtained using the dilution probe.

Additional research that may indicate that probes perturb measurements of total nitrogen oxides has been performed by England, et al. (1973); however, in this work, only nitric oxide data are presented. Consequently, definitive statements on the loss of total NO_x cannot be made. For uncooled, stainless-steel probes in rich flames, the NO measurements are significantly less than for cooled probes. As described previously this behavior is not at all unexpected for $\emptyset > 1.0$ (rich flames). In spite of the fact that the paper indicates a fall-off in NO for these uncooled probes even for $0.6 < \emptyset < 1.0$, this may be an artifact of the curve-fitting technique (no actual data points are published). In any case, no detailed mechanism has been presented to explain these data. For two cooled probes and even an uncooled quartz tube, NO profiles are nearly identical for the lean flames and are similar for fuel-rich flames. Slight discrepancies on the fuel-rich side may be due to NO/NO_2 interconversion rather than loss of total NO_x.

In summary, there is only one known report that suggests that changing probes may change the total concentration of nitrogen oxides by a significant amount (other than uncooled probes in rich flames). This study by Bryson and Few shows that a tubular inlet probe produces higher values (by 50%) than two other probes. Although insufficient data are available, it is possible that phenomena associated with the higher operating pressure, an external stagnation zone, or different flow rates may contribute to the observed results. Moreover, it should also be noted that apparent differences in NO_x may be observed between different probes if NO/NO_2 interconversion varies between the probes and NO_2 exiting from one of the probes is lost in water traps or an inefficient converter.

III.A.3 Losses in Sampling Line

As Tuttle, et al. (1973) have discussed, NO_2 can be lost in sampling lines for any of various reasons. These include reduction of NO_2 on particulate filters, loss in water traps, or loss or reduction of NO_2 in unconditioned stainless-steel sampling lines. Dimitriades (1967) claimed to have observed NO_2 losses in both water traps and Drierite columns, but these losses are not quantified and it consequently is difficult to estimate the impact on a measurement where water removal prior to analysis is necessary. Dimitriades does, however, comment that this loss is specific to NO_2 and that he did not observe similar losses of NO. The same comment cannot be made for the other items listed above. For example, it has been observed in our laboratory that unconditioned stainless-steel lines will also produce an apparent loss of nitric oxide. This loss mechanism can usually be eliminated by flowing an NO calibration gas through new lines for 15 minutes to 1/2 hour. Once conditioned, no evidence was found that indicated the necessity to repeat this process. In regards to the loss of NO_2 on filter paper containing carbon or soot particles, Tuttle, et al. observed losses of NO_2 using an NDUV detector

(for NO_2) but did not look for the possible conversion to NO or for similar losses of NO due to the presence of soot. Gas-phase, NO-hydrocarbon reactions are typically as well known and as fast as NO_2-hydrocarbon reactions; by analogy, one might expect similar reactions between NO and deposits of soot.

Each of the above problems represents a real concern and should be considered in the construction of any sampling or analysis system. Presumably, the line conditioning problem can be easily rectified by using teflon coated tubing and fittings throughout or using clean stainless-steel tubing which has been conditioned for several (> 15) minutes using an NO or NO_2 calibration gas. Nitric acid should not be used as a cleaning agent since it leaves nitrates and/or nitrites as residues.

Water condensation is a more difficult problem to solve. Bryson and Few (1978) ran without a water trap and then between measurements flushed out the lines with dry nitrogen in the analyzer to remove any condensed water. (This procedure complicates data reduction since, as discussed Section III.A.4, water can have a strong effect on the response of the CLA and was not accounted for by Bryson and Few.) Although this technique eliminates the retention of large quantitites of water within the analyzer some condensed water along the inner walls must remain and presumably could contribute to NO_2 absorption. The best methods would include the modification of the analysis equipment so that (1) the entire system (both sampling and analyzer) are heated substantially above the dew point (based on the maximum pressure in the sampling system and the initial water concentration) or (2) sample line and analysis instruments all operate at reduced pressure (low enough to prevent condensation). For example, for a liquid-fueled gas turbine engine operating at an overall stoichiometry less than 0.33, it can be estimated that all lines should be heated above 35°C if the maximum sample pressure is only 800 torr (15.5 psia). Although these modifications represent changes over the present specifications in the Federal Register (1973, 1976), it is not clear whether such steps are necessary since the loss of NO_2 in a trap is not understood quantitatively and may be dependent on trap geometry and capacity, among other things.

The loss of NO_x due to the presence of soot on particulate filters (or even coated on sample lines) is a more difficult problem to address. Presumably, no easy solution can be found for a combustion system that produces large quantities of soot. Fortunately, Federal requirements for smoke emissions help to reduce potential complications due to soot in sampling lines. As in the above case for water absorption, losses cannot be estimated quantitatively.

III.A.4 Response of Chemiluminescence Analyzer

As mentioned previously in Section III.A.2, the response of a commercial chemiluminescent analyzer (CLA) is dependent not only on the concentration of nitric oxide but also on the fluid mechanical properties and quenching efficiency of the carrier gas. Response changes due to changes in quenching efficiency have been reviewed by Matthews, et al. (1977). From the well-known chemiluminescent reaction sequence

$$NO + O_3 \rightarrow NO_2^* + O_2 \qquad \text{(III-12)}$$

$$\rightarrow NO_2 + O_2 \qquad \text{(III-13)}$$

$$NO_2^* + M \rightarrow NO_2 + M \qquad \text{(III-10)}$$

$$NO_2^* \rightarrow NO_2 + h\nu \qquad \text{(III-11)}$$

it is clear that Reactions III-10 and 11 are in competition. The presence of species such as water and carbon dioxide which are more efficient than nitrogen at quenching the excited NO_2 molecule (NO_2^*) will produce less of a response than when nitrogen is the carrier for equivalent concentrations of nitric oxide. The presence of species that are less efficient at quenching (e.g., argon) correspondingly will produce a greater response.

These comments are true only in the case of a CLA for which the pressure in the reaction chamber is maintained constant (such as the original design by Fontijn). Unfortunately, the technique used to maintain constant pressure in the reaction chamber of low pressure commercial units is via flow restriction using capillary tubes. Since the flow rate through these tubes is dependent upon on the fluid mechanical properties of the carrier, the pressure and, of course, the concentrations of NO and the quenching species (M) in the reaction chamber are dependent on these same properties. This phenomena was observed several years ago by one of these authors (M. F. Zabielski) when comparing mass spectrometric and chemiluminescent data when argon was used as the carrier. In this case, the chemiluminescent detector was found to have a reduced response relative to measurements with nitrogen carrier; this direction is opposite to that predicted according to an analysis of quenching phenomena. Subsequently, Dodge, et al. (1979a) modelled this problem by assuming frictional choking in the capillary tubes. Stimulated by the original UTRC work, Folsom and Courtney (1979) performed a detailed empirical study on the effect of carrier gas on the responses of commercial Beckman and Thermo Electron instruments. Although Folsom and Courtney qualitatively explained their data in terms of relative viscosity and quenching data, the model developed at UTRC (Dodge, et al. 1979a) appears to be in good quantitative agreement with the data obtained both at UTRC and by Folsom and Courtney on the Thermo Electron instrument. (The UTRC model would have to be modified for the atmospheric pressure instruments (e.g. Beckman or McMillan) due to a different design.

In general, corrections due to differences in a carrier of pure nitrogen and that of combustion gases are not large (typically < 10%). Exceptions to this rule include flames using an unusual carrier (argon, for example) or no carrier at all; samping systems where the water is not removed (especially for stoichiometries near $\phi = 1.0$); or samping systems were the sampled gases are diluted with a species other than nitrogen. In these cases, the combination of viscous and quenching effects ought to be considered, since the response change of a CLA can amount to as much as 15% or possibly more.

III.A.5 NO_X Converter

The purpose of an NO_X converter is to reduce nitrogen dioxide to nitric oxide via the overall reaction

$$2NO_2 \rightarrow 2NO + O_2 \qquad \text{(III-14)}$$

in the presence of a heated metallic surface (usually stainless-steel). The NO thus formed, along with the initial NO, is detected in a chemiluminescent analyzer. The NO_2 concentration is obtained by subtracting from this response the instrument response when the converter is bypassed.

Problems associated with the operation of the converter have been discussed in detail by Tuttle, et al. (1973). The problems can be placed into the three classifications: anomalies, inefficiencies, and NO_X reduction. Tuttle, et al., for example, report an anomaly observed by A. Nelson of Pratt and Whitney Aircraft. In this case, a span gas of 91 ppm NO in nitrogen but void of NO_2 (verified by the Saltzmann technique) indicated a concentration of 95 ppm when passed through the detector. As opposed to a decrease or apparent loss of NO, this increase appears very unusual since it suggests a generation of nitric oxide. Although Tuttle reports this as an anomoly, it is likely that the calibration of the instrument shifted (if the operator did not adjust for changing flow rates due to the pressure drop across the converter) or perhaps nitric acid was used as a cleaner which may outgas nitrogeneous species. It is more typical that a slight but noticeable reduction in indicated NO (several percent) will be observed when a span gas of NO is directed through the converter. Presumably this loss is due to a reduction of nitric oxide (to nitrogen) in the converter.

Practically, the best efficiency for conversion of NO_2 to NO is about 97 to 98 percent, and efficiencies of 90 to 97 percent are typically achieved for fuel-lean gases. These efficiencies, however, are dependent on NO_2 concentrations and type, condition, and temperature of the converter. Most converters, for example, will perform, at least momentarily, when fuel-rich gases with NO_X are passed through, however, stainless-steel converters at high temperatures will last only a matter of seconds before total NO_X is destroyed. Molybdenum converters are more useful since they efficiently convert NO_2 to NO without loss of total NO_X for up to a minute or so (depending on flame stoichiometry and converter temperature). The increased activity of molybdenum for fuel-rich gases is due to its lower operating temperature ($\sim 450°C$ for molybdenum vs. $\sim 700°C$ for stainless-steel). The activities of the converters are easily recovered by flowing an oxygen rich mixture through the heated tubes for a few minutes. In fact, alternately flowing air through the converter when sampling fuel-rich flames is a common procedure. This technique should be used with caution, however, since resultant surface oxidation deteriorates the converter and may reduce its conversion efficiency.

III.A.6 Summary

In the above discussion, it is shown that many phenomena may contribute to erroneous measurements of nitrogen oxides. These include interconversion between NO and NO_2, loss of total NO_X, and misinterpretation of data (assuming use of CLA). Interconversion and loss can occur in the probe, sample line (water trap and filter included) or converter. Perhaps the biggest errors may be caused by the use of uncooled probes sampling fuel-rich gas. Under the same flame conditions, NO_2 measurements (using a converter/CLA) can only be made through careful use of the converter. In any case, efficiency checks on the converter operation should always be made. In the case of lean or stoichiometric flames, only one report (Bryson and Few) was found that indicated substantial discrepancies (~50%) in NO_X when measured using different water-cooled probes. These discrepancies may be due (at least in part) to differences in sample line pressure and/or flow rate. The results of another report which indicates discrepancies (Bilger and Beck) are unreliable since at least one of the probes was poorly matched to the combustion system. The only other significant probe effect is the conversion from NO to NO_2 due to oxidation by the HO_2 radical. This reaction, however, has been found to be of significance only when relatively low concentrations of NO are present (~ 50 ppm). It would be expected that at larger concentrations when the NO/HO_2 ratio is large both in the flame and probe, oxidation of NO via the HO_2 radical is relatively unimportant.

III.B Quenching in Gas Sampling Probes

Gas samples extracted from a flame environment are quenched by a rapid reduction in either pressure or temperature, and typically both. For a bimolecular reaction, a reduction in pressure by a factor of ten will reduce reaction rates by a factor of 100. Decreasing the gas temperature from 2000 to 1200 K for a reaction with an activation energy of 40 kcal/mole (typical for overall hydrocarbon oxidation) will decrease the reaction rate by a factor of 750. The quenching of flame gases is required not only to stop ongoing reactions (non-equilibrium conditions) but also to prevent a shift from equilibrium (or quasi-equilibrium) conditions such as may be present in a post flame zone. Ideally, a probe should quench or "freeze" the flame gases exactly at the concentrations present where the probe tip is located.

Techniques used to quench flame gases include quenching by dilution, convection, or expansion and each of these have been discussed in some detail by Tiné (1961). Briefly, quenching by dilution is accomplished by adding a low temperature diluent to the flame gases which acts to absorb heat from the extracted sample. Quenching by convection is performed by heat transfer to cooled walls within the probe and quenching by expansion is accomplished by

accelerating the gases supersonically through a nozzle to drop the static temperature and pressure. Although expansion cooling is undoubtedly the fastest ($\sim 10^8$ K/sec vs. $\sim 10^6$ K/sec for cooling by convection), the associated phenomena are not well understood and two major drawbacks accompany this technique. First of all, convection cooling to cooled walls must also take place while the gas is flowing supersonically; otherwise, upon return to subsonic flow conditions, the static gas temperature will return near to flame temperatures. Secondly, substantial pressure losses, both friction and normal shock losses, are suffered. Details of these phenomena will be discussed later in this chapter.

In spite of the many years that probes have been in use, there exist many uncertainties in regard to their quenching behavior. Beal and Grey (1953) have argued that any of the above three techniques provide sufficiently high quenching rates to freeze the concentrations of stable species at or near concentrations present in the flame zone. Alternatively, Halpern and Ruegg (1958) have found that changes in quenching rates due to changes in probe design, internal diameter, and sample flow rate may vary measured ratios of CO/CO_2 and H_2/H_2O. These latter conclusions may be subject to error since the authors apparently used probes that were comparable to the size of the burner. The presence of a large, cooled probe will significantly perturb the flame environment. Other authors have reported discrepancies in CO and NO measurements for various flame conditions using different probes (Bryson and Few, 1978; Bilger and Beck, 1975; and England, et al., 1973) but it is not clear whether these discrepancies are due to differences in quenching rates rather than to flame perturbations, stagnation of the flow, or sampling line/analysis phenomena. It should be noted that species existing in low concentrations (several hundred ppm or less) are especially susceptible to any of the above effects. Examples include NO, NO_2 and in lean flames, CO. Small absolute changes ($\sim$ 25-50 ppm) can reflect a large relative change for these molecules. In fact, increased rates of quenching may not necessarily solve problems associated with measuring these species since radical termination on the walls or in the gas phase may perturb concentrations of these species. Indeed, a model developed by Kramlich and Malte (1978) makes the unusual prediction that higher quench rates increase the conversion (in the probe) from NO to NO_2.

Not only are there uncertainties in the effect of quenching rates, but also actual knowledge of quenching rates is unknown. Typically, approximate fluid mechanic models are used to estimate cooling rates and pressure reductions; however, virtually no experimental evidence exists to verify these calculations. For example, the operation of quartz microprobes has been misunderstood for years. Fristrom and Westenberg (1965) argued by analogy that since a large diverging nozzle sustains a supersonic flow, a small probe nozzle should perform similarly. Although this extrapolation is somewhat suspect, many experimenters have operated on this premise with no experimental verification and very little, if any, theoretical analysis (e.g., Friedman and Cyphers, 1955; Lyon, et al., 1975; Kramlich and Malte, 1978; Lengelle and Verdier, 1973). More recently, questions regarding these conclusions have been raised

in the literature (Bilger, 1975, Amin, 1977; Seery, et al., 1977; Cernansky and Singh, 1979) with fewer and fewer experimenters tacitly assuming the existence of quenching by expansion. Even so, arguments used to question supersonic expansion are primarily phenomenological with only a few studies attempting to examine analytical details of the fluid mechanics (Seery, et al., 1977; Cohen and Guile, 1970; Amin, 1977) and with virtually no experimental investigation of the problem.

The lack of understanding of this problem can be explained by the fact that the fluid mechanic and thermal status of the sample gas in a probe is altered by a number of factors. These include: heat transfer from the uncooled probe tip to the sample gas and from the sample gas to the probe coolant; skin friction; flow area changes; pressure losses associated with shock systems, sudden area expansions, and turns within the sample passage; and, chemical reaction. For probes designed to achieve an aerodynamic quench (see III.B.2.a), sudden-expansion losses, turn losses, and chemical reaction are neglected and shock losses are avoided until the aerodynamic quenching region of the flow is completed. To understand the influence of the competing mechanisms, it is convenient to assume that the sample flow is both steady and one-dimensional and that manufacturing techniques are sophisticated enough so that the internal geometry of the probe (especially in the region of the probe tip) is reasonably close to the geometry analyzed. (The wall temperature distribution within the probe tip is difficult to calculate and, for small diameter probes, the internal shape of the tip is difficult to control during manufacture and also difficult to examine once constructed.)

Even though a model may be developed to describe heat transfer, skin friction, shock losses, and the effect of area changes, each of these phenomena produces different relative effects as the probe operating conditions are varied. Consequently, it is necessary to examine each experimental condition individually and a probe designed from such a study is usually a compromise.

The above discussion indicates the complexities of the operation of a probe in terms of kinetics, fluid mechanics, and heat transfer. Due to the discrepancies between optical and probe measurements observed by McGregor, Few and coworkers, and the above problems, the present program focused on understanding probe and sample line behavior and its impact on sample analysis. Although substantial effort was placed on examining possible homogeneous mechanisms for NO reduction, no mechanism was found that predicts loss of nitrogen oxides within water-cooled probes. Interconversion between NO and NO_2 may affect NO measurements and was observed in this study under certain conditions. This phenomena, however, was of little importance since, in the comparisons of optical and probe measurements, NO_X was approximately equal to NO. Moreover, recent studies on this problem (Johnson, et al., 1979; Kramlich & Malte, 1978) suggest that total NO_X is conserved. Knowledge of the NO_2/NO ratios may be important in understanding the total emissions problem (NO_2 can be visible in sufficient concentrations and NO_2 acts as an initiator in the photochemical smog cycle).

Fluid mechanics and heat transfer mechanisms were also examined in this study. Particular effort was focused on the phenomena of aerodynamic cooling since this technique is not well understood and since potentially the most significant benefits (i.e., the fastest quenching rates) can be obtained.

III.B.1 Kinetics of NO Decomposition

The loss of nitric oxide within a gas sampling probe, if indeed it occurs, should be explainable in terms of either hetero- or homogeneous phenomena. As reviewed in the TASK I report (Dodge, et. al., 1979), very little information is available on reaction mechanisms or rates for NO decomposition on walls. Nevertheless, for walls that are directly water cooled, virtually no NO can be lost on either quartz or stainless steel walls for a typical residence time in a probe of less than one second. (This statement assumes that the walls are properly conditioned, as in the case of sampling lines.) Near the orifice of a probe tip, wall temperatures may be significantly higher than 300 or 400 °C and in cases even approach the material softening point. Under these circumstances, the surfaces are certainly catalytically active and the potential for altering flame concentrations exists. Although a detailed analysis of molecular diffusion was not performed for this work, it was estimated that if the residence time in this portion of the probe is held to less than 10 microseconds, then the molecules undergo only a few collisions with the wall. Since the efficiency of NO decomposition should be significantly less than one, then decompositions of NO by collisions with a hot wall should be negligible.

Homogeneous mechanisms for the decomposition of NO have been examined by many workers (e.g., Hanson, et. al., 1974; Flower, et. al., 1975; and Koshi and Asaba, 1979). A listing of possible reactions which lead to the gas phase reduction of NO_x are listed in Table III-C. Reactions that oxidize NO to NO_2 are not included here since no net loss of NO_x results. (Assuming, of course, that care was taken to avoid loss of NO_2 in the sampling line and/or sampling system.) If the temperature is assumed to be constant, an estimate of the contribution of each of the reactions in Table III-C can then be made. For small fractional conversions of NO, the fraction of NO consumed by Reaction x is estimated by

$$\text{fraction} = \frac{\Delta[NO]}{NO_o} = k_x\,[x]\,\Delta t \qquad \text{III-23}$$

$$(\text{or} = k_x\,[x][M]\,\Delta t \text{ where applicable})$$

TABLE III-C

REACTION MECHANISM FOR NO DECOMPOSITION

Reaction Number				Rate Constant[1] A	n	E/R	Ref.
III-15	$NO + NO$	$\rightarrow$	$N_2O + O$	4.9×10^{12}	-	33,770	Koshi and Asabi (1979)
III-16	$NO + O$	$\rightarrow$	$N + O_2$	2.32×10^{9}	1	19,445	Hanson, et. al. (1974)
III-17	$NO + N$	$\rightarrow$	$N_2 + O$	1.63×10^{13}	-	-	Baulch, et. al. (1973)
III-18	$NO + M$	$\rightarrow$	$N + O + M$	1.41×10^{21}	-1.5	77,250	Baulch, et. al. (1973)
III-19	$NO + H$	$\rightarrow$	$N + OH$	1.35×10^{14}	-	24,760	Flower, et. al. (1975)
III-20	$NO + H_2$	$\rightarrow$	$H + HNO$	5.75×10^{12}	-	28,890	Baulch et. al. (1973)
III-21	$NO + H_2O$	$\rightarrow$	$OH + HNO$	2.0×10^{14}	-	36,510	Baulch, et. al. (1973)
III-22	$NO + H + M$	$\rightarrow$	$HNO + M$	1.8×10^{16}	-	-300	Jensen and Jones (1978)

[1] $k = AT^n \exp(-E/RT)$, units in cm^3/mole, sec

where [x] represents the concentration of the collision partner and k_x, the rate constant of Reaction x. The time increment, Δt represents an estimated quenching time, after which the reaction is effectively frozen due to a drop in the rate constant, concentrations, or both. Rate constants were obtained from literature values and are listed in Table III-C. Concentrations of stable and radical species were equated to the maximum equilibrium value for the three flat flames examined in this study. The concentration of NO was assumed to be 5000 ppm, a value larger than the maximum seed concentration used in this (TASK II) or the TASK III study. These concentrations, in terms of mole fraction, are listed in Table III-D and the fraction of NO lost due to each of these reactions, as calculated by Equation III-23, is also given. The calculations are based on a (local) probe pressure of 1/2 atmosphere and have been done for average static temperatures of 2000 and 1400 K. In addition, the quench time was assumed to be one millisecond. Even by assuming an uncertainty of one order of magnitude in rate constants or concentrations, it is clear from these results that only the (overall) three body reaction could possibly contribute to loss of nitric oxide. The conclusion that a three body reaction dominates under conditions of elevated temperature and reduced pressure is extremely unusual. It is more likely that the negative temperature dependence used for this reaction is too weak and, in fact, the rate constant decreases much more rapidly at high temperatures than indicated by the rate constants given in Table III-C. Other (overall) three body reactions typically have significantly higher negative activation energies. Since this rate constant has only been measured up to temperatures of 700 K, it should be expected that errors will result by extrapolation of the rate constant to flame temperatures. In addition, Reaction III-22 should be less important than indicated by Table III-D since the hydrogen atom concentration will decrease rapidly as the gas is cooled.

Even if this reaction does cause conversion of NO to HNO, the product will primarily reform nitric oxide after abstraction of the hydrogen atom, i.e.,

$$R + HNO \rightarrow RH + NO \qquad \text{(III-24)}$$

which occurs at nearly collision frequency. In this reaction, R represents any radical species. Some HNO could possibly be lost via

$$HNO + HNO \rightarrow N_2O + H_2O \qquad \text{(III-25)}$$

$$HNO + NO \rightarrow N_2O + OH \qquad \text{(III-26)}$$

or possibly by

$$HNO + H \rightarrow NH + OH \qquad \text{(III-27)}$$

or

$$HNO + O \rightarrow NH + O_2 \qquad \text{(III-28)}$$

followed by

$$N_2O + R \rightarrow RO + N_2 \qquad \text{(III-29)}$$

and

$$NH + NO \rightarrow N_2 + OH \qquad \text{(III-30)}$$

TABLE III-D

ESTIMATED FRACTIONS OF NO DECOMPOSITION

Reaction Number	Reaction Partner	Estimated Mole Fraction[1] of Reaction Partner	Fraction of NO Decomposed[2] Due to Each Reaction	
			2000 K	1400 K
III-15	NO	5×10^{-3}	3.5×10^{-6}	3.6×10^{-9}
III-16	O	1.5×10^{-5}	1.3×10^{-5}	2.0×10^{-7}
III-17	N	7.7×10^{-8}	3.8×10^{-6}	5.5×10^{-6}
III-18	M	1.0	8.1×10^{-10}	1.3×10^{-16}
III-19	H	5.7×10^{-5}	9.9×10^{-5}	7.0×10^{-7}
III-20	H_2	2.6×10^{-2}	2.4×10^{-4}	7.0×10^{-7}
III-21	H_2O	.15	1.1×10^{-3}	6.3×10^{-7}
III-22	H xM	5.7×10^{-5} 1.0	1.0×10^{-2}	2.2×10^{-2}

[1]See text

[2]From Equation III-23, assuming that pressure = 1/2 atm, Δt = 1 millisecond

but none of these reaction mechanisms is considered very likely. Reaction III-25 is sterically improbable and undoubtedly represents a multistep process. In any case, its reaction rate is dependent on the square of the HNO concentration which would be quite low. Reaction III-26 is slow since it has a significant activation energy of 26 kcal/mole (Wilde, 1969). Reaction III-27 is similarly slow due to its high endothermicity ($\sim$24 kcal/mole). If the oxygen atom concentration is high enough to allow Reaction III-28 to proceed at a high rate, then it is highly likely that the radical NH will be oxidized to form NO rather than reduced to form N_2.

Other reaction mechanisms (such as to produce HNO_2) were also examined, but conclusions similar to those above were obtained. No mechanism could be found which indicated loss of NO_x in a water-cooled sampling probe. Based on the analysis, the following quenching criteria were selected.

1. In the first portion of the probe tip where high wall temperatures (> 600 K) may exist, the residence time of the gas must be less than 10 microseconds.

2. The gas sample must be "quenched" within 1 millisecond, and

3. The gas is considered to be "quenched" when the total temperature falls below 1000 K (with an initial temperature approximately 1800 K).

This last criteria is based on the fact that after 1 millisecond radicals will have undergone hundreds of collisions with the walls. Recombination of these radicals, therefore, must occur within 1 millisecond and equilibrium radical concentrations at 1000 K are too low to allow any further reactions with NO before the gas is further cooled to water temperature (typically less than 100 milliseconds).

III.B.2 Description of Computer Program for Probe Analysis

The UTRC Probe Design computer program is based upon an equation which describes the change in local Mach number as a function of heat transfer, skin friction, area variations and thermal property changes for a steady, one-dimensional flow. Using the influence coefficient approach of Shapiro (1953), this equation is

$$\frac{dM^2}{M^2}(1-M^2) = -2\left(1 + \frac{\gamma - 1}{2}M^2\right)\frac{dA}{A} + (1 + \gamma M^2)\frac{dQ}{c_p T_s} + \gamma M^2\left(1 + \frac{\gamma - 1}{2}M^2\right)4f\frac{dx}{D}$$

$$-(1 + \gamma M^2)\frac{d\mathcal{M}}{\mathcal{M}} - (1 - M^2)\frac{d\gamma}{\gamma} \qquad \text{(III-31)}$$

where M is the Mach number; γ, the ratio of specific heats; A, the cross-sectional area; Q, the heat transfer rate; c_p, the heat capacity at constant pressure; T_s, the static temperature; f, the skin friction coefficient; x, the axial distance from the probe orifice; D, the tube diameter; and $\mathcal{M}$, the molecular weight. The heat transfer rate is calculated from

$$dQ = h(T_r - T_w)\,\pi D dx \qquad \text{(III-32)}$$

where h is the heat transfer coefficient, T_r is the recovery temperature,[1], and T_w is the wall temperature. To determine the wall temperature distribution within the probe tip, a computer program called TCAL was used (see end of this section). For both the portion of the probe tip and the constant area section that are cooled directly by the water in the coolant passage, the wall temperature is determined by the overall heat transfer rate from the sample gas to the coolant. To provide a conservative (i.e., low) estimate of the heat transfer from the sample to the water, a higher than anticipated coolant temperature (150 °C) was used in the calculations. The heat transfer coefficients reported by Kays (1955) for laminar flow and Rohsenow and Choi (1961) for turbulent flow were used. For the skin friction term (4f), correlations reported by Eckert and Drake (1959) were used; these correlations are applicable to fully developed laminar and turbulent flow in smooth tubes.

To calculate the profiles of temperature, pressure, etc., the terms in Equation III-31 are evaluated at a given axial location and the new Mach number at the next axial location is calculated by a simple, forward marching procedure. The gas properties at the new location may then be calculated using standard relationships, such as the ideal gas law. When the flow is supersonic initially, conditions downstream of a normal shock system are calculated using the Rankine-Hugoniot relationships. The position of the shock is determined using one of two procedures. The position may be specified by the user to occur at a physically realistic location in the probe (e.g., at a bend or sudden area increase). Alternatively, the shock may be positioned by the program so that the stagnation pressure behind the shock is just equal to the desired back pressure.

The program performs various checks on the calculations to verify the stability of the computational procedure. For example, the program compares

---

[1]In continuum flow, the flow velocity is necessarily zero at the wall due to frictional forces. This deceleration of the flow results in an increase in the flow temperature near the wall. The flow temperature at the wall is termed the recovery temperature and is always somewhat less than the temperature that would result from decelerating the flow isentropically to zero velocity (i.e., the stagnation temperature) (Schlichting, 1960).

the computed results with results obtained using differential equations for selected flow parameters (Shapiro, 1953). In addition, the step size is selected small enough so that results are essentially independent of the step size. Typically, the initial step size is between one and two orders of magnitude smaller than the orifice diameter.

In order to estimate the internal wall temperature distribution of the probe tip, it is necessary to analyze the heat transfer between the tip and the external environment, sample gas, and cooling water. Heat transfer calculations were performed using TCAL, a computer program formulated at Pratt & Whitney Aircraft to evaluate the temperature distribution and heat fluxes in combustors, turbines, and other structural members in gas turbine engines. In the program, a finite difference representation of the heat conduction equation (a time-dependent version of Laplace's equation) is solved by a relaxation technique. The inputs to the program include a description of both the geometry and material properties for the hardware being analyzed, the properties of fluids around the hardware, and the heat generated on the surface or within the device. Optional boundary conditions include time dependent surface and internal heat generation. Material properties are permitted to vary with temperature and boundary temperatures are allowed to vary with time.

III.B.2a. Sudden Expansion Losses

The computer program (probe design deck) used in this study for analysis and design of gas sampling probes assumes that the gas flow is one-dimensional. It, furthermore, requires that the flow within the probe be attached to the probe walls; flow separation is not modeled. In the case of probes designed to operate with a choked orifice followed by a supersonic expansion, this requirement is usually satisfied. If this type of probe is operated unchoked, then it is probable that the subsonic flow within the expanding probe tip will separate from the probe walls due to the high divergence angle of these walls. Detailed analysis of the boundary layer accompanying subsonic flow in the tip of one the large probes used in this study revealed that the subsonic flow is indeed separated. Furthermore, it was demonstrated experimentally that for probe operation at high back pressure (>1/2 external pressure) the probe orifice was unchoked. Consequently, the following procedure was included to account for the pressure loss associated with separated internal flow.

During the process of diffusing a subsonic flow, frictional forces and the adverse pressure gradient may be sufficient to dissipate the forward momentum of the flow, i.e., the flow will separate. Practical subsonic diffusers limit the wall angle of the device to a few degrees. Wall angles greater than this limit (such as encountered with flows over rearward facing steps or with flows in probes with short, high area ratio tips) tend to cause flow separation. The loss in stagnation pressure due to flow separation is termed the sudden expansion loss.

The sudden expansion loss may be calculated by assuming that the static pressure in the separated region is equal to the (unknown) static pressure at station 2 (see Fig. III-1). Thus, for one-dimensional flow, the continuity and momentum equations may be applied to the control volume shown in Fig. III-1 (dashed line). After some manipulation, the system of equations becomes:

$$\frac{P_{T_2}}{P_{T_1}} = \frac{\left(\frac{f}{P_T}\right)_1 + \left(\frac{P}{P_T}\right)_1 \left(\frac{A_2}{A_1} - 1\right)}{\frac{A_2}{A_1} \left(\frac{f}{P_T}\right)_2} \qquad \text{(III-33)}$$

$$\frac{P_{T_2}}{P_{T_1}} = \frac{(A/A^*)_2}{\frac{A_2}{A_1} (A/A^*)_1} \qquad \text{(III-34)}$$

where $f = P(1 + \gamma M^2)$ and represents the stream thrust per unit area. A is the flow area, M, the Mach number, P, the static pressure, P_T, the stagnation pressure, and γ, the ratio of specific heats. A^* is the area at the throat and the subscripts 1 and 2 refer to the upstream and downstream conditions, respectively. Writing Equations III-33 and 34 in terms of the Mach numbers, M_1 and M_2, and the area ratio, A_2/A_1, and solving the equations simultaneously yields an equation which may be solved explicitly for M_2. Then, the pressure ratio, P_{T2}/P_{T1}, may be calculated from either Equation III-33 or 34. The sudden expansion loss is $1 - P_{T2}/P_{T1}$. It is, of course, assumed that the initial conditions (M_1, P_1) and the points of flow separation and reattachment (which defines A_2/A_1) are known to sufficient accuracy.

III.B.2b. Aerodynamic Quench

From extensive use of the computer program, some qualitative features on the operation and design of 'aeroquench' probes have been obtained. These facts are reviewed here along with a more detailed description of the phenomena of aerodynamic cooling.

FIG. III-1

MODEL FOR CALCULATING SUDDEN EXPANSION LOSS

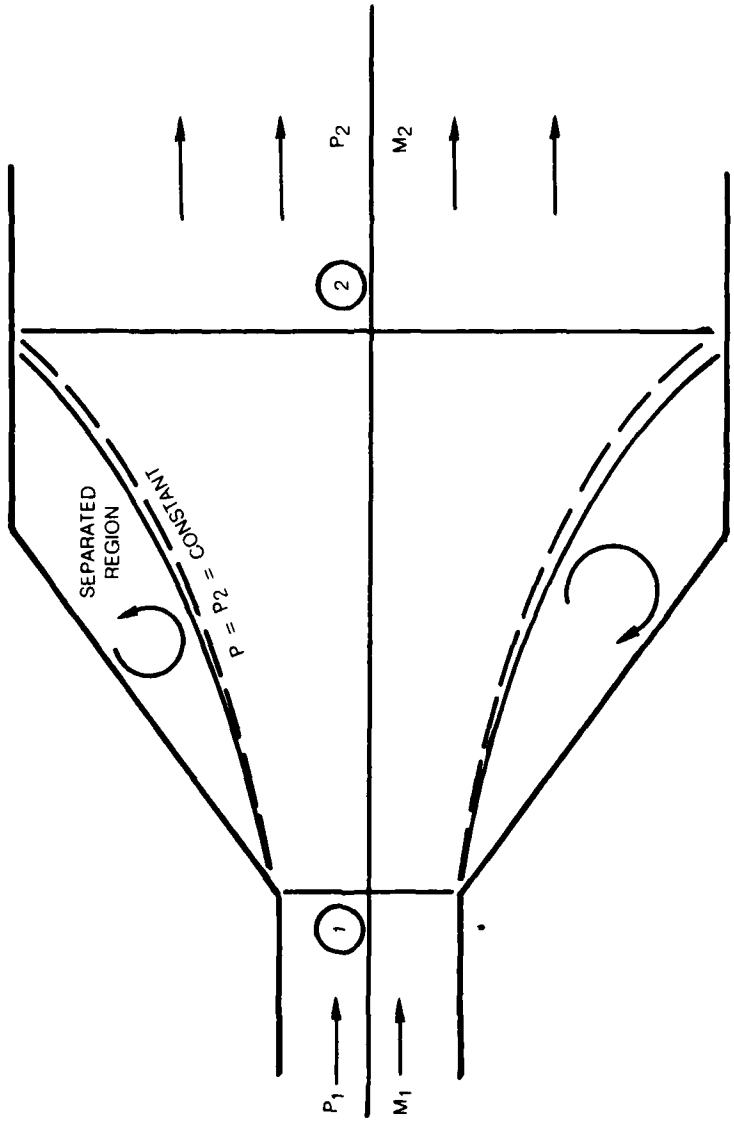

79-10-85-24

An aerodynamic quench in a sampling probe is accomplished by reducing the static temperature to some level determined from the kinetic rates and maintaining it at this level until the stagnation temperature of the gas is also reduced to near this level. The reduction of the static temperature is achieved by accelerating the flow to a high supersonic Mach number. During this process, the random kinetic energy in the gas is converted to directed translational energy and, hence, a net cooling of gas occurs. The reduction of the stagnation temperature is achieved via heat transfer to cooled walls of the probe. (The stagnation temperature is the temperature the gas will reach if decelerated adiabatically to zero velocity.) This heat transfer to the walls is of prime importance since without it the gas would eventually shock heat during its recovery to subsonic flow conditions and return to temperatures approaching the original flame conditions. Since an aerodynamic quench is obtained by accelerating the flow, a significant stagnation pressure loss results due to friction. Therefore, whether an aerodynamic quench can be achieved is highly dependent upon the pumping system used with the probe. The pumping system sets the back pressure which is the maximum pressure behind the shock system that terminates the supersonic portion of the flow.

In a probe designed to quench aerodynamically, the flow is accelerated from a Mach number of unity at the orifice to a high supersonic Mach number via the area expansion in the probe tip. This expansion must be large enough to achieve the reduction in static temperature required yet not so large as to cause friction to reduce the stagnation pressure below that achievable by the pumping system. Larger area ratios would increase the Mach number and consequently increase frictional losses. The flow then enters the constant area section where the stagnation temperature is reduced by heat transfer. Some heat transfer also occurs in the tip but is generally only a small part of the total heat transfer because the residence time of the flow is short in this region. In the constant area portion, both the stagnation pressure and the supersonic Mach number of the flow are reduced due to friction. If calculations indicate that the Mach number is reduced to unity in the constant area section, either a shock must instead occur at some upstream location where the shock may be stabilized or the flow in the probe is subsonic throughout. In either case, no aerodynamic quench is possible. The constant area section must terminate prior to the occurrence of choking but only after the desired reduction in stagnation temperature is achieved. This section is generally terminated by a sudden expansion to stabilize a shock system that reduces the Mach number to a subsonic value. The expansion must be large enough to result in a relatively low Mach number so that additional stagnation pressure losses are small; otherwise, the flow will choke in the subsonic portion of the probe. It is important to note that the probe must not contain a bend prior to the desired shock system location.

III.C Design of Probes

Using the above assumptions for the probe model and experimental conditions, two sets of probes were designed. One set was designed for sampling over the flat flame burner, while the other was designed for sampling exhaust from the IFRF burner or the FT12 combustor. In these design studies, the primary design criteria was to reduce the gas temperature below 1000 K within one millisecond (see Section III.B.1.a). Furthermore, it was assumed that the back pressure was 0.35 atmospheres (266 torr), a pressure that should be easily achievable for most sampling systems. A special effort was made to develop a probe design for which true aerodynamic quenching would be expected.

III.C.1 Probes for Combustor Measurements

For sampling the exhaust of the IFRF burner and the FT12 combustor, two water-cooled probes were designed: one for cooling by expansion and the other quenched by convection. These probes are denoted the reference probe and EPA probe respectively and drawings of these probes are depicted in Fig. III-2. As apparent from this figure, pressure taps and thermocouples have been located in these probes to facilitate comparison of experimental and computed data. Externally, both probes are identical and photographs of the reference probe with its water-cooled mount are shown in Figs. III-3 and III-4. Due to their size, they have been denoted macroprobes. They were each designed to enter from a side window of the combustor but with a right angle bend to face the oncoming flow. The probes are sufficiently long so that they could traverse across the internal dimension of the combustor along the optical path.

The geometry of the reference probe with two sections of constant area follows the guidelines described earlier (Section III.B.2b) for a probe that quenches by expansion. As will be apparent, the second expansion has been located far enough downstream so that the recovery shock returns the gas to temperatures near 1000 K when the initial gas temperature is 1800 K. Also observe that the tip has been carefully contoured to minimize the possibility of coalescence of compression waves (i.e., shock waves) by providing a smooth transition at the junction of the tip and the first constant area section. It is very important to note that even with this ideal design, aerodynamic quenching could not be achieved (based on computer program prediction) unless the back pressure was reduced to below 7 percent ($\sim$ 50 torr) of the ambient flame pressure which in this case was atmospheric pressure. This pressure was much lower than the desired operating pressure of 0.35 atmospheres and, as described in the experimental section, creates some special sampling problems.

A calculated profile showing the static temperature and pressure and the total temperature vs. time is shown in Fig. III-5 for assumed flame temperatures of 1800 and 1400 K. In the case of the higher temperature, internal positions from the probe tip are also provided. Although these curves indicate that the static temperature rapidly decreases to below 1000 K (in less

FIG. III-2

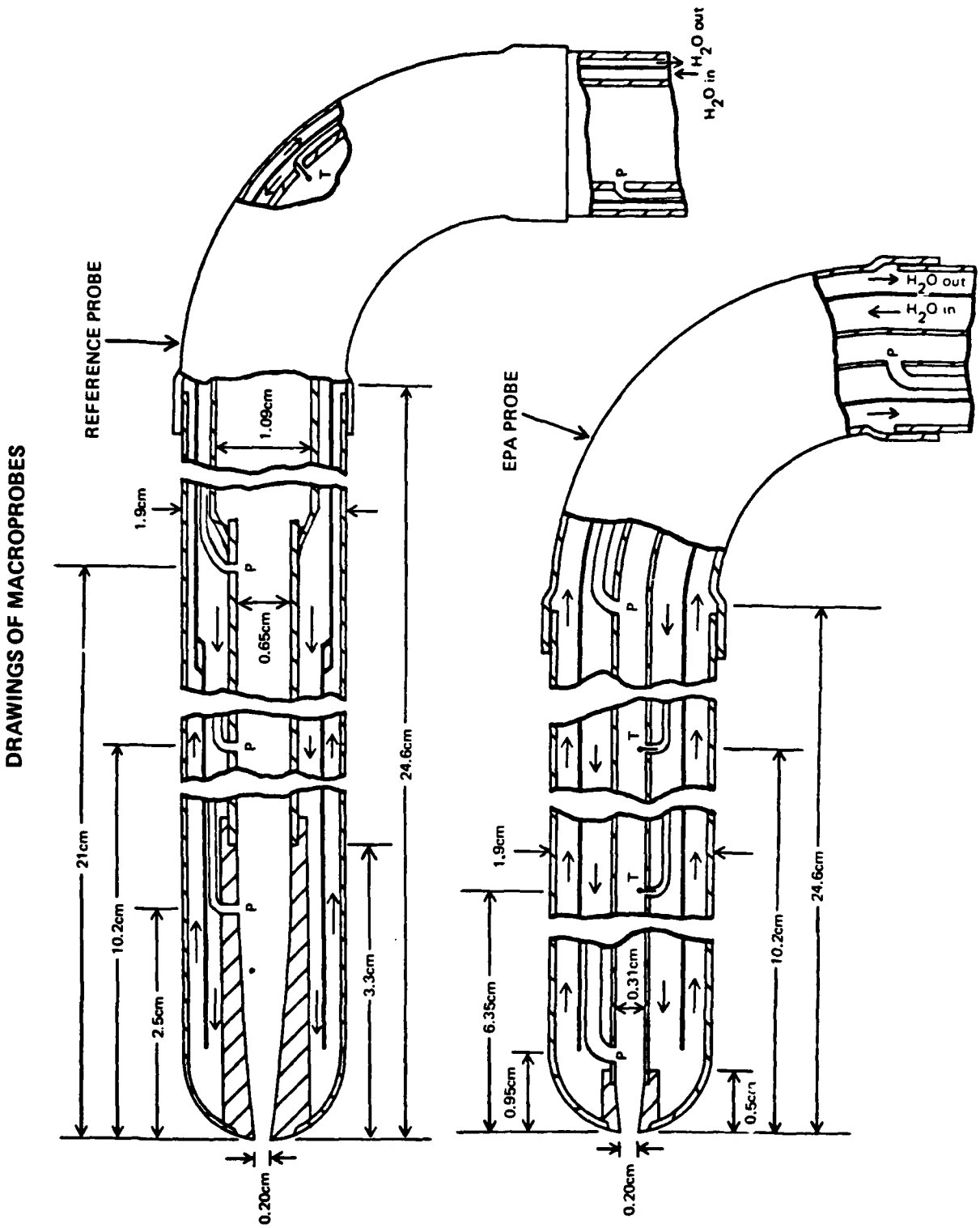

79-10-85-23

REFERENCE PROBE

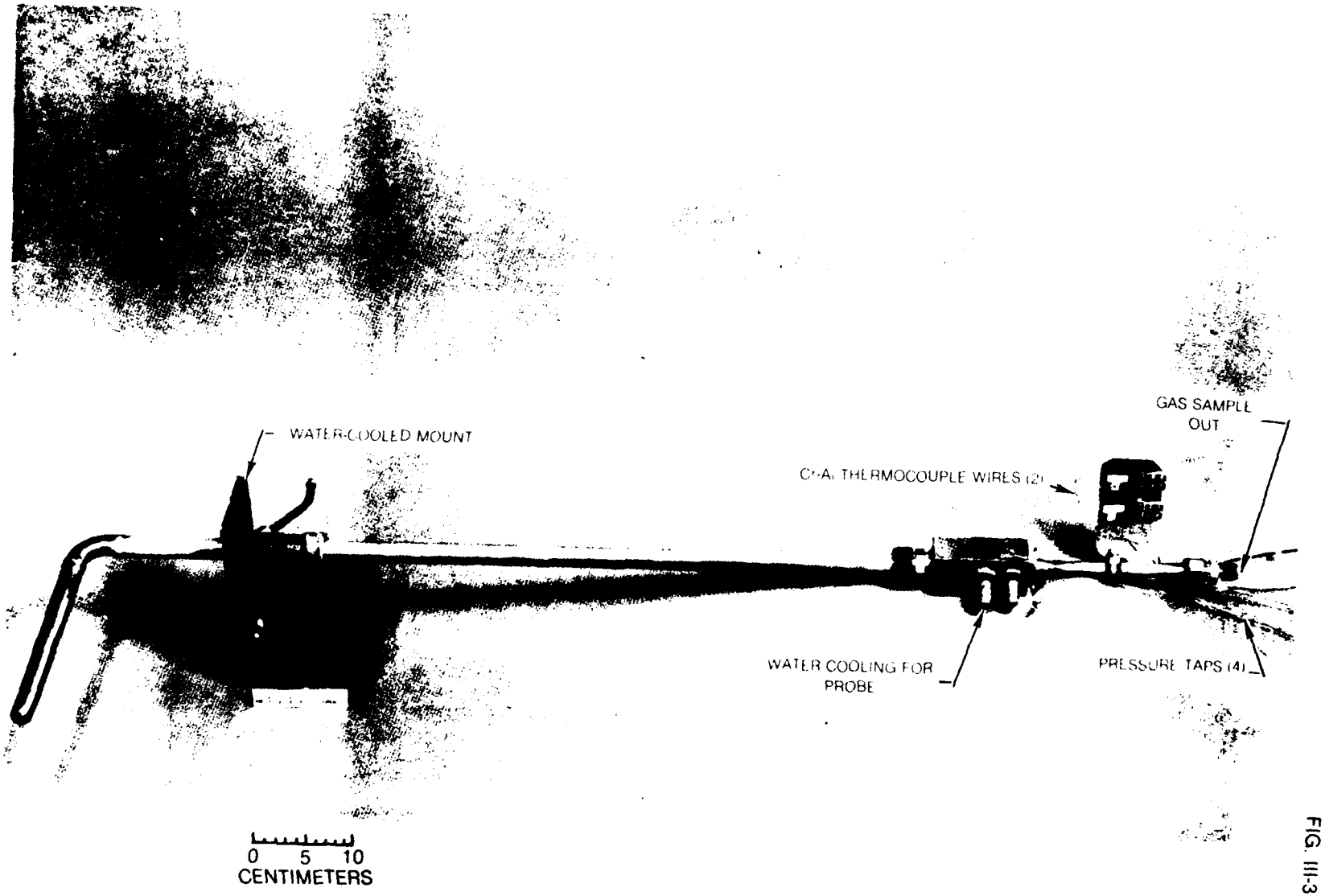

FIG. III-3

79-10-85-1

TIP OF REFERENCE PROBE

FIG. III-4

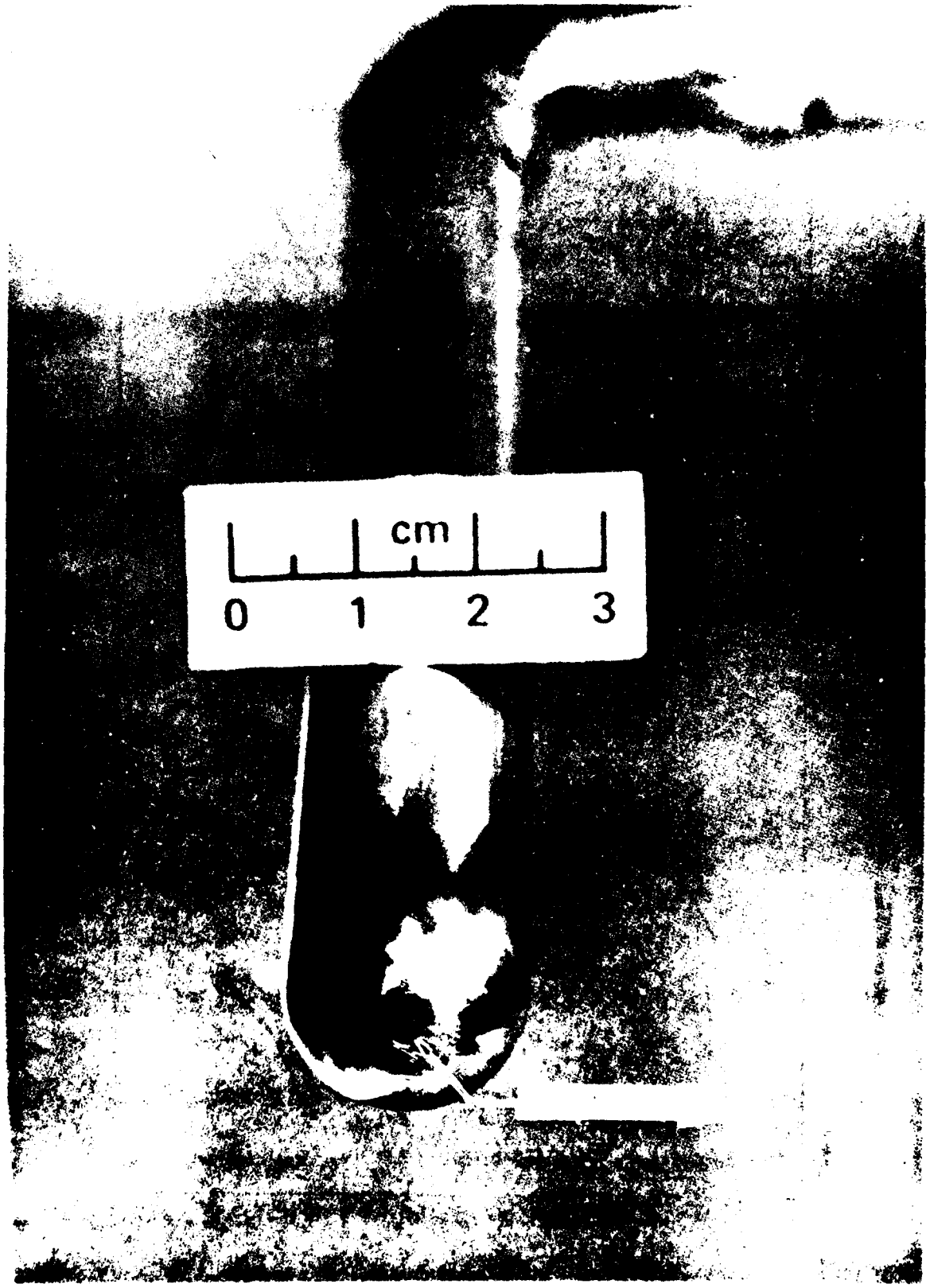

79 10 85-2

CALCULATED TEMPERATURE AND PRESSURE PROFILES FOR REFERENCE PROBE

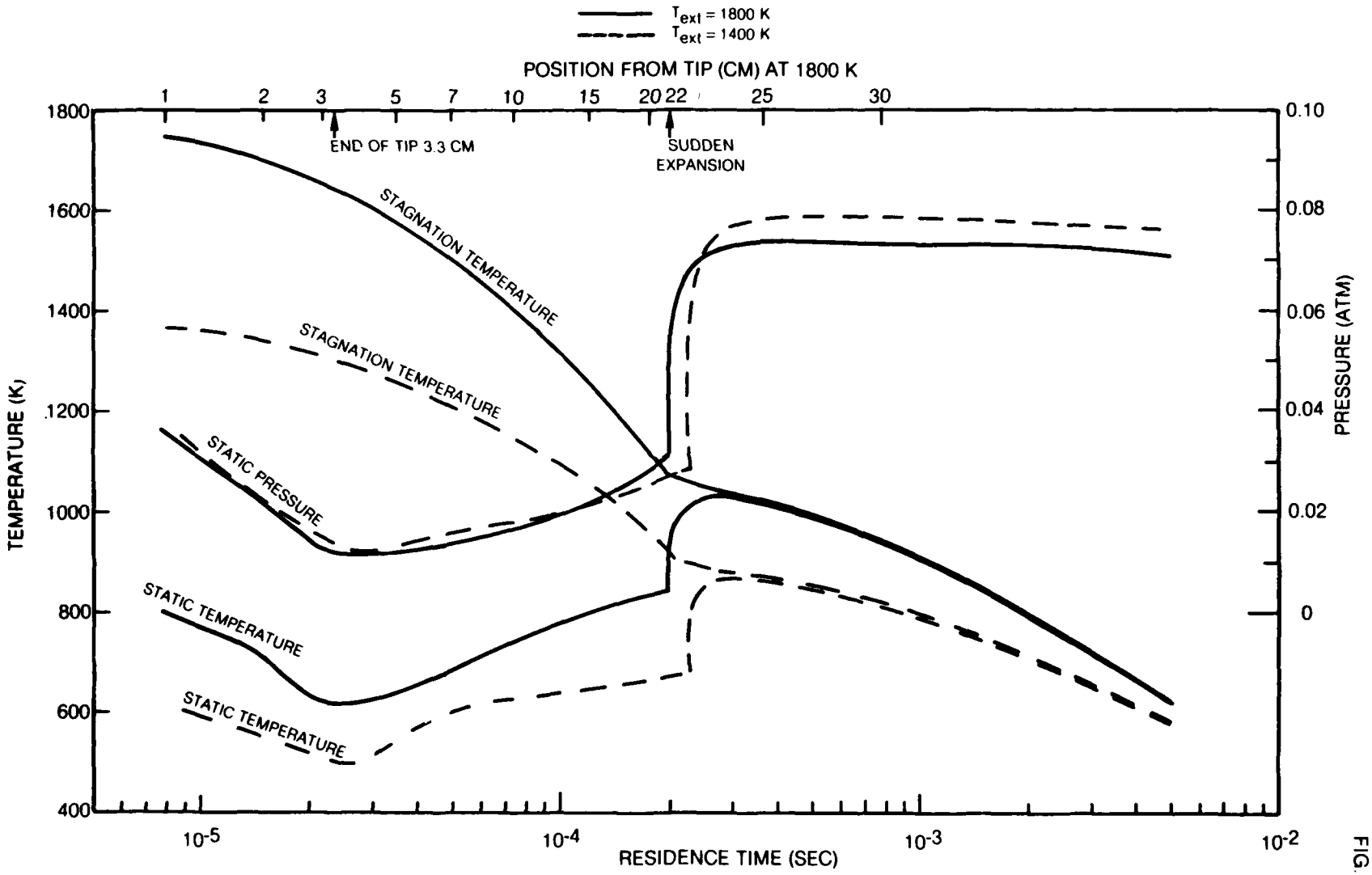

FIG. III-5

79-10-65-21

than 10 microseconds), the total temperature is still high and does not fall below this level until about 1/2 millisecond for 1800 K inlet temperatures. The two primary features in the static temperature curves are the minimum at about 25 microseconds indicating the termination of the divergence in the tip and the rapid rise due to shock recovery at about 200 microseconds.

Calculated cooling curves for the EPA probe which cools primarily by convection are shown in Fig. III-6 for the two assumed inlet temperatures, 1400 and 1800 K. For these profiles a back pressure in the probe was assumed to be 0.35 atmospheres (266 torr). According to these calculated curves, the static temperature (nearly equivalent to total temperature for subsonic flow) reduces to below 1000 K in approximately 0.3 milliseconds. For comparison, calculated data from the reference probe when operated at the same back pressure is presented. In this case, the reference probe cools by convection. This probe which was designed to achieve an aerodynamic quench is clearly relatively poor at cooling by convection since the static temperature does not reach 1000 K until 2.3 milliseconds, a difference of nearly one order of magnitude from the EPA probe. The inflection near this location is due to the area change at 22 centimeters from the tip.

For both probes, when cooling by convection, it may be noted that the program indicates the existence of a normal shock within a centimeter of the tip orifice. In each case, temperature recovery occurs within several microseconds and returns the gas from less than 1000 K to within approximately 100 K of the original gas temperature. It is this operating mode that is probably typical of most probes previously believed to be aerodynamically quenched. The probe is indeed choked, the gas flows supersonically for a period, and the initial quenching rates are rapid with temperatures falling below 1000 K; however, a shock system quickly forces the gas to the elevated temperatures and the initial quenching, although real, is only temporary. Further examination of the EPA probe design with the computer program indicated that no back pressure existed for which the shock system could be pulled into the constant area section and produce an aerodynamic quench. The difficulty was not due to the small discontinuity in the slope at the end of the tip but rather due to excessive friction and pressure losses in the probe.

III.C.2 Probes for the Flat Flame Burner

Several probes were selected for sampling over an atmospheric $CH_4/O_2/N_2$ flat flame. The orifice diameter for these probes (miniprobes) was selected to be 0.025 inches (635 microns) which was large relative to the quartz microprobes used in the first phase of this program but was necessary to supply the mass flow required by the analytical instrumentation. Using this orifice diameter and assumed flame conditions of 2000 K and one atmosphere, no practical geometry could be found over an experimentally realizable back pressure range for which an aerodynamic quench, as defined above, could be achieved. Consequently, all design efforts for these probes were focused at convection cooling below 1000 K and within one millisecond.

FIG. III-6

CALCULATED COOLING CURVES FOR MACROPROBES

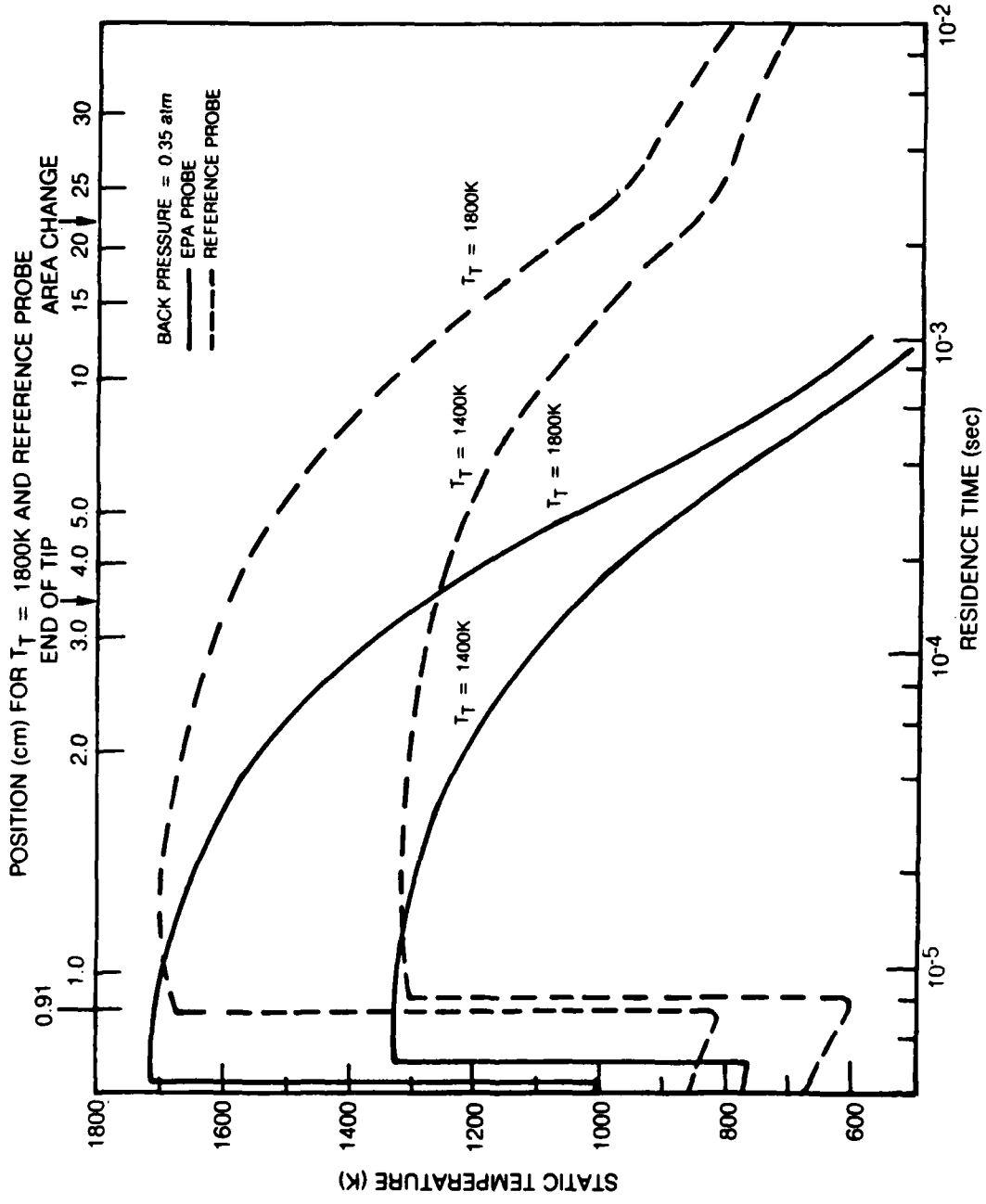

79-10-85-4

Designs of two water-cooled probes were selected for cooling by convection. One probe was entirely stainless-steel. The computer calculations, however, indicated that the wall temperature of this probe was reduced to only about 750 K at the location for which the gas residence time was approximately 10 microseconds. This temperature was not considered low enough to minimize wall reactions in the probe tip. In order to satisfy this quenching criterion, a copper tipped, water-cooled probe but which is otherwise identical to the stainless steel probe was also constructed. Calculations for the copper-tipped probe indicated not only that the wall temperature fell to around 500 K within a gas residence time of 10 μsec but also that the initial cooling rate of the gas was significantly faster. A relatively blunt tip does offer an alternative to the change in material, but this was not considered feasible since such a probe could significantly perturb the flame and since flow separation at the entrance of the tip (due to the large angle) was considered to be very likely. A catalytic surface effect due to the copper was considered possible but believed to be negligible because of the short residence time in the tip. A drawing and photograph of the stainless-steel probe are shown in Figs. III-7 and III-8 respectively. The third, water-cooled probe was constructed completely of quartz. Its design was similar to the quartz microprobe used in Task I of this study (Dodge, et al., 1979), however, the orifice was enlarged to 635 microns by shortening the tip (see, for example, the description by Fristrom and Westenberg (1965)). For comparison, an uncooled stainless-steel probe was constructed which, except for a smaller outside diameter (0.635 cm) and no cooling passages, was geometrically identical to the other metallic probes.

Model predictions for the copper tipped and stainless-steel tipped probes are compared in Fig. III-9. The positions apply to the stainless-steel probe although they also approximate the positions for the copper tipped probe. Clearly, there is little difference between the calculated cooling curves for these probes after approximately one millisecond of residence time; however, the initial cooling rates are sufficiently faster with the copper tip so that at residence times less than 200 microseconds, gas temperatures are nearly 150 K cooler. Note that for both of these probes, the gas flow chokes at the tip, accelerates supersonically and then shock heats within one centimeter of the probe orifice.

The effect of back pressure on temperature profiles and cooling rates was also examined. Model predictions for the copper-tipped probe at two back pressures, 0.35 and 0.167 atm (266 and 127 torr, respectively), are shown in Figure III-10. It is clear that at the lower back pressure the recovery shock occurs later in time and at a cooler static temperature, the static temperature returns to temperatures 100 K lower than those at the higher back pressure, and the total temperature (nearly the same as the static temperature under subsonic flow) reduces to below 1000 K in about 140 microseconds, approximately half the time required at the higher pressure. In addition, a 50% drop in the back pressure provides another advantage to quenching since the rates of bimolecular reactions are dropped by a factor of four, and even unimolecular reaction rates slow by a factor of two.

FIG. III-7

DRAWING OF MINIPROBE

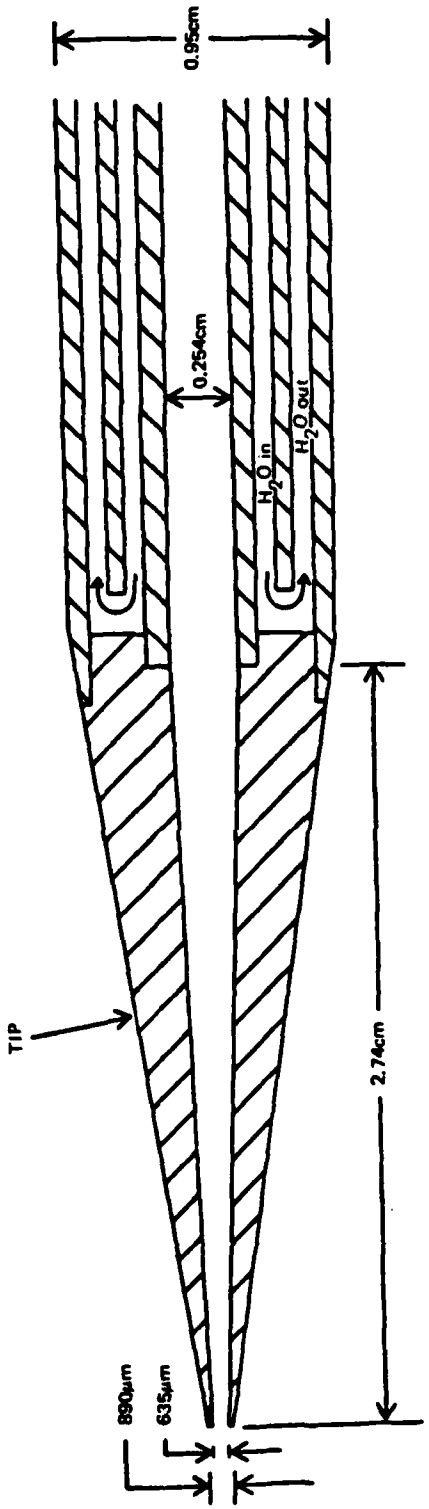

79-10-85-22

STAINLESS STEEL TIPPED MINIPROBE

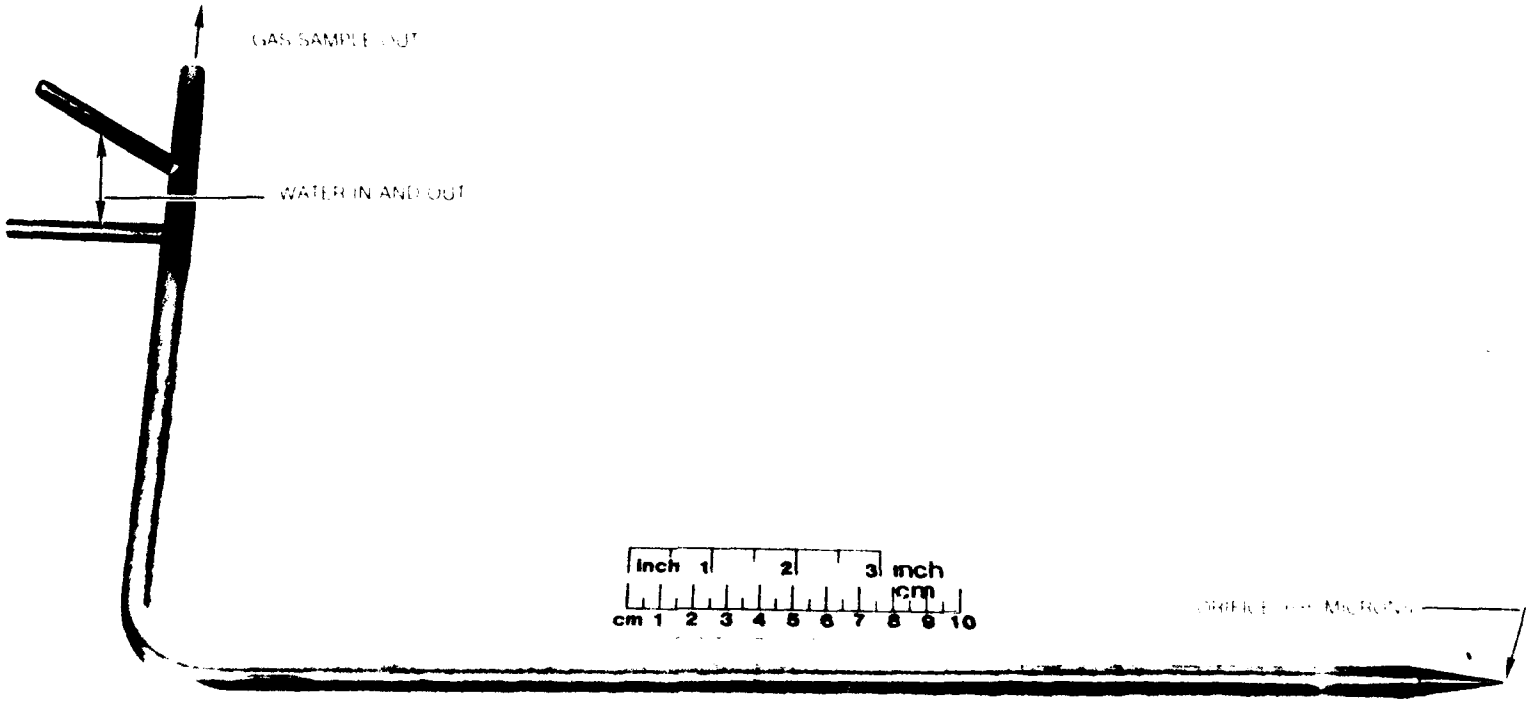

FIG. III-8

79-10-85-3

CALCULATED COOLING CURVES FOR MINIPROBES

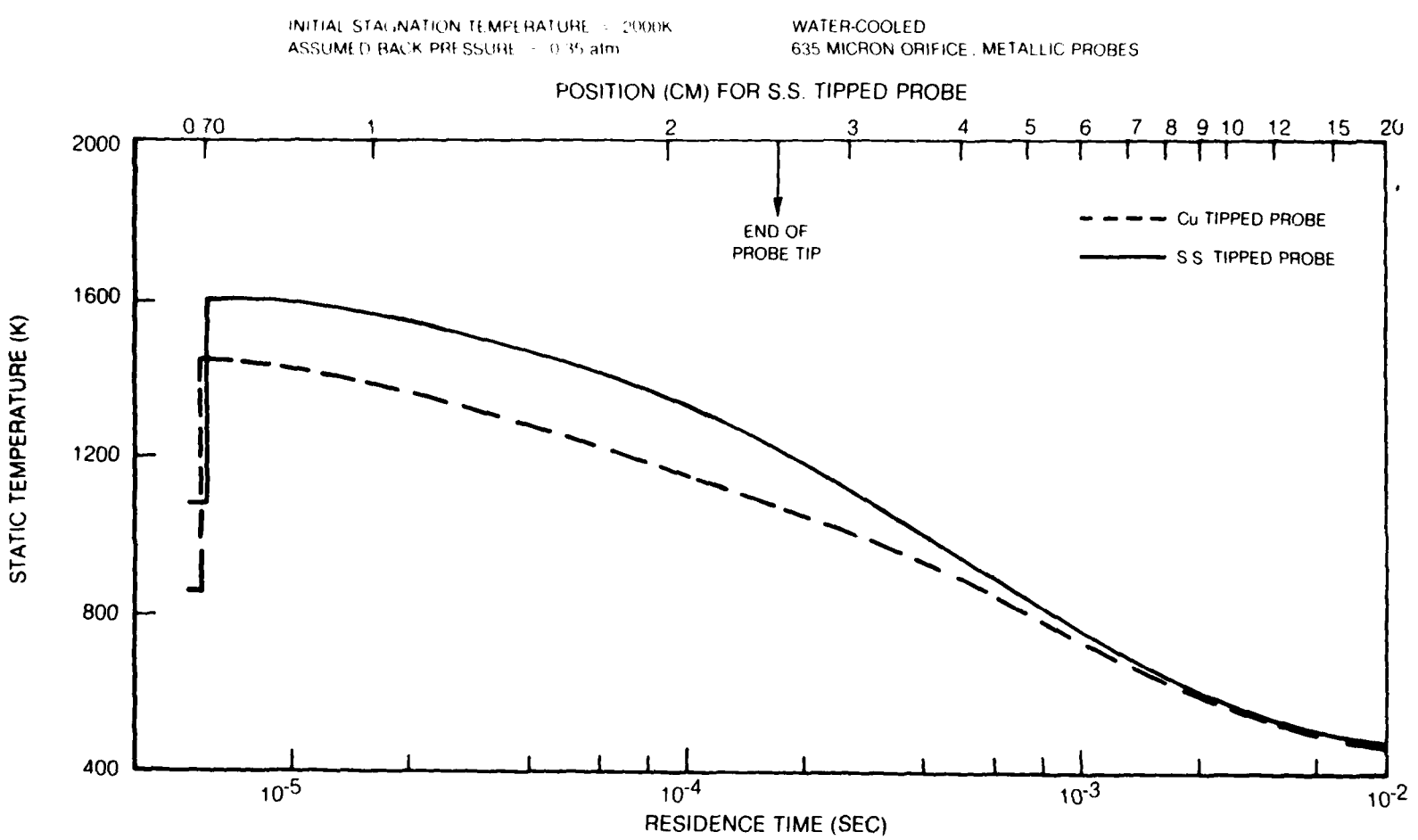

FIG. III-9

79-10-85-5

CALCULATED COOLING CURVES FOR MINIPROBES AT VARYING BACK PRESSURE

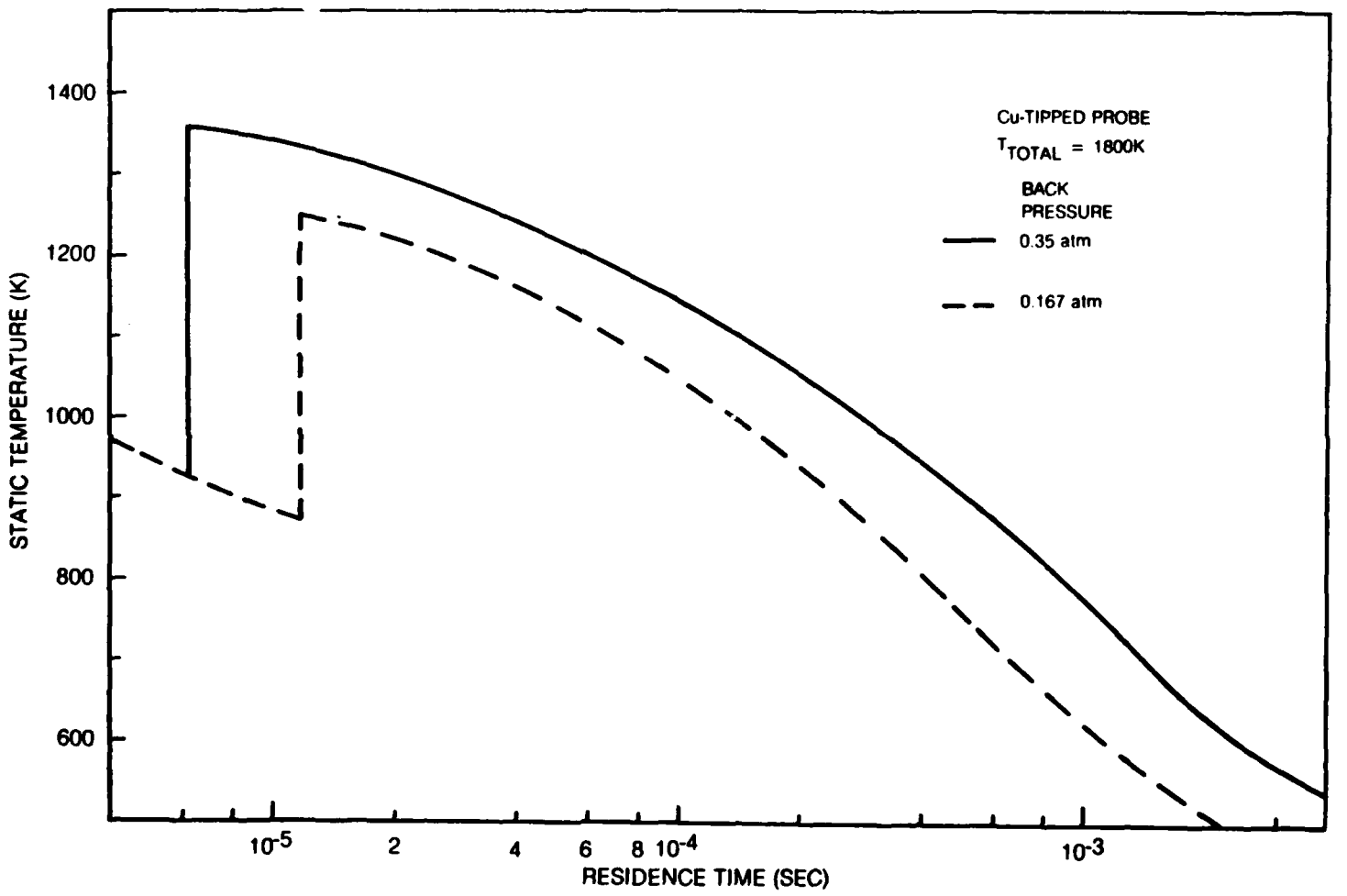

FIG. III-10

79-10-85-5

Detailed calculations were not performed for the quartz probe or the uncooled probe. The primary differences for these probes will of course be surface material for the former and, for the latter, surface material at elevated temperatures and lack of rapid cooling (some cooling is expected since the probe itself will radiatively and conductively cool and this cooling in turn is passed onto the gas via conduction).

III.C.2a Microprobe

In the course of analyzing the behavior of probes, quartz microprobes were also examined since they had been used in the first part of this program. These calculations using the current version of the UTRC Probe Analysis computer program indicate that supersonic flow cannot be sustained within the tip region of so-called "microprobes". Since supersonic flow can be maintained in larger probes (if the back pressure is set at a prescribed level), it is desirable to explain the differences in the flow characteristics within each type of probe in terms of the physical dimensions of the probes.

For a constant property flow, it can be shown that the local Mach number varies according to:

$$\frac{dM^2}{M^2} \frac{1 - M^2}{1 + \frac{\gamma - 1}{2} M^2} = -2 \frac{dA}{A} + (1 + \gamma M^2) \frac{dT_o}{T_o} + \gamma M^2 \, 4f \frac{dx}{D} \qquad \text{(III-35)}$$

where M is the local Mach number, A, the area, γ, the ratio of specific heats; T_o, the stagnation temperature; f, the skin friction coefficient, x, the distance from the probe orifice, and D, the internal diameter.

Since this relationship holds for a flow passage of any size, the difference between flows within small and large probes must lie in the relative contribution of each term (area change, heat transfer, friction). For a supersonic flow ($M > 1$) within a passage of increasing area ($dA > 0$) and with cooling ($dT_o < 0$), the Mach number will increase if the absolute value of the area change and heat transfer terms in Eq. (III-35) exceed the frictional contribution; the Mach number will decrease if the opposite is true.

For example, consider the following case for both a micro-and macroprobe. Assume that the probes are used to sample a flow whose stagnation pressure and temperature are one atmosphere and 2000 K, respectively. Assume that the flow is choked at the entrance of a probe whose tip is a conical section with a half-angle of 7 degrees.

For a microprobe, assume that the initial probe sample passage diameter is 0.01 cm (4 mils). It can be shown that the flow accelerates initially (even in the absence of heat transfer). The Mach number reaches a peak value of 1.71

at 0.015 cm from the tip and thereafter decelerates to unity (chokes) at 0.167 cm. This second choke point is unrealistic and indicates that instead a shock must occur near the tip or that subsonic flow must exist throughout. The reversal of the Mach number change is explained by noting that the flow in this case is laminar. It can be shown for such a flow that as the distance from the orifice increases, both the area change and heat transfer terms decrease and the frictional term remains approximately constant. Thus, the friction term eventually dominates the change in the Mach number equation.

For a macroprobe, assume that the initial diameter is 0.2 cm (0.079 in.) which is identical to the orifice of the macroprobes in this study. In this case, the flow within the probe is turbulent. It can be shown for fully developed turbulent flow that all contributions to the change in Mach number decreases as the diameter of the passage increases. Calculations indicate that friction effects eventually dominate (as they do in the laminar case) and can choke the flow under the right circumstances; however, the distance to the choke point may be long enough to provide sufficient length to achieve an aerodynamic quench. Choking is avoided by encouraging the formation of a normal shock (such as by a sudden expansion) and slowing to a low subsonic Mach number. Consequently, the rate of frictional losses is drastically reduced.

Thus, in either case, the friction contribution eventually dominates the variation in Mach number. If supersonic flow exists within a microprobe, it cannot be sustained for any useful length; rather a normal shock must exist very near the probe tip and a low subsonic Mach number must exist thereafter. This unrealistic shock location (within a few orifice diameters of the tip) together with the fact that boundary layer growth has been ignored, lead to the conclusion that supersonic flow is not likely within a microprobe. Boundary layer growth is less important in a macroprobe, and the required shock location is more realistic. Thus, supersonic flow can exist within a macroprobe.

IV. EXPERIMENTAL RESULTS

The objectives of the experimental measurements on the three combustors were two fold. First of all, probe measurements of seeded nitric oxide would be made, compared with expected concentrations, and causes for any existing discrepancies between the various probe measurements and/or the expected concentrations analyzed. Secondly, sufficient probe data (specifically, concentration and temperature profiles) must be obtained so that subsequent optical measurements can be properly interpreted. These measurements along with experimental data on probe behavior are presented in this chapter.

IV.A. Flat Flame Burner

Three flame stoichiometries, $\phi = 0.8$, 1.0, and 1.2, were examined and the run conditions are listed in Table II-A. With the nitrogen purge passing through the optical ports, vertical and horizontal temperature profiles were obtained. A typical horizontal profile (for $\phi = 0.8$) is shown in Fig. IV-1. These measurements are corrected for radiation losses as outlined in Task I Report by Dodge, et al. (1979) and were obtained along the optical axis. The burner surface was located 2 centimeters below this axis while the visible flame sheet was a few millimeters above the burner surface. Estimates of uncertainties in the radiation corrections and individual and repeated measurements are indicated in the error bars. Vertical profiles of uncorrected thermocouple temperatures for the three flames are shown in Fig. IV-2. Since the optical beam is less than a centimeter in diameter and centered at 2 centimeters above the burner, the beam encompasses a region for which deviations (due to height) are less than $\pm$ 15K. As may be observed by comparing these two figures, radiation corrections are on the order of 140 K for these flames.

Measurements of stable species using the Scott Instrument package and the quartz, water-cooled probe (all water-cooled probes produced the same results within 10 percent) are reproduced in Table IV-A. Equilibrium data at the adiabatic flame temperature (Gordon and McBride, 1971) for the flat flames are also presented in this table for comparison. It may be noted that reasonable agreement is obtained between the measured and equilibrium values. Noticeable differences are observed for the CO and CO_2 concentrations. Although these differences may be due to interconversion within the probe, most of these differences may be explained by differences in actual and adiabatic flame temperatures and to incomplete combustion of carbon monoxide. Only in the case of the stoichiometric case ($\phi = 1.0$) is the measured total of the CO and CO_2 concentration significantly different from the equilibrium calculations ($\sim$ 8%). (Data on unburned hydrocarbons are not reported since their concentrations even in the fuel-rich flame were less than 1000 ppm.)

HORIZONTAL TEMPERATURE PROFILE OVER $CH_4/O_2/N_2$ FLAT FLAME

$\phi = 0.8$

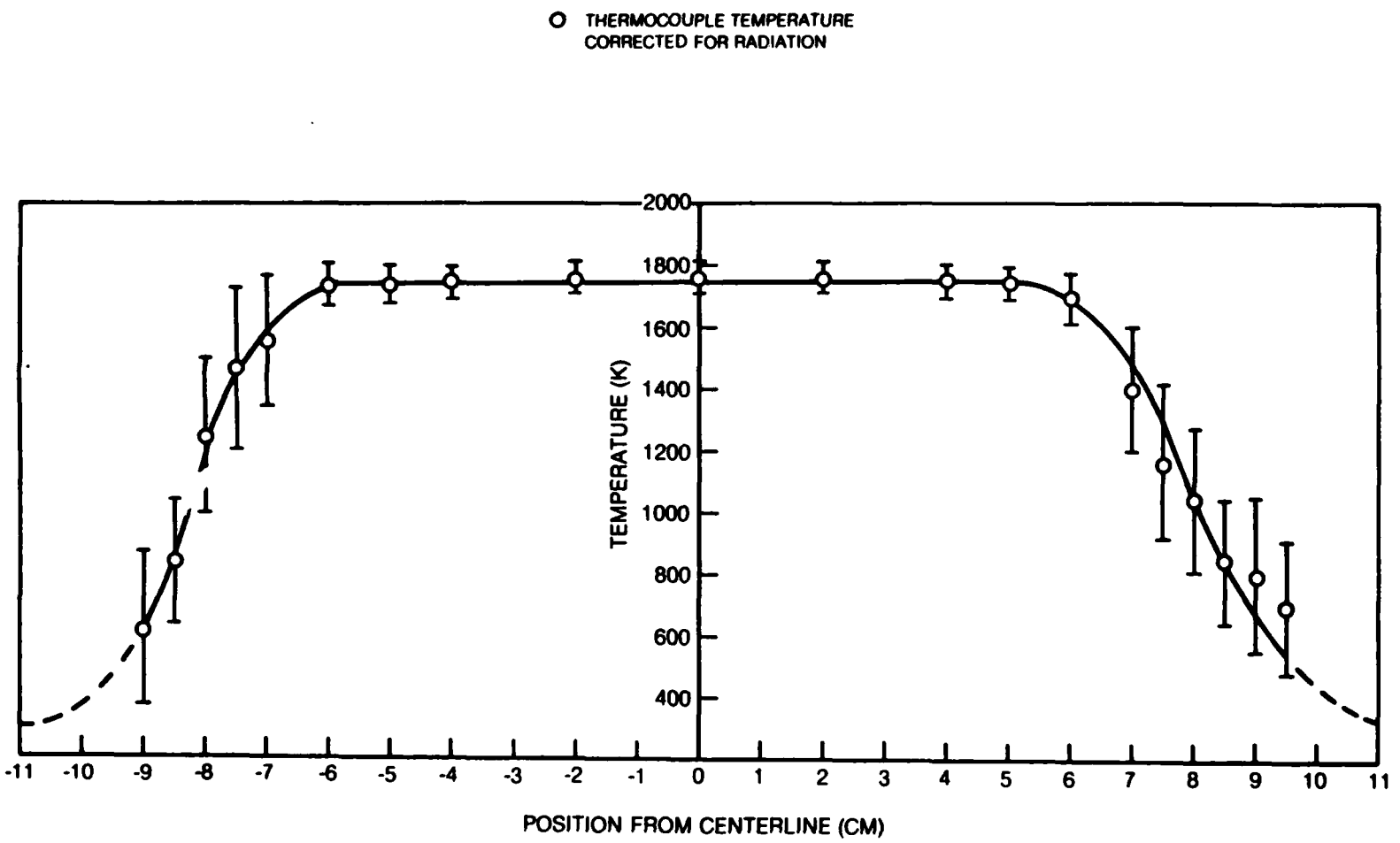

FIG. IV-1

FIG. IV-2

VERTICAL TEMPERATURE PROFILE OVER $CH_4/O_2/N_2$ FLAT FLAME

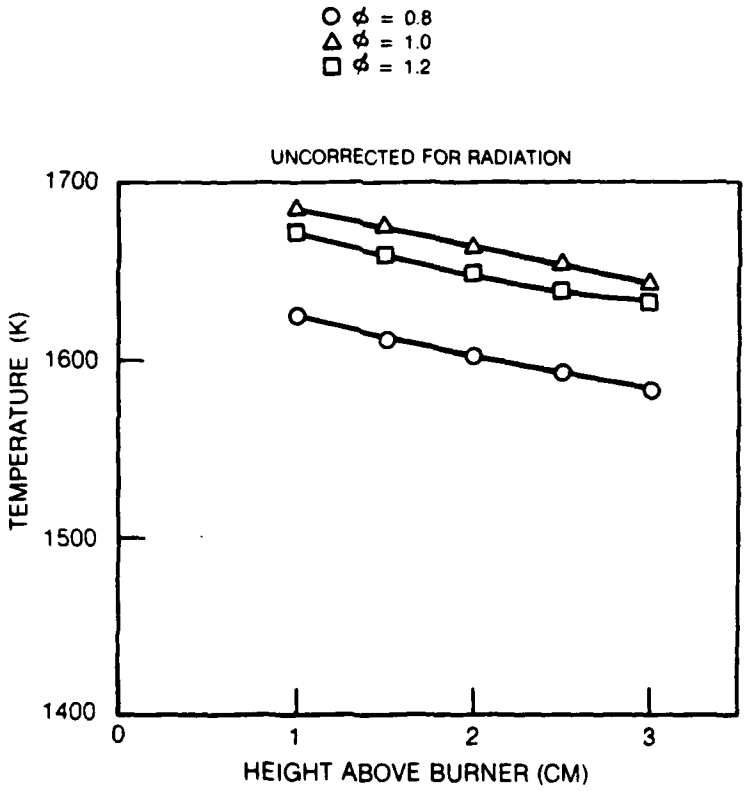

79-10-85-14

TABLE IV - A

MOLE PERCENT OF STABLE SPECIES FOR
THE FLAT FLAME BURNER
(Wet Basis)

Experimental

ϕ	O_2[1]	CO[1]	CO_2[1]	H_2O[2]	N_2[3]	Temp. (K)
0.8	3.2	.0137[4]	6.6	12.6	77.6	1740
1.0	0.2[4]	.064	6.55	14.1	78.7	1815
1.2	-	4.1	4.8	17.8	73.3	1800

Equilibrium[5]

ϕ	O_2	CO	CO_2	H_2O	N_2	Temp. (K)
0.8	3.15	0.0051	6.43	12.9	77.4	1765
1.0	0.13	0.109	7.09	14.3	78.1	1905
1.2	0.7ppm	3.60	5.50	15.7	72.6	1904

1. Measured values but corrected for the presence of water vapor.
2. Water estimated from known input conditions.
3. Nitrogen calculated by difference.
4. Error ± 40% of value.
5. Based on equilibrium flame temperature.

Except where noted, the uncertainity in the experimental concentrations is approximately ± 5% of reported (experimental) value.

Measured concentrations of nitric oxide were on the order of 5, 30, and 30 ppm for the three flames, respectively. These values at flame temperatures and for the given optical path length are much smaller than that necessary to produce a reasonable signal-to-noise ratio for the optical measurements. Typically, concentrations of 700-1500 ppm are required for the UV resonant lamp measurements and even higher NO densities are required for the infrared gas correlation technique. Consequently, all subsequent studies were made using nitric oxide premixed with the inlet gases.

Using the stainless steel tipped, water-cooled probe and the TECO CLA, nitric oxide horizontal profiles were obtained for a given seed level. Profiles, normalized to the input seed level for the flames $\phi = 0.8$ and $\phi = 1.2$ are shown in Fig. IV-3. Data for the $\phi = 1.0$ flame is nearly identical to the data for the $\phi = 0.8$ flame except the centerline fraction is slightly higher (~ 0.88) for an NO seed level of 840 and 980 ppm calculated on a wet and dry basis, respectively. For the lean flame, NO_x values were typically 5 to 7 percent higher than the NO and, for the stoichiometric and rich flames, they were about 3 percent higher than measured NO. The excellent repeatability of the burner and sampling conditions is indicated by the double set of points on the right-hand side of this figure.

Vertical profiles for the three flames and the three water-cooled probes are reproduced in Fig. IV-4. (Note, the data in this figure are not normalized.) Agreement between these profiles is generally quite good (within 6%) except for relatively low values obtained by the stainless steel tipped probe when sampling the rich flame. Since the front part of this tip (~ 1 cm) becomes very hot (with a red-orange glow), it is believed that catalytic reactions take place similar to those occurring in an NO_2 to NO converter. This conclusion is consistent with the computed results from TCAL indicating that the stainless steel tip is insufficiently cooled. Although residence times in this portion of the probe are very short ($\ll 1$ msec), the wall temperatures very near the orifice are significantly hotter than in a stainless steel converter (1100 to 1200 K vs. 1000 K). The profile may be associated with the presence of hydrogen that would be expected to decrease with height above the flame. Although this mechanism was not verified, it seems highly likely considering the strong NO_x reducing effect that hydrogen has in hot stainless steel tubes (Benson and Samuelsen, 1976, 1977). The relatively low values obtained in the $\phi = 0.8$ flame for the copper-tipped probe are unexplained. Although this difference of 7 percent may be due to a catalytic effect of a copper surface, it is unclear why good agreement is found for the other flames. In any case, this difference is considered to be small.

From the above results, it is seen that the recovery of the nitric oxide seeded into the flame is not quantitative. At the seed concentrations, approximately 15, 12, and 38 percent of the initial NO was lost for the $\phi = 0.8$, 1.0, and 1.2 flames, respectively. Attention was directed to determining whether the loss occurred in the inlet gas lines (for the unburned/premixed gas), in the flame itself, or the probe/sampling system. Losses in the post-flame zone were believed to be unlikely since essentially flat vertical profiles were obtained (Fig. IV-4).

NORMALIZED NITRIC OXIDE PROFILES OVER $CH_4/O_2/N_2/NO$ FLAT FLAME

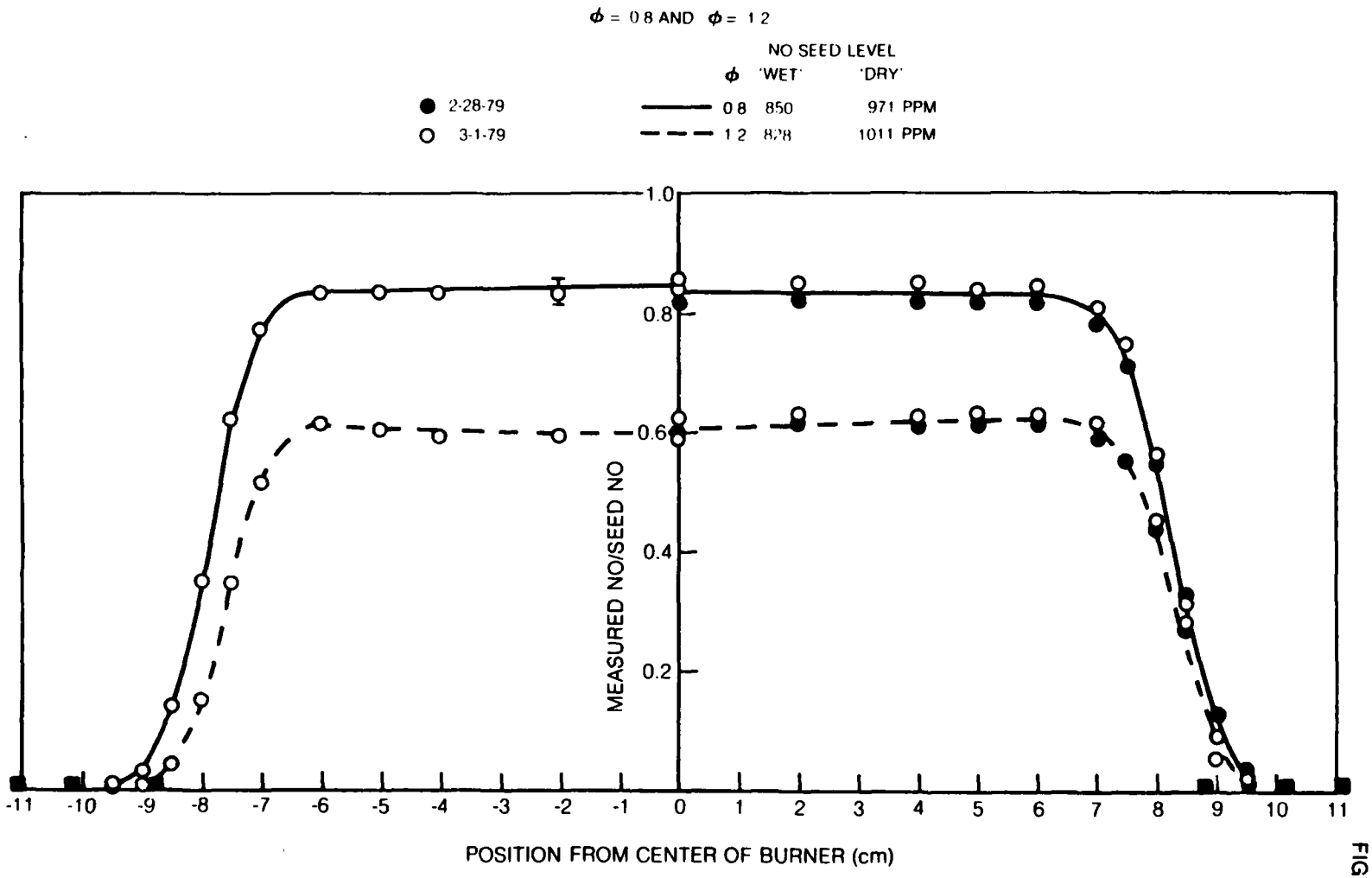

FIG. IV-3

79-10-85-12

FIG. IV-4

VERTICAL PROFILES OF NITRIC OXIDE OVER FLAT FLAME BURNER

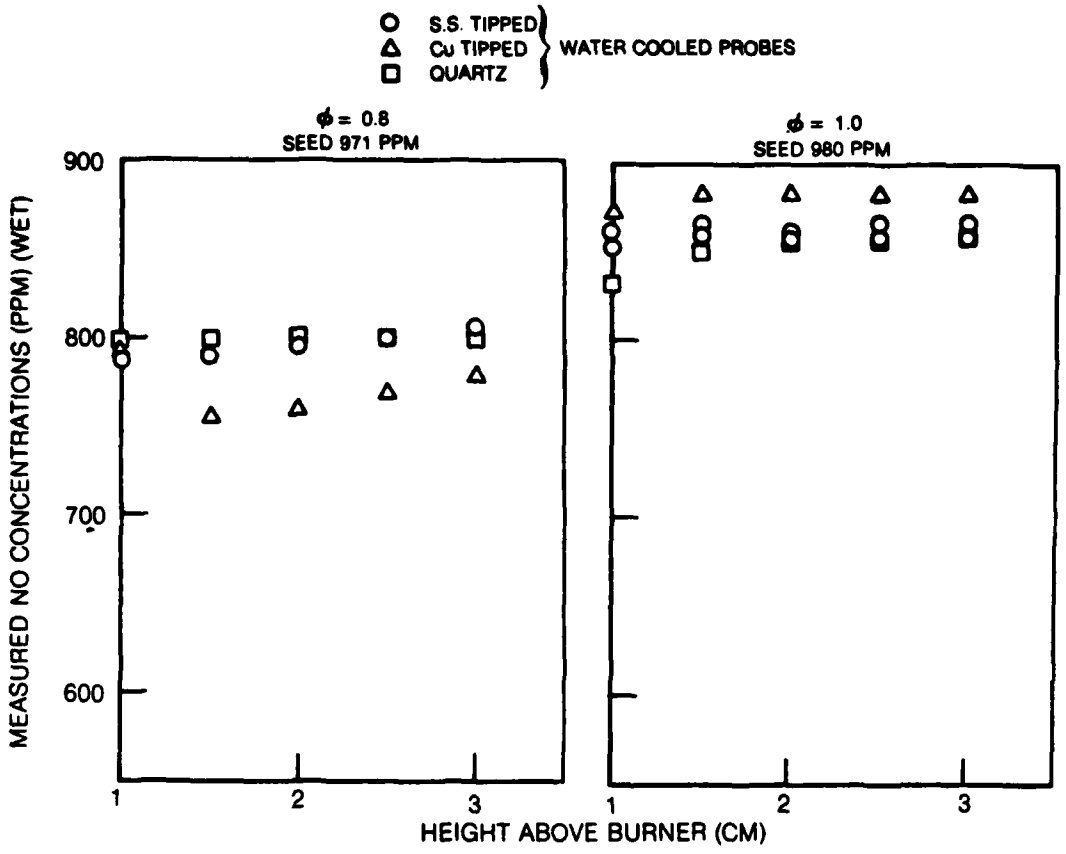

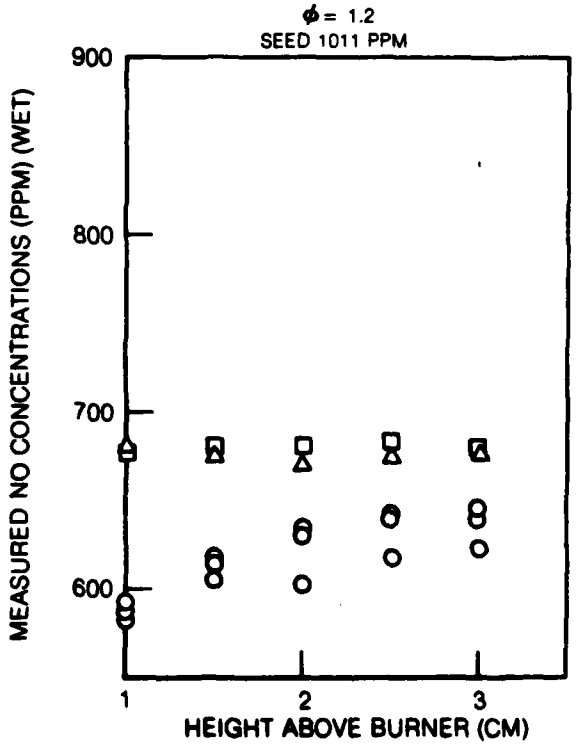

79-10-85-11

These loss figures can be slightly adjusted to account for phenomena associated with the flame and experimental apparatus. First of all, some NO_2 was present as indicated by NO_x readings, and, consequently, the percent losses can be decreased by 3 to 5 percent. Although it is uncertain whether the presence of NO_2 is due to the flame or probe, the fraction of NO_2 was not large enough relative to experimental uncertainties to warrant a detailed investigation. Alternatively, if one assumes that the NO formed in the flame without seed NO is also formed when NO is added, then the losses in the stoichiometric and rich cases can be increased by approximately 3 percent (about 30 ppm in 1000). The estimated losses at centerline of NO may be decreased by about 3 to 5 percent due to dilution from the nitrogen purge in the optical ports (see Dodge, et. al., 1979). Uncertainties also include the inaccuracies in blending from the mixing apparatus and in the calibration and analysis. It is estimated that the sum of these uncertainties is on the order of 3 percent since measured NO concentrations generally agreed to within 3 percent of the calculated values when NO was blended only with nitrogen, and the gas sample was extracted within 1 mm of the burner surface with no flame present and with the nitrogen purge off. This procedure provides an extremely powerful and important experimental tool to check the operation of the complete apparatus. It was used to verify not only the accuracy of the blending methods but also the integrity and behavior of the sampling system. For example, this procedure was used several times to identify the existence, although generally not the location, of sample line leaks and indicated the necessity for conditioning new stainless steel lines used in the sampling line or detector system (see Section III.A.3). This technique is particularly advantageous over other alternative tests such as a vacuum check for leaks, since it can easily be performed prior to and after any given experiment and does not require the opening and resealing of the sample line or probe connection to the sample line. (Moreover, it also identifies the existence or lack thereof of other loss mechanisms of NO such as line conditioning or other line losses.)

With all of the adjustments and uncertainties mentioned above, the percent NO_x lost for these flames becomes 9, 8 and 34 percent respectively with an uncertainty of about $\pm$ 5 percent in each number, i.e., for the lean flame, the estimated real loss can range from 4 to 14 percent. If the natural NO formed in the flame is not included, then these numbers become 9, 5, and 31 percent for the ϕ = 0.8, 1.0, and 1.2 flames, respectively.

To check whether NO was conserved prior to the exit from the surface of the burner, the following test was made. The probe tip was placed near the surface (within 0.4 cm) but still above the flame sheet and NO and NO_x measurements were made. Then the mass flow of the carrier gas (N_2) was increased to push the visible flame sheet well above the probe tip ($\sim$ 2 cm) and NO and NO_x measurements were repeated. This test was performed using the copper tipped probe on the lean and the rich flames with approximately 1000 ppm of

seed NO and no nitrogen purge. With the flame below the probe tip for the lean flame, the probe measurement indicated a 9 percent loss of NO_x. With the flame pushed above the tip and correcting for increased diluent in the flame, measurements of NO_x were 2 percent higher than the calculated value, with 10 percent of this NO_x measured as NO_2. In the case of the NO_x value, exact corrections due to changes in the viscosity and quenching efficiency of the carrier gas (Dodge, et. al., 1979a) were not made since the constituency of the carrier was uncertain after it passed through the converter. Estimates for both NO and NO_x, indicated that less than a 3 percent correction would be required. For the rich flame, NO_x measurements indicated a loss of 31 percent of the seed NO with the probe at 0.4 cm above the burner; but with the flame pushed above the probe tip, the loss was only 6 percent of the original NO and at least half this amount could be due to viscosity and quenching effects. The remaining differences are considered to be negligible. Again, 10 percent of the measured NO_x was NO_2. (In the rich case, the NO_x converter (molybdenum) could be operated for a short period of time, approximately one minute or so, before reconditioning was necessary).

These results indicate that NO_x is conserved in the gas handling apparatus and up to the burner. One may argue that by lifting the flame off the burner, the temperature in the sintered copper surface is reduced and consequently catalytic action which would depend on stoichiometry is reduced. It is not believed that this is the case, however, due to other evidence obtained at UTRC, (discussed later in this section).

These measurements also verify the operation of the sampling line and analysis system. First of all, the status of the sampling system is the same as it would be during sampling of the flame since these were sequential measurements and since other gases were sampled along with nitrogen and nitric oxide. The other gases presumably were CH_4 and O_2 although some CO, CO_2, H_2, and H_2O could be formed in the hot tip. The presence of NO_2 is probably due to Reaction III-3, i.e., $NO + NO + O_2 \rightarrow 2NO_2$. Using an analysis similar to that described in Section III.A.1a, this reaction can convert approximately 5 percent of the NO to NO_2 in the sampling system when sampling the unburned gases.

The only remaining possibilities are NO losses in the flame zone or in the probe. To shed further light on this problem, NO measurements were made at various levels of seed for the three flames. These data are reported in Fig. IV-5. Examination of these data indicate that the loss mechanism is concentration dependent. In the rich flame, for example, 63 percent of the NO is recovered (as NO) at 1000 ppm whereas at 2900 ppm only 52 percent is recovered. At least in the case of the rich flame, it is unlikely that any NO will be converted to NO_2 in the sampling line via Reaction III-3 since virtually no oxygen exists in the combustion products. These data are in fact not unique since very similar results have been obtained by Falcone (1979) using a quartz probe. For reference, equilibrium concentrations for NO (Gordon and McBride, 1971)

FIG. IV-5

NITRIC OXIDE MEASURED VS. NITRIC OXIDE SEED

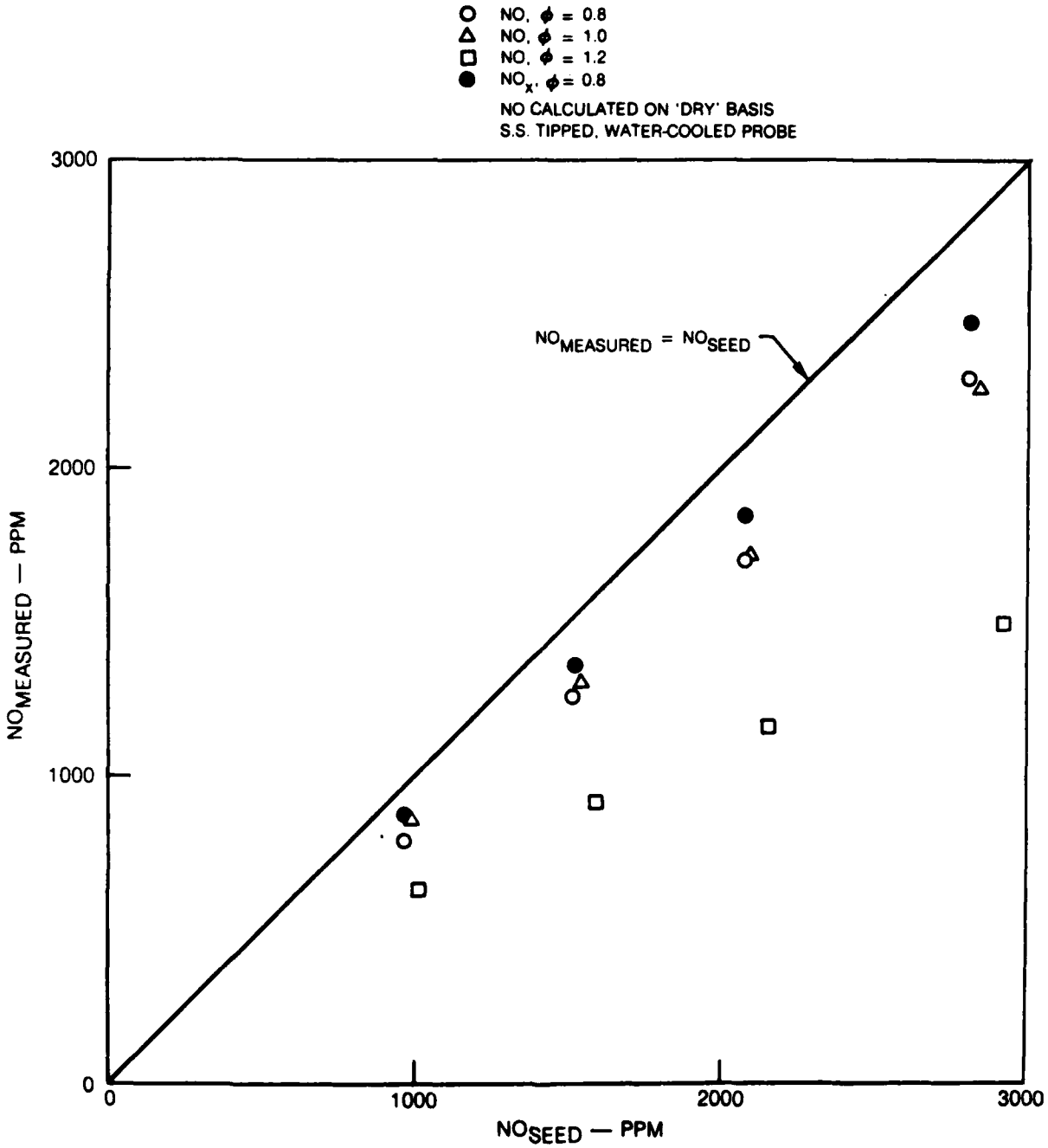

79-10-85-15

at the measured flame temperatures and for the three stoichiometries 0.8, 1.0, and 1.2 are approximately 1400, 300, and 3 ppm, respectively. Highest NO equilibrium concentrations are obtained in the lean case since flame temperatures are not that much different and since significantly more oxygen is present in this flame (see Table IV-A).

The data presented in Fig. IV-5 are not sufficient to identify which of the two, i.e., flame front or probe or possibly both are responsible for the loss of NO. These data do, however, indicate two facts. First of all, the phenomena is concentration dependent. (This fact is important when analyzing data for subsequent optical measurements for which a wide range of NO concentration was supplied.) Secondly, these results are not only consistent with possible losses in a water-cooled probe (for which a mechanism does not exist) but also are consistent with a move towards equilibrium conditions in the flame. Reactions would only be rapid in the reaction zone of the flame rather than the post flame zone since concentrations of reactive species are the highest in these regions, e.g., superequilibrium radical concentrations. Consequently, losses in the post flame zone would be minimal which is in agreement with experimental measurements. Although reaction mechanisms may be similar to that suggested by McCullough, et. al., (1977), a detailed analysis was not considered feasible here due to the existence of very high gradients (temperature and concentration) and the resultant difficulty of incorporating uncertain transport properties of reactive species at elevated temperatures. Although it could be argued that in the lean case, the equilibrium concentration of 1400 ppm is higher than the lowest concentrations where losses were still observed, it should be remembered that at least a portion of the loss would be occurring in the early part of the reaction zone where temperatures and therefore equilibrium concentrations are much lower.

Although the above data are inconclusive, it is considered most likely that the loss of NO is primarily due to flame kinetics rather than to probe phenomena. This conclusion has been reached since the differences between NO measured using the different probes is small relative to the magnitude of loss of NO, especially and quite noticeably in the case of the rich flame. Similarities between the different probes are observed in spite of noticeable changes in surface material and quenching rates. Furthermore, several experiments were performed where the back pressure was varied from about 100 to 600 torr. Again, these data reproduced the above results well in spite of changes in quenching rate (see, for example, the discussion in Section III.C.2) and even unchoking the sampling orifice. In addition, experiments have been performed in an adjacent laboratory at UTRC (Seery and Zabielski, 1979) using a molecular beam/mass spectrometer system to sample a low pressure (1/10th atmosphere) $H_2/O_2/Ar$ flame seeded with various concentrations of NO. In the lean flames, NO is quantitatively recovered in the post flame zone, but in the reaction zone a profile of nitric oxide has been observed, decreasing at first (by as much as 35-40 percent) and then recovering back to the seed value. In

the rich cases, initial rates of NO decay are similarly fast but little or no recovery of NO is observed. These results, which are analogous to the observations in this program on a $CH_4/O_2/N_2$ seeded flame, strongly indicate that the observed descrepancies are due to flame rather than probe phenomena.

Although the data when analyzed in relation to kinetic theory suggests that the destruction of NO occurs in the flame and not in the probe, these data are not sufficient to draw a conclusion. The ultraviolet absorption data, however, which will be reported in TASK III Report are in agreement with the probe data. This agreement between data obtained by two separate methods is sufficient to conclude that destruction does take place in the flame. Since the reaction zone where NO loss occurs is extremely small due to the high pressure (1 atm), the present measurements cannot be used to elucidate the kinetic details of the loss mechanism. Measurements made at subatmospheric pressure on the other hand, could prove useful.

IV.A.1. Uncooled, Stainless Steel Probe

As described earlier, the uncooled probe is geometrically similar to the other metallic probes. This probe, as expected, glowed red when placed in the exhaust of the flame. Using this probe, NO measurements were similar to measurements obtained when using the cooled probes for the lean flames although the results were somewhat dependent on the residence time of the uncooled probe in the flame. Data are reported in Table IV-B and times between scans are typically 5-10 minutes. For the stoichiometric flame, the observed NO was approximately 25-30 percent less, and for the rich flame values ranged from the same as that measured using cooled probes to only 20 percent of that value depending on probe history and probe back pressure, i.e., residence time. For example, at 220 torr back pressure and when the flame is quickly changed from the lean to rich flame ($\sim$15-30 seconds), cooled and uncooled probes behave similarly but in less than a minute the indicated NO begins to fall and after 10 to 15 minutes a stable, but lower value (by a factor 0.66) is obtained. Then by increasing the back pressure to 430 torr which correspondingly increases the residence time substantially, the NO drops further to only 20 percent of the initial value.

The behavior of the uncooled probe, is not unexpected since similar results have been obtained by England, et. al., (1973) and since similar effects are common for a stainless steel NO_2-NO converter when sampling rich flame gases.

IV.B. IFRF Burner

Initially, temperature profiles were measured and their dependency on burner operating conditions (i.e., swirl number, position of fuel nozzle, and design of fuel nozzle) and location within the combustor was examined. The primary objectives of these tests were to (1) find stable and repeatable

TABLE IV - B

MEASURED CONCENTRATION OF NO (PPM) USING
UNCOOLED, STAINLESS STEEL PROBE OVER FLAT FLAME BURNER[5]

	ϕ	0.8[1]	0.8[2]	1.0[1]	1.2[1]	1.2[2]	1.2[3]	1.2[4]
height	1.5	772	717	655	242	227	225	147
above	2.0	762	712	630	237	222	217	142
burner	2.5	755	710	545	232	220	215	137
(cm)	3.0	752	702	500	230	215	215	132
Back pressure (torr)		225	213	219	218	218	218	435
Direction of Scan		down	down	down	down	down	up	down
Seed level (ppm)		971	971	980	1011	1011	1011	1011

1. First scan
2. Second scan
3. Third scan
4. Fourth scan
5. These data may be compared directly to data for cooled probes presented in Figure IV-4.

operating conditions and (2) obtain reasonably flat temperature profiles in order to simplify the reduction of the optical data. The selected burner conditions are described in Section II-C. Probe locations as far downstream as practical were selected to insure that only combustion products and not unburned or partially burned gases were sampled and that the temperature profiles were relatively flat. Six operating conditions were chosen and these are listed in Table II-B. Two swirl levels were examined and at each swirl number, three stoichiometries were tested. Although flames at lower swirl numbers were tested, these flame conditions were relatively unstable and therefore unsuitable for these experiments.

A typical temperature profile (corrected for radiation and conduction) for the run condition $\phi = 0.8$, swirl = 1.25, are shown in Fig. IV-6. These data were taken using the aspirated thermocouple described in Section II.C.3. The dotted lines represent estimates based on measurements in the wings. The change in swirl produced no measurable difference for any of the stoichiometries. The shape of the temperature profiles for the rich and stoichiometric flames are similar to the lean flame with the centerline temperature varying according to stoichiometry (see Table IV-C). In the wings, temperature measurements (uncorrected for radiation or conduction) were made using a chromel-alumel thermocouple (0.010" wire diameter) inserted through the open optical ports. The measured temperatures are much lower than are expected for adiabatic temperatures of a C_3H_8/air flame. The low temperatures observed are due to cooling from the water-cooled walls of the expansion diameter.

Stable species were measured using the SCOTT Instrument package and both the "EPA" and reference probes. No differences were observed between these probes and measured concentrations were independent of back pressure. Experimental data are listed in Table IV-C and equilibrium calculations based upon the measured (not the adiabatic) temperature are also given. Data for only one swirl level is given here since the data for the other swirl numbers is essentially identical. In general, agreement between equilibrium and experimental values are reasonable except for the CO_2 (and to some extent CO) values for which the measured values are about 9% low. It is believed that this difference is due to uncertainties in the fuel flow rate and/or the CO_2 calibration curve. The high experimental water value (estimated by mass balance) for the rich flame is due to the presence of about 3.5% molecular hydrogen (equilibrium value) and the equilibrium value of water is realistic. The presence of H_2 was not accounted for when estimating the concentration of water.

Concentrations of nitric oxide were measured to be approximately 48, 40 and 25 ppm for the $\phi = 0.8$, 1.0 and 1.2 flames respectively. NO_x was typically, 4 to 5% higher than these numbers for the $\phi = 0.8$ and 1.0 flames and was not measured for the rich flame. Since these levels were too low (even with the relatively long path length) to provide adequate signal-to-noise ratios in the optical measurements, nitric oxide was blended with the inlet air.

TEMPERATURE PROFILE ACROSS IFRF COMBUSTOR

ϕ = 0.8, SWIRL = 1.25

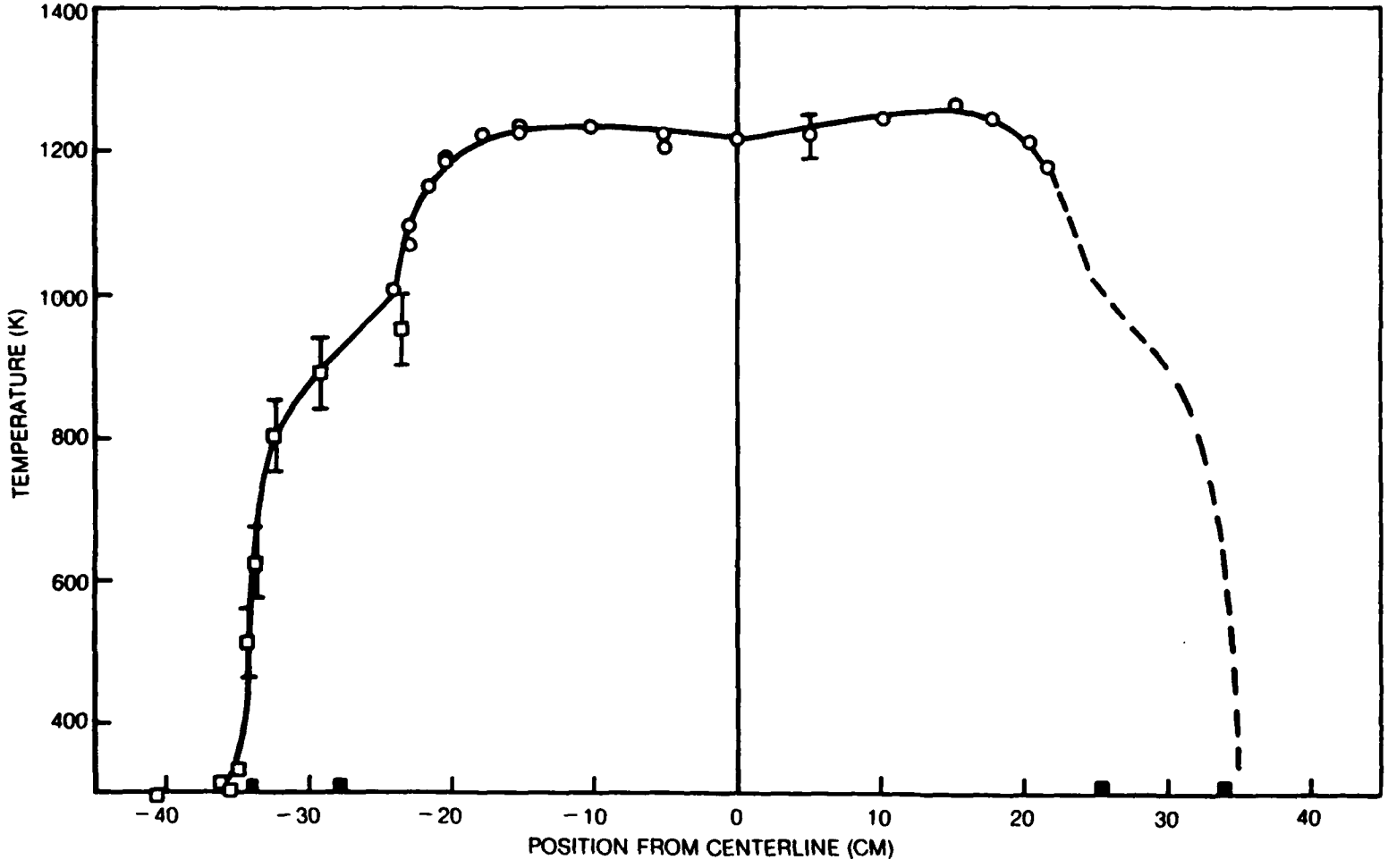

FIG. IV-6

TABLE IV-C

Mole Percent of Stable Species
for IFRF Burner[1]
(Wet Basis)

Experimental

ϕ	O_2[2]	CO[2]	CO_2[2]	H_2O[3]	N_2[4]	Temp. (K)
0.8	4.2	9ppm[5]	8.8	11.7	75.3	1200
1.0	-	0.063[5]	10.6	15.6	73.8	1280
1.2	-	3.0	9.0	17.3	70.7	1220

Equilibrium[6]

ϕ	O_2	CO	CO_2	H_2O	N_2	Temp. (K)
0.8	3.92	<1 ppm	9.45	12.6	73.1	1200
1.0	<1 ppm	0.021	11.6	15.5	71.9	1280
1.2	<1 ppm	3.65	9.56	13.9	68.3	1220

1. Although two flames were examined (two different swirls) at each stoichiometry, measured values of these stable species were essentially the same.

2. Measured values but corrected for the presence of water vapor.

3. Water estimated from known input conditions.

4. Nitrogen calculated by difference.

5. Error ± 40% of value.

6. Based on measured temperatures

Except where noted, the uncertainity in the experimental concentrations is approximately ± 5% of the reported (experimental) value.

Typical profiles of nitric oxide across the optical axis, normalized to the seed concentration of NO, are shown in Fig. IV-7. The profile data were obtained using the 'EPA' probe and did not vary over the back pressure range examined (100-350 torr). The dotted lines are estimated extrapolations based on other similar flame measurements. Data for the other flames are quite similar. Also included on these profiles are experimental data obtained using the reference probe at two back pressures. At these conditions both the theoretical model and experimental pressure profiles inside the probe (presented in Section IV.D) indicate that the flow in the probe is subsonic except for possibly a small region in the tip. Thus, the flow is convectively cooled. No differences between NO measurements using the reference probe and the EPA probe are observed when operating both in the convectively cooled mode. For all presssures examined and for both probes NO_x measurements were typically within 2 or 3 percent of the NO measurement. For Fig. IV-7, the NO seed values for the ϕ = 0.8, 1.0 and 1.2 flames were 184, 189 and 182 ppm dry and 162, 160, and 150 ppm wet, respectively. In these calculations the 'dry' concentrations were estimated assuming the vapor pressure of water at 3 torr remained in the sample gas with a total pressure of approximately 500 torr.

Measurements were also made when supersonic flow (verified by pressure profiles) extended into the first constant area section of the reference probe. The data are reproduced in Table IV-D and are compared with measurements made using the same probe but at higher back pressures, i.e., when the gases were convectively cooled. Although these data are within about 10%, there appears to be some difference between the NO measured at a low back pressure (90 torr) versus that measured at higher back pressure. In addition, the NO_{meas}/NO_{seed} ratios are smaller than those obtained at lower seed concentrations and reported in Fig. IV-7. This latter result, in fact, is not surprising since the results from the flat flame burner also show a concentration dependence. The former results apparently indicate a small difference between a probe that convectively cools and one that aerodynamically cools; however, it is more likely that the observed differences are associated with the very low operating pressure of the sampling system. For example, due to the very low pressures, the pumps could deliver only half (1 cfh) the normal flow (2 cfh) to the CLA. In either case, most of the gas was extracted with a 17.5 cfm vacuum pump immediately at the exit of the probe. Although the CLA was recalibrated to the lower flow rate, a small leak of only 2 to 3% would be difficult to detect under normal flow conditions yet would amount to a 4-6% dilution when only half the flow passed through the sample line. In addition, less water would be extracted at the refrigerator since the total pressure is lower. The resultant increase in water concentration will not only act to dilute the sample on a relative basis, but also will provide more efficient quenching of the chemiluminescent reaction (see Section III.A.4) and consequently decrease the response of the CLA. It is estimated that an increase in the water concentration from 1% to 3% will decrease the CLA response (due to both chemiluminescence quenching and sample dilution effects) by 4 to 5%. Consequently, it is believed that the differences observed in Table IV-D are not due to differences in quenching rates of the gas sample but rather due to a decrease in sample line pressure and associated phenomena.

NORMALIZED NITRIC OXIDE PROFILES ACROSS IFRF COMBUSTOR

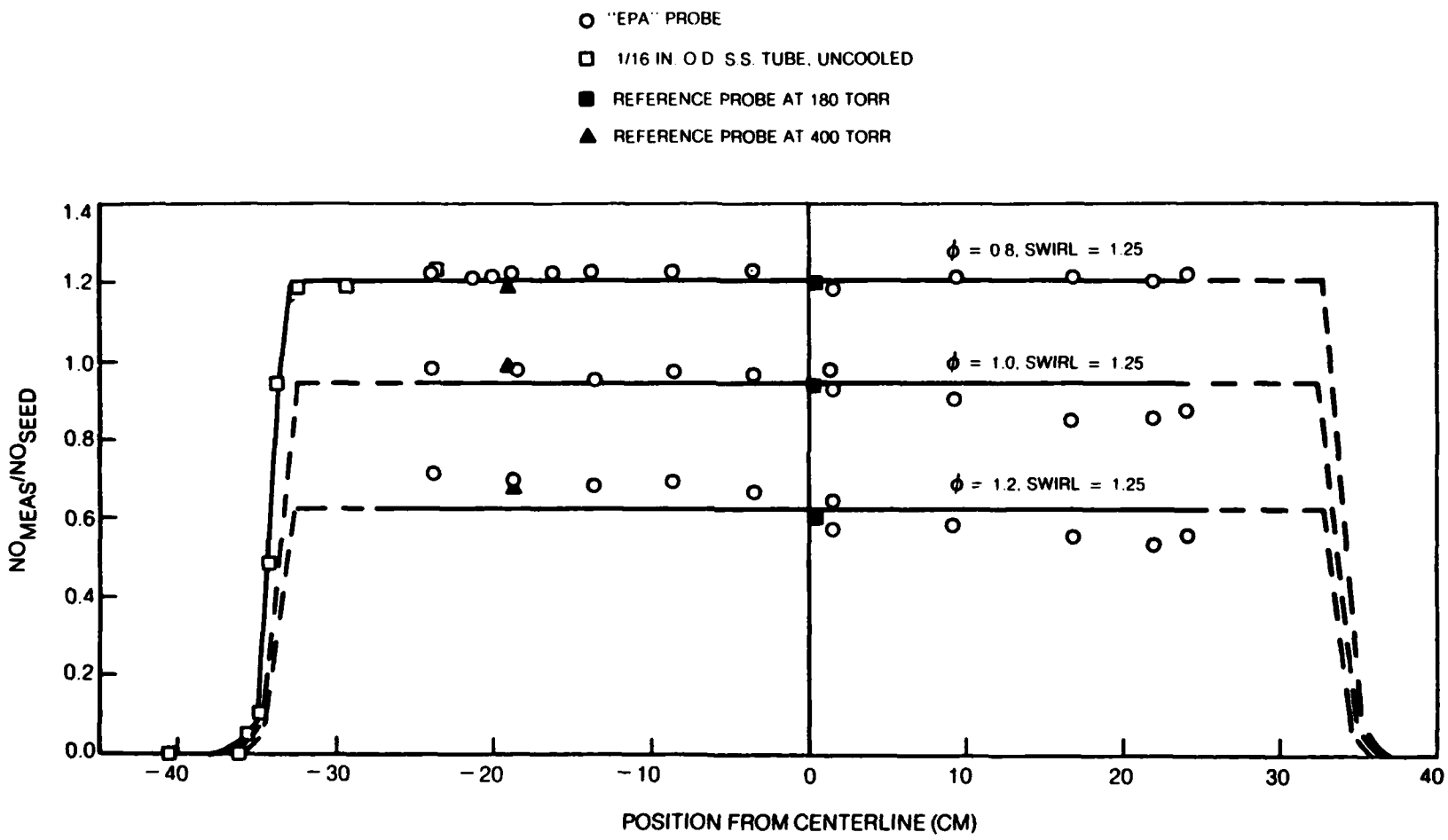

FIG. IV-7

79-10-85-20

TABLE IV-D

Comparison of Nitric Oxide
Measurements Using the Reference Probe
IFRF Burner

	ϕ = 0.8 Swirl = 1.25 Seed = 960 ppm	ϕ = 1.2 Swirl = 0.63 Seed = 470 ppm	
NO (ppm)	895 ± 40	240 ± 10	Back Pressure = 190 torr (0.25 atm)
NO_x (ppm)	880	--	
NO (ppm)	--	246	Back Pressure = 380 torr (0.5 atm)
NO (ppm)	830	220	Back Pressure = 90 torr (0.12 atm)[1]
NO_x (ppm)	820	—	

1. Supersonic flow extends into first constant area section of reference probe.

Additional information on the performance of the reference probe is provided in Section IV.D.1.

IV.C FT12 Measurements

Three flight conditions, idle, cruise, and maximum continuous were simulated for this series of tests. The corresponding operating conditions are given in Table II-C. Temperature profiles across the optical axis (same as for the IFRF measurements) are shown in Fig. IV-8 for idle and cruise conditions. These data were obtained using the Pt/Pt-13% Rh, aspirated thermocouple. The profile for maximum continuous is very similar in shape and magnitude to that for cruise. Also shown in the figure are data from a vertical profile which indicate no difference between the different quadrants. In addition to these measurements, centerline temperature measurements using coherent anti-stokes Raman spectroscopy (CARS) were made (Eckbreth, et. al, 1979). For the CARS measurements, the temperatures were 580K, 875K and 875K for the idle, cruise, and maximum continuous conditions respectively. These data agree quite well with the centerline thermocouple data obtained at the same position i.e., 590, 900 and 920K.

Measurements of CO, CO_2, and O_2 using the SCOTT instrument package and the EPA probe are listed in Table IV-E. For comparison, equilibrium data based on the input conditions and measured gas temperature are also presented. Good agreement is observed between the experimental and equilibrium data except for carbon monoxide and an unexplained, high experimental value for carbon dioxide at maximum continuous. The high concentrations of CO measured behind the FT12 combustors are due to a quenching of the reaction from air dilution within the combustor. With the reference probe, the CO_2 and O_2 concentrations were not measured. Carbon monoxide concentrations were the same as with the EPA probe when the reference probe was operated both in the convective cooling mode and with supersonic flow extending into the first constant area section of the probe.

Without seed, concentrations of nitric oxide (total nitrogen oxides) on centerline were on the order of 3(15), 5(28), and 6(30) ppm for the simulated flight condition idle, cruise, and maximum continuous, respectively. These values varied as much as 20-30% from day to day for any given probe but specific variations due to probe type or back pressure were not observed. The cause of the uncertainty may be variations in input conditions for the combustor or calibration of the CLA at these low NO levels. Careful attention to obtaining accurate base line values was not given since this program focused on NO seed levels much higher than 25 ppm. In any case, it is interesting to note that the NO_2/NO ratios were typically quite high, on the order of five. The source of the NO_2 is not due to the reaction in the sample line.

$$NO + NO + O_2 \rightarrow 2\ NO_2$$

TEMPERATURE PROFILE DOWNSTREAM OF FT12 COMBUSTOR

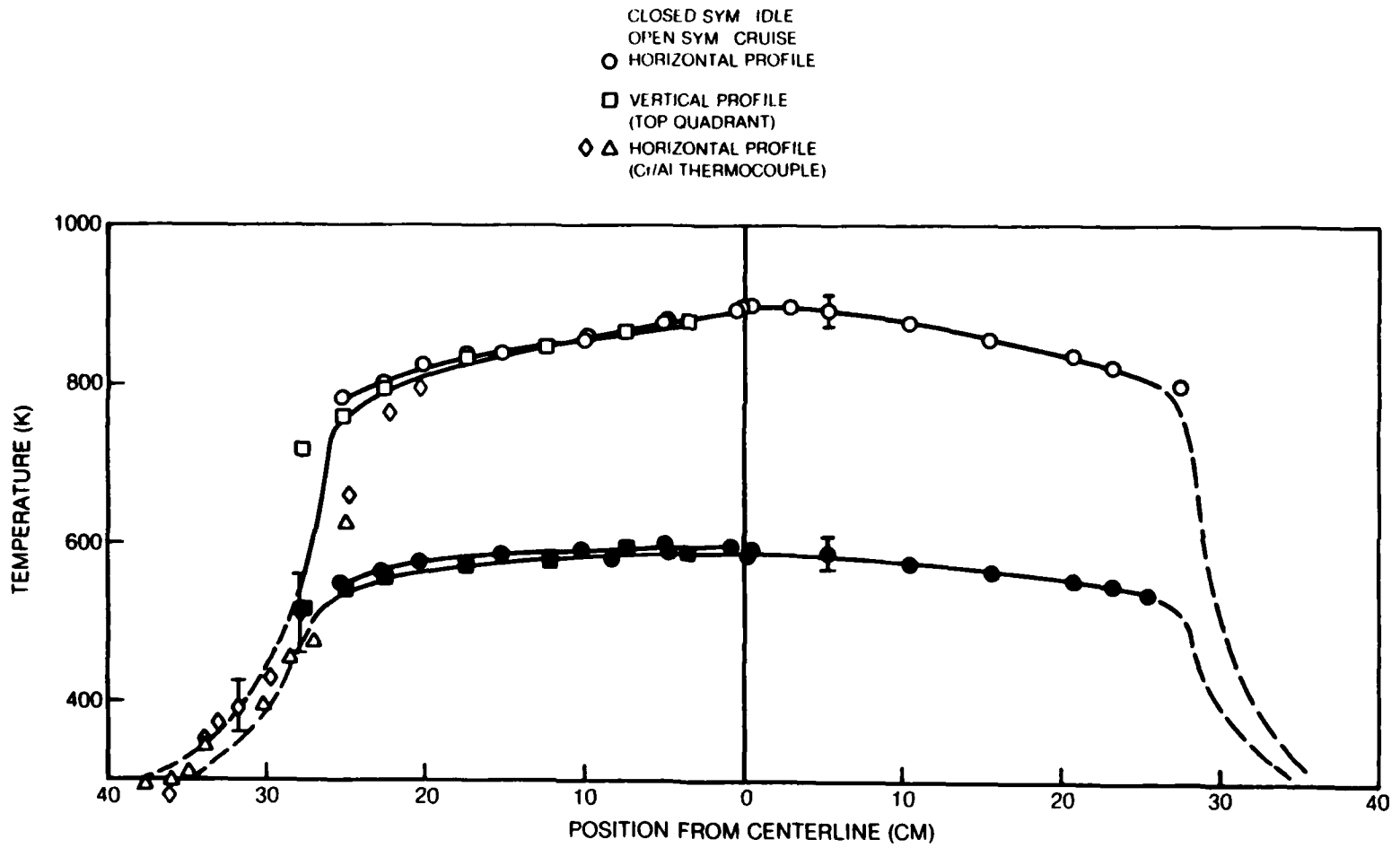

FIG. IV-8

79-10-85-18

TABLE IV-E

Mole Percent of Stable Species
for FT12 Combustor
(Wet Basis)

Experimental

	ϕ	O_2[1]	CO[1]	CO_2[1]	H_2O[2]	N_2[3]	Temp. (K)
Idle	0.14	19.0	0.25	1.7	1.9	77.15	580
Cruise	0.19	16.8	0.20	2.8	2.6	77.60	870
Max. Cont.	0.20	16.5	0.17	3.3	2.7	77.33	900

Equilibrium[4]

	ϕ	O_2	CO	CO_2	H_2O	N_2	Temp. (K)
Idle	0.14	17.9	<1 ppb	1.94	1.94	77.3	580
Cruise	0.19	16.8	<1 ppb	2.60	2.58	77.0	870
Max. Cont.	0.20	16.6m	<1 ppb	2.77	2.74	77.0	900

1. Measured values but corrected for the presence of water vapor.

2. Water estimated from known input conditions.

3. Nitrogen calculated by difference.

4. Based on measured temperatures

The uncertainity of the experimental concentrations is approximately ± 5% of the reported (experimental) value.

since the rate of this reaction is strongly dependent on the NO concentration and sample line pressure. Experiments with high seed values of NO ($\sim$800 ppm) in air at much higher sample line pressure (750 vs 180 torr) indicated only 3% conversion to NO_2. Instead, it is more likely that NO_2 is formed from NO in the combustor during the addition of relatively cold air, in the post flame region downstream of the combustor, or in the probe from the reaction with HO_2 (see discussion in Section III.A.1). Insufficient information is available to determine conclusively which is the primary mechanism, however, it appears unlikely that probe reactions are responsible due to the relatively low temperature of the gas and the necessarily low radical concentrations.

Profiles of nitric oxide were obtained with seed levels of NO at 327, 326, and 326 ppm for the idle, cruise, and maximum continuous flames. Normalized profiles of nitric oxide for the idle and cruise conditions are plotted in Fig. IV-9. These data were obtained using the EPA probe. Also shown are profiles of total nitrogen oxides. For maximum continuous, the centerline fraction of NO (NO_x) recovered relative to the seed value was 0.89 (1.08). In these gas samples, it is clear that there are relatively large fractions of NO_2. For example, idle conditions convert more than 40% of the total NO_x to NO_2. For the same reasons discussed in the previous paragraph, it is believed that the NO_2 is probably formed in the combustor or post flame zone rather than the probe or sampling line. Greater losses of NO are observed at idle in spite of the relatively lean stoichiometry possibly because at this level mixing is less intense and local variations in stoichiometry may be larger and may last longer than those at the other power levels. In the very fuel rich eddies, losses similar to those in the flat frame burner undoubtedly take place.

Also shown in Fig. IV-9 are experimental measurements of nitric oxide using the reference probe. For most of these data the back pressure was approximately 300 torr. Although good agreement is obtained between measurements with this probe and the EPA probe, some differences are noted for one set of NO_x measurements at cruise and idle. The FT12 assembly had been removed from the test assembly and reinstalled before this second set of NO and NO_x measurements were made. Small shifts in alignment of the fuel nozzle or variations in input conditions may be responsible for the changes in NO_x recovery although no corresponding change in the gas temperature was observed.

The reference probe was also used to sample flame gases at reduced pressure ($\sim$95 torr) where supersonic flow conditions extended into the first constant area section of this probe (see discussion in Section IV-D). In Table IV-F these values are compared to measurements taken at high back pressure with the same probe. The agreement is excellent.

FIG. IV-9

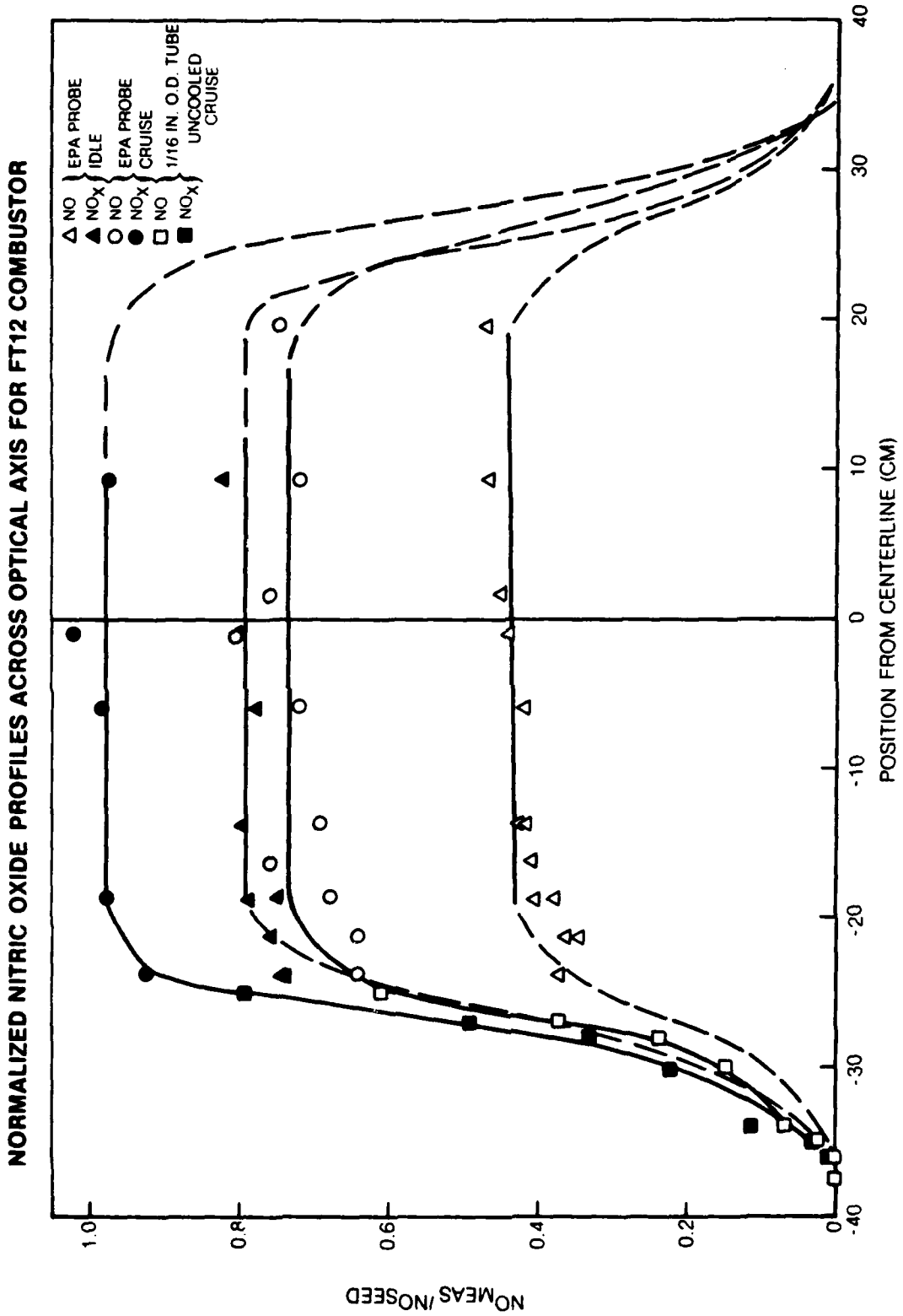

79-10-85-19

TABLE IV-F
Comparison of Nitric Oxide Measurements Using
the Reference Probe - FT12 Combustor

		Idle	Maximum Continuous
Back Pressure ~ 205 torr (0.27 atm)	NO	395	740
	NO_x	480	800
Back Pressure* ~ 95 torr (0.13 atm)	NO	385	740
	NO_x	478	790

* Supersonic flow extends into 1st constant area section of reference probe

IV.D Experimental Verification of Probe Model

To verify the predicted aerodynamic behavior of gas sampling probes, two types of measurements were made. First, internal pressure measurements were made for the reference probe to identify if and when it operated in the aerodynamic quench mode. The smaller probes were not instrumented due to physical limitation. Secondly, mass flow measurements were made for probes of three sizes, macro-, mini- and microprobes, to compare with theoretical values. These data include not only measurements of the maximum possible flow for a given probe but also the variation of mass flow as a function of probe back pressure.

IV. D.1 Pressure Profiles for the Reference Probe

To verify the operation of the reference probe, three static pressure taps were positioned along the constant area section and one was placed after the bend. A detailed design of the probe including the location of these pressure taps is given in Fig. III-1. The last pressure tap was used to approximate the stagnation pressure at the exit of the probe and this piece of data is of prime importance in estimating the location of shock recovery. Typical static pressure data obtained when sampling the exhaust from the FT12 combustor are shown in Fig. IV-10. The solid and dotted lines in the figure are calculated profiles when the stagnation pressure at the exit of the probe (back pressure) was assumed to be equal to the static pressure after the bend. For these calculations, this assumption can be shown to provide a reasonable estimation. As can be seen, the agreement between the theoretical and calculated profiles is excellent. The mechanism for reducing the static pressure to the measured value was a normal shock whose position and, therefore, strength varied with back pressure.

AD-A097 545 UNITED TECHNOLOGIES RESEARCH CENTER EAST HARTFORD CONN F/G 21/2
NITRIC OXIDE MEASUREMENT STUDY. VOLUME II. PROBE METHODS.(U)
MAY 80 M B COLKET, M F ZABIELSKI DOT-FA77WA-4081
UNCLASSIFIED UTRC/R80-994150-2 AFESC/ESL-TR-80-13 NL

END
DATE
FILMED
DTIC

PROFILES OF STATIC PRESSURE FOR THE REFERENCE PROBE

$T_{EXTERNAL}$ = 900 K

$P_{EXTERNAL}$ = 1 atm

SOLID LINES — CALCULATED PROFILES

SYMBOLS — EXPERIMENTAL MEASUREMENTS

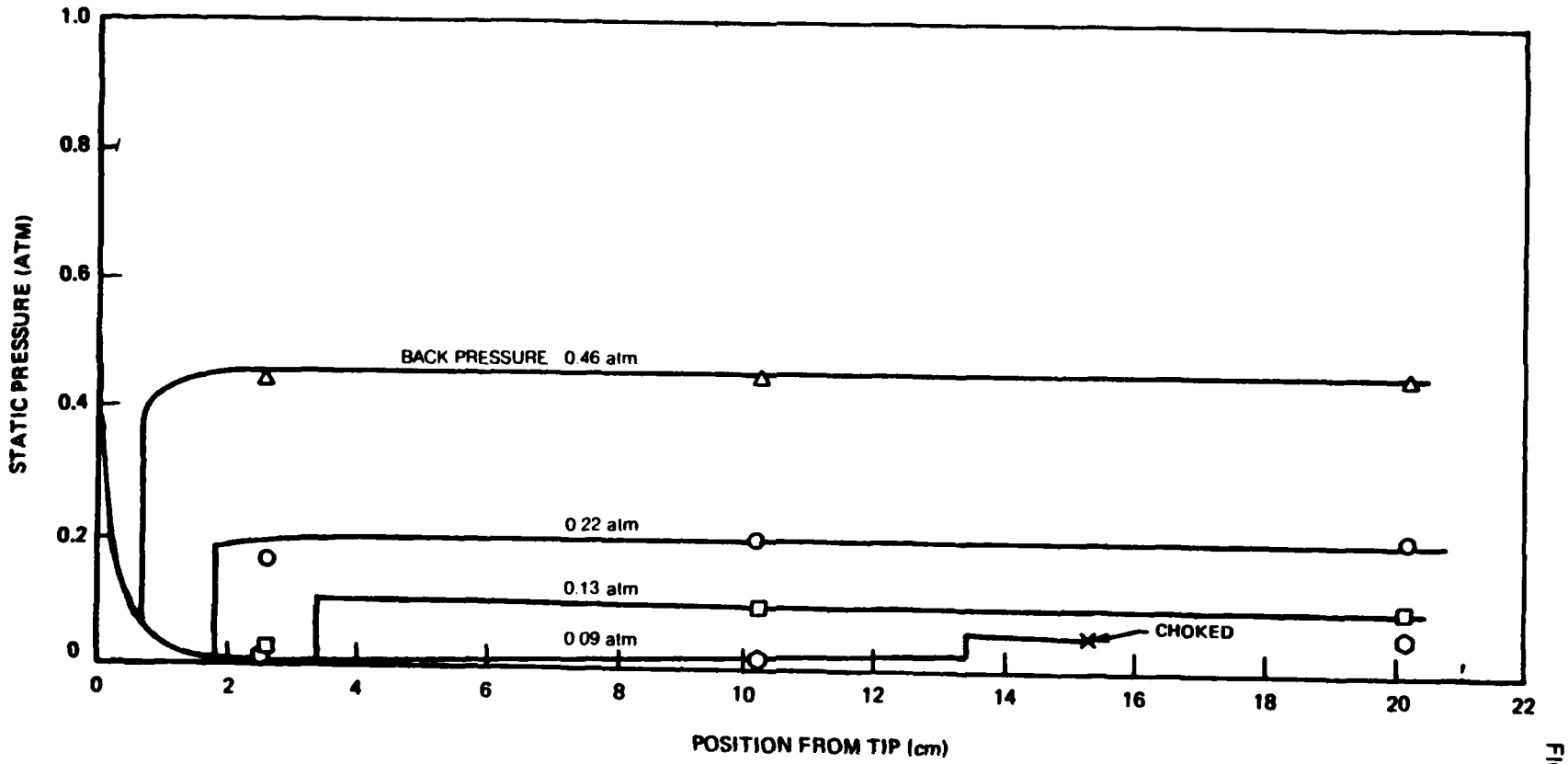

FIG. IV-10

The calculations indicate that at the lowest back pressure the flow chokes prior to the exit of the constant area section. Since the flow in a constant area tube can choke only at the exit of the tube, the predicted choke location is in error due apparently to uncertainties in the back pressure and the skin friction correlation used in the analysis. In any case, the experimental data presented in Fig. IV-10 confirm the analytical result that an extremely low back pressure is needed to extend supersonic flow for a substantial distance into the probe.

Experimental verification of calculated temperature profiles was considered impractical since the presence of a thermocouple in the supersonic region will trigger a shock wave. Even if placed downstream of the recovery shock, thermocouple temperatures would probably be ambiguous since the thermocouple will also be cooled by its water-cooled jacket. Nevertheless, some temperature measurements were made using the chromel-alumel thermocouple depicted in Fig. III-2. Although the measurements typically were within 50K of the theoretical calculations, this agreement may be fortuitous.

NO measurements taken with the reference probe operating at low back pressure are given earlier in this chapter. Typically, for these measurements, the back pressure was 0.12 atmospheres. Under these conditions, the very low pressure measurements at the first pressure tap verified that supersonic flow exists at least past this position. For the IFRF burner at $\phi = 1.0$, a computer analysis indicates that the shock occurred 5.2 centimeters from the probe tip (45 microseconds). The static gas temperature recovered to 1080K (compared to the external flame temperature of 1280K) and cooled below 1000K in a total time of 170 microseconds. Alternatively, at a back pressure of 1/3 atmosphere, the computer calculations indicate that the shock occurs 0.9 cm from the tip (8.6 microseconds). After this shock, the static temperature increased to 1205K but did not fall below 1000 K until 750 microseconds. Clearly, there is substantial difference between these two modes of operation. When the gas flow was supersonic past the first pressure tap, the time above 1000K was nearly 6 times less than that when the flow was primarily subsonic (0.125 vs 0.74 milliseconds).

It was desirable to extend the aerodynamic quench made by reducing the back pressure further and simultaneously measuring the nitric oxide concentration; however, this was not possible because of the low pumping speed of sampling pumps operated at low pressures. At a back pressure of 90 torr (0.12 atm), the maximum flow rate through the sampling lines was only one cubic foot/hour ($\sim$ 7.9 scc/sec) which was barely sufficient to operate the chemiluminescence analyzer. Only this amount of flow could be obtained in spite of the use of many metal bellows pumps (see Section II.D.1a) in the gas sample line and the vacuum pump associated with the CLA. To extend the supersonic flow all the way through the constant area section, the pressure taps indicated that the back pressure had to be reduced to $\sim$ 50 torr. At this low sampling line pressure, the collection of sampling pumps would not supply sufficient flow to the CLA.

IV. D.2 Mass Flow Measurements

Measurements of mass flow through the micro-, mini-, and macroprobes were made using low pressure drop, Hastings mass flow meters (ALU-100, -5K, and -20K, respectively). Description of the experimental method used for these measurements is provided in Section II-E. Hot flow data were obtained for each class of probes and cold flow measurements were made only for micro- and miniprobes. For the macroprobe at room temperature, the mass flow was too large for accurate readings on the Hasting meter (mass flow rate through probe $\sim 1/\sqrt{T}$).

IV. D.2a Macroprobe

Experimental measurements were made using the reference probe when sampling exhaust from the FT12 burner can at each simulated flight condition. Exhaust from the FT12 rather than from the IFRF burner was used for these tests since water condensation did not present a problem. In the case of the IFRF burner, approximately 15% of the exhaust was water vapor and even though the mass flow meter and associated lines were heated it was found that water condensation was a problem at high probe pressure. The condensation was due to nonuniformites in heating the large lines necessary for these tests and severely interfered with the mass flow measurements. Data from cruise conditions are normalized in Fig. IV-11 to the maximum mass flow measured. The analytical results for the macroprobe are presented as the solid line. It can be seen that a subsonic condition exists that will yield a relative mass flow of 0.69 at a back pressure of 0.9 atm and that, below approximately 0.6 atmospheres, the probe orifice will be choked. If the probe orifice is choked, then the flow in the tip is supersonic and is not likely to separate. Friction losses and normal shock losses in this case are sufficient to reduce the calculated pressures to the measured values. By accounting for sudden expansion losses, agreement between the theoretical and measured profiles is excellent.

IV.D.2b Miniprobe

Experimental measurements of mass flow were made using the stainless steel tipped, water-cooled probe when sampling over the flat flame burner, $\phi = 0.8$, and room temperature air. These mass flow data have been normalized and are plotted in Fig. IV-11 as a function of back pressure. Also shown are calculated profiles based on sudden expansion losses. The cause of the differences between the calculated and relative mass flow curves is uncertain and may be due to assumptions used in the model for sudden expansion. Another possible explanation is that the tip geometry is not known precisely and that the points of flow separation and flow reattachment have been taken as the beginning and end points, respectively, of the tip. The area ratio, therefore, needed to calculate the sudden expansion loss is not known exactly. In addition, the

RELATIVE MASS FLOW VS. BACK PRESSURE FOR SEVERAL PROBES

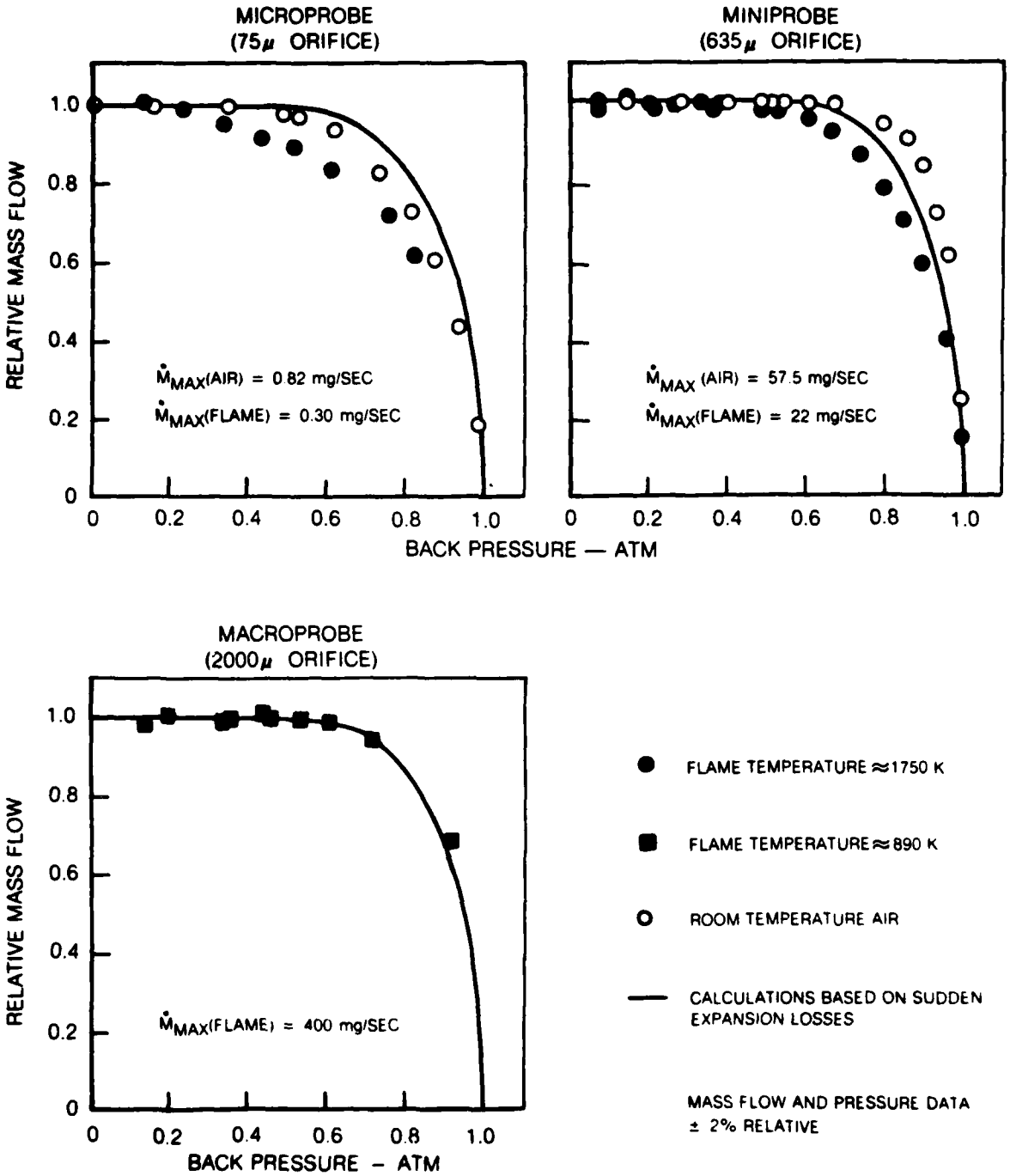

79-10-85-25

mass flow profiles exhibit some differences between the cold and hot flows; however, these differences cannot be explained using our current understanding of the fluid mechanics and heat transfer within probe tips. Additional research is required to identify the controlling phenomena.

IV.D.2c Microprobe

Measurements using a quartz, water-cooled microprobe with an orifice diameter of 75 microns (0.003 inches) were also made over the flat flame burner ($\phi = 0.8$) and for room temperature air. A photograph of a similar probe is shown in the Task I report (Dodge, et. al, 1979). Normalized mass flow profiles are provided in Fig. IV-11. For the cold flow, the data indicate that the flow chokes for all back pressures below (approximately) one-half atmospheres. This choking point is consistent with not only the experimental data from the macro- and miniprobes, but also with equations developed by Shapiro (1953) for the required pressure drop for choking at a minimum area. Air, for example, will choke with a pressure ratio (static pressure at minimum area to stagnation pressure) of 0.53. This ratio is relatively independent of changes in gas properties. For the hot flow data, a substantial difference is observed when compared to the other results. The flow does not choke until at least a back pressure below one-fifth of an atmosphere. This result is in qualitative agreement with the computer calculations (for probe design) that indicated that this microprobe cannot be choked (see Section III.C.2a). Based on both an analytical study and experimental measurements, one must conclude that under described conditions the flow does not choke (except possibly at very low back pressure) and consequently will not quench the gas aerodynamically. This conclusion is in direct conflict with assumptions regarding probe behavior in other investigations and suggests that some earlier conclusions based on (assumed) very high rates of quenching may have to be reanalyzed.

The experimental and analytical results for the microprobe do not agree as well as for the larger probes. In addition to the uncertainties mentioned previously, it should be noted that the dump loss calculation procedure used here becomes singular at a high area ratio. The curve in Fig. IV-11 was calculated for the highest area ratio prior to the breakdown of the calculation procedure ($\sim$550), while the actual area ratio was approximately 4500. The results for the cold flow condition indicate that a choked orifice may exist over a range of back pressure if the appropriate sudden expansion loss is applied. On the other hand, the sudden expansion model for this loss is not adequate to explain the variation in the hot flow data which indicates that the probe orifice is not choked.

IV.D. 3 Discussion

The experimental mass flow vs. back pressure profiles indicate that, except for the microprobe operated at high gas temperatures the probe orifices become choked

at the proper back pressure. The back pressure to ambient pressure ratio at which choking occurs is approximately 0.5 and is consistent with calculations for choked flow through an orifice plate (Shapiro, 1955). The probe design model assumes that the flow within the probe is not separated. For the probes examined in this study, however, separated flow occurs when the probe is operated unchoked. Except in the case of the microprobe operated in a high temperature gas stream, calculations accounting for sudden expansion losses yield mass flows in agreement with the measured data.

It should be noted that the probe design model is generally used to design probes for which a sudden expansion loss is not important. Either the flow is supersonic throughout the probe tip (as in designs exploiting an aerodynamic quench) or the tip area ratio and flow angle are small enough that the subsonic flow in the tip does not separate. Microprobes are designed to minimize the disturbance that the probe causes to the flame front. Unfortunately, the geometry of a microprobe requires a better understanding of its internal flow characteristics than heretofore appreciated or included in the analysis.

V. RESULTS AND DISCUSSIONS

In order to study the processes involved in the probe sampling of NO and, ultimately, to compare probe and optical measurement methods properly, three combustion devices were designed and characterized under a variety of operating conditions. The most controlled of these devices was a flat flame burner. Temperature and NO concentration profiles for methane/nitrogen/oxygen flames were obtained at various heights above this burner. The stoichiometries characterized were 0.8, 1.0, and 1.2. Centerline temperatures in the post-flame regions varied from 1740 K to 1815 K depending on stoichiometry and height. Thermal NO produced in these flames ranged from 5 ppm to 30 ppm. Since these concentrations were considered too low for making accurate optical absorption measurements, NO was seeded into the flame at concentrations of 850 ppm to 4500 ppm. The amount of seeded NO recovered in the post flame region was dependent on stoichiometry and will be discussed below.

The second device employed was a swirl burner designed after that of the International Flame Research Foundation (IFRF). Temperature and NO concentration profiles were obtained for unseeded and NO-seeded propane-air flames. The stoichiometries used were 0.8, 1.0, and 1.2. In addition, tangential or swirl flows were introduced onto the air flow. Swirls (S) of 0.63 and 1.25 were used where swirl is defined as the ratio of tangential momentum to axial momentum divided by the radius of the exit. Peak temperatures measured by suction pyrometry and corrected for radiation and convection ranged from 1200 to 1280 K. Thermal NO concentrations ranged from 25 to 48 ppm and were principally dependent on stoichiometry. Seeded concentrations were varied from 130 ppm to 890 ppm. The amount of NO recovered was also dependent on stoichiometry. Temperature and concentration profiles were obtained 87.5 cm downstream of the quarl. Data obtained in four quadrants indicated axial symmetry. The bulk of exhaust was contained in an expansion chamber of 50.0 cm diameter. To simplify optical access, windowless ports with purging across the exit of the optical ports were used. Temperature and concentration profiles through and external to the ports were obtained.

The third combustor, which was also installed into the above expansion chamber, was a modified Pratt & Whitney FT12 combustor. The modifications consisted of a reduction in length from 41.1 cm to 29.5 cm and the closing of several air holes to provide axial symmetry. The distance from the combustor exit to the probe (optical axis) was 78.0 cm. The combustor was operated at three conditions: idle, cruise, and maximum continuous. The fuel/air ratios were 0.0106, 0.0143, 0.0152, respectively. Operating air pressure was Mach number scaled from 6.0 atm to 1.0 atm. The scaling was performed because of facility limitations and to facilitate accurate definition of the optical path. Centerline temperatures for the three operating conditions were 580 K, 870 K, 900 K, respectively. Thermal NO produced spanning the range from 3 ppm to 6 ppm, while

total NO_x values ranged from 12 to 35 ppm. In order to obtain adequate signal-to-noise ratios in the optical measurements, the air flow was seeded with NO in concentrations from 270 ppm to 790 ppm. As with the flat flame burner and IFRF combustor, the amount of NO recovered was dependent on fuel/air ratio (stoichiometry).

The measurement of NO by extractive sampling is a procedure consisting of three elements each of which must be considered in detail. The first of these is the removal of the sample from the flame without seriously perturbing the flame while rapidly reducing sample temperature and pressure. The second element involves the transfer of the gas from the probe to the analyzer. This transfer includes, usually, the removal of water and particulates. The third element is the actual analysis of NO with a chemiluminescent analyzer. This study has been concentrated on the first two elements. However, information obtained outside this particular study has been applied to the third element.

Two separate sets of probes were designed and evaluated and set for the flat flame burner measurements and the other set for the combustor tests. For each set of probes, a special effort was made (using a computer code for probe design) to select a probe geometry that was capable of cooling the gas aerodynamically. For the flat flame burner, the probes used were: (1) a water-cooled quartz miniprobe; (2) a water-cooled, stainless steel miniprobe; (3) a water-cooled, stainless steel miniprobe with a copper tip; and (4) an uncooled stainless steel miniprobe. Each of these probes had an orifice diameter of 635 μ, and the metallic probes had an area ratio of 16. The area ratio for the quartz probe was 62. In addition, a water-cooled quartz probe with an orifice of 75 μ and an area ratio of 4500 was also examined, however, only mass flow measurements were made with this probe. For the large combustor, two water-cooled stainless steel macroprobes were designed. The first of these, which was defined as the EPA probe (in compliance with the Federal Register requirements), had an orifice diameter equal to 0.080 in (2 mm) and an area ratio of 2.4. The second macroprobe, which was defined as the reference probe, had an orifice diameter of 0.080 in (2 mm) but with dual expansion areas. The area ratio of the first relative to the tip was 10.6 while the second ratio relative to the tip was 29.7.

In addition to properly sizing the probe to minimize temperature and flame perturbation, these probe designs were analyzed in relation to the available kinetics of NO decomposition and the aerodynamics necessary to achieve quenching of NO reactions.

A consideration of gas phase reactions through which NO could be destroyed revealed that if the gas sample was rapidly cooled ($\sim$1 msec) to below 1000 K, NO loss would not occur. In addition, it was estimated that catalytic effects would be minimized if exposure to walls whose temperature was greater than 600 K was kept at 10 μsec or less. This kinetic analysis is consistent with the results of this study obtained with probes satisfying the above conditions. The

aerodynamic behavior of these probes were studied with a computer model based on the original work of Cohen and Guile (1970). This program predicts the changes in static temperature and pressure as a function of time and position in the probe. Parameters considered were area changes, heat transfer rates, skin friction, and probe back pressures. In addition, mass flow is calculated for specified combustion stream temperatures and pressures, geometries, and back pressures. The most important prediction of this model was that microprobes and miniprobes (as defined above) cannot achieve an aerodynamic quench. In such a quench, the gas is supersonically expanded to reduce the static temperature and pressure rapidly but does not shock heat until the stagnation temperature is significantly reduced below source conditions via convective cooling to the walls. Cooling sufficiently rapid relative to kinetic rates, however, can still be achieved only by convective cooling to the walls under subsonic flow conditions.

For the macroprobes (large scale), a study of various geometries for sampling from many temperatures, revealed that an aerodynamic quench is possible. The reference probe was constructed from the model predictions. The design for the EPA probe was selected for rapid cooling by convection. The significant results obtained will be reviewed below.

The second element of NO extractive sampling, i.e., sample transfer, can be subject to two related problems. The first is the conversion of NO to NO_2. The second is the loss of NO_2 once converted from NO. The principal mechanism for the conversion is

$$NO + NO + O_2 \rightarrow 2NO_2$$

This conversion is related directly to the partial pressure of O_2 and to the square of the partial pressure of NO present. Since the reaction is relatively slow, conversion can be minimized by minimizing the sample transfer time. For laboratory flames, this reaction is only important for lean flames and, more critically, for high seed levels of NO. For large scale combustors which typically have an overall lean stoichiometry, the above reaction is important. Federal Register (1976) regulations for sample transfer time (2 seconds) seem adequate. A vital part of the sample transfer process, however, is the time spent in the analytical instrumentation. For some instruments, this time can be considerable. An example of this problem was considered and analyzed experimentally. The rate coefficient for the above reaction was obtained with good agreement ($\sim$50%). The Federal Register (1976) requires 9 seconds to 15% response for NO_x. For low values of NO ($\sim$100-200 ppm) this seems adequate; however, for high concentrations (> 1000 ppm) careful consideration of this reaction is important to the measurement of NO. If conversion of NO to NO_2 occurs, then NO loss (NO_x loss) is possible in water traps and particulate filters as has been previously documented (Tuttle, et. al., 1973).

The final element to be addressed is sample analysis with a chemiluminescent detector. For laboratory flames with unusual carriers such as He and Ar, significant errors in calibration are possible due to quenching differences and viscosity effects associated with sampling handling. These problems are avoided by having calibration gases gravimetrically prepared in the desired diluent and, if possible, analyzed by an alternative method. For laboratory and combustor flames in air, measurements made on wet samples can have errors in excess of 10%.

The probe measurements of seeded-NO over the flat-flame burner indicated the following. First, within the random errors of the measurements, no significant differences were observed between the water-cooled quartz, water-cooled all stainless steel, and water-cooled copper tipped stainless steel probes even though there was significant visible radiation from the all stainless steel probe and none from the copper tip. A range of back pressures (100 torr to 700 torr) were employed but the results were independent of this parameter. The uncooled stainless steel probe produced results similar to the water-cooled probes in the lean flame. For the stoichiometric and rich flames, NO results were significantly lower. In addition, for all stoichiometries a systematic difference between the NO-seed value and the NO measured by the water-cooled probes was observed. These differences were the greatest for the rich flame while for the lean and stoichiometric flames the differences were approximately the same. For all stoichiometries, the amount of NO destruction was dependent on seed concentration. This fact by itself was not sufficient to conclude that the NO was being destroyed in the flame and not in the probe. However, the optical measurements obtained in TASK III of this study indicate that the loss is occurring in the flame front. The specific reaction for this loss was not analyzed. It is possible, nevertheless, to suggest that the NO concentration is slowly driving towards equilibrium. Similar results were observed on the IFRF diffusion flame. Here, as with flat flame, the amount of NO_2 observed cannot explain the loss. For the FT12, a loss was observed for all operating conditions. Although these conditions are lean overall the locally rich regions in the combustor are responsible for the loss.

The macroprobes used in making the NO measurements on the large scale combustors revealed no significant differences in detected NO. The reference probe was operated both in the aerodynamic quench mode and in the convective quench mode with no significant difference in detected NO. It is important to note that the low back pressure required to operate a probe in the aeroquench mode is difficult to achieve. The results do not warrant the effort necessary to make these measurements.

Finally, the validity of the computer model for the probe design model was investigated. Pressure measurements made internal to the reference probe verified the predictions of this model and demonstrated that a probe could be operated in an aerodynamic quench mode albeit at extremely low back pressures.

Mass flow measurements for varying back pressures were in agreement with the predictions for the mini- and macroprobes when sudden expansion losses were considered. Mass flow measurements on the microprobe indicated that when sampling at atmospheric pressure and high temperatures ($\sim$ 1800 K) the flow in the probe is not choked until at least below 0.2 atm. This is significantly lower than that predicted by cursory analysis ($\sim$ 0.5 atm). The nonchoking of the probe was accurately predicted with the detailed fluid flow analysis contained in the probe design model.

VI. CONCLUSIONS

Based on the results of this study, the following major conclusions can be drawn for well designed and properly operated probes sampling the exhaust gases of gaseous and liquid fueled combustors.

1. Water-cooled quartz, stainless steel, and copper-tipped miniprobes yield the same NO concentrations when sampling products from methane/oxygen/nitrogen flames with seeded NO at temperatures up to 2000 K and irrespective of stoichiometry. This similarity in behavior occurs over a wide range of probe back pressures; hence, no advantage is gained from back pressures less than 0.5 atm when sampling atmospheric pressure flames.

2. Uncooled stainless steel probes give NO concentrations slightly smaller (10-15%) than the cooled probes mentioned above for lean methane/oxygen/nitrogen flames ($T \sim 1800K$). For stoichiometric and rich flames, the NO concentrations are significantly less and, at least for the rich flames, the amount of loss is dependent on the probe back pressure. The destruction of NO in this uncooled probe is similar to that encountered in NO/NO_2 converters operated in the absence of oxygen. Hence, uncooled stainless steel probes are only suitable for sampling NO in the presence of oxygen.

3. In general, for miniprobes and microprobes, aerodynamic quenching is not possible because of fluid mechanical and geometric constraints. However, rapid-cooling of the sample gases (within a few milliseconds) can be achieved by convective heat transfer to the probe walls.

4. For microprobes, mass flow measurements indicate that, in the sampling of high temperature gases, choked flow does not occur at the classical pressure ratio. This result was predicted by the probe model and suggests that quenching processes may be less efficient than those estimated in previous studies. A kinetic analysis indicates that quenching rates are still sufficiently fast for sampling NO in exhaust gases; the impact of slower quenching rates on gases sampled from reactive flame zones may have to be examined.

5. Unlike the small scale probes, it is possible to construct a large scale water-cooled probe that can produce aerodynamic quenching of the sample; however, measurements made on both gaseous and liquid fueled combustion systems yielded essentially the same results regardless of the quenching mode, i.e., aerodynamic or convective. Given this fact plus the complexity of probe construction and the difficulties in achieving the low probe back pressures required of the aerodynamic mode, there is no advantage to aerodynamic quenching in the measurement of NO.

6. The model predictions of pressure distribution and mass flow within the large scale probe agreed well with the experimental data. In addition, the model accurately predicted that the microprobe would not choke at the classical pressure ratio when sampling at high temperatures. Based on these results, it can be stated that the fluid dynamic and heat transfer processes have been adequately described in the model for the case of fluid mechanical choking at the probe orifice.

7. A kinetics analysis of gas phase reactions known to destroy NO indicated that no significant loss of NO would occur during the sampling process if the sample temperature was reduced to 1000 K in approximately 1-2 milliseconds. The results of this study are consistent with this analysis.

8. A review of the literature indicated no definitive study where large differences (> 20%) between measurements of total nitrogen oxides from different probes were observed when properly designed probes and sampling lines were used and correct calibration of the chemiluminescent analyzer was performed. A properly designed probe is one that does not perturb the flame environment, does not stagnate the flow, is water-cooled, operates at a back pressure to external static pressure ratio low enough to aid in quenching of reactions, and finally has hot walls (> 600 K) which are limited only to the front portion of the tip such that the local gas residence time is on the order of 10 microseconds or less. Proper sampling lines are those in which the residence times are short relative to the time required for the conversion of NO to NO_2 and the loss of NO_x in water traps and particulate filters. Correct calibration of the chemiluminescent analyzer consists of accounting for the influence of gases other than N_2 on the introduction of NO into the chemiluminescent reaction chamber and the collisional deactivation of excited NO_2.

REFERENCES

Allen, J. D.: Combustion and Flame, 24, 133 (1975).

Amin, H.: Combustion Science and Technology, 15, 31 (1977).

Baulch, D. L., D. D. Drysdale, and D. G. Horne: "Critical Evaluation of Rate Data for Homogeneous, Gas Phase Reactions of Interest in High Temperature Systems". The University, Leeds, England, 1970.

Baulch, D. L., D. D. Drysdale, D. G. Horne, and A. C. Lloyd: Evaluated Kinetic Data for High Temperature Reactions, Vol 2, Butterworth, London, 1973.

Beér, J. M. and N. A. Chigier: Combustion Aerodynamics, Ed. by J. M. Beér, John Wiley and Sons, Inc., New York, 1972.

Benson R. and G. S. Samuelsen: Presentations at the Western State Section of the Combustion Institute, Fall Meeting, Paper No. 76-39, October 18-20, 1976 and Spring Meeting, Paper No. 77-7, April 18-19, 1977.

Benson, R., G. S. Samuelsen and R. E. Peck: Presentation at the Spring Meeting Western State Section of the Combustion Institute, Paper No. 76-11, April 19-20, 1976.

Beal, J. L. and Grey, J. T.: Journal of the American Rocket Society 23, p. 174 (1953).

Bilger, R. W.: Probe Measurements in Turbulent Combustion. PURDU-CL-75-02, Purdue University, School of Mechanical Engineering, May 1975.

Bilger, R. W. and R. E. Beck: Fifteenth Symposium (International) on Combustion, The Combustion Institute, Pittsburgh, 541 (1975).

Bryson, R. J. and J. D. Few: "Comparisons of Turbine Engine Combustor Exhaust Emissions Measurements Using Three Gas-Sampling Probe Designs", AEDC-TR-78-7, November (1978).

Cernansky, N. P.: AIAA Aerospace Sciences Meeting, Paper No. 76-139, Washington, D. C., January, 1976.

Cernansky, N. P. and S. Singh: "Sampling and Measuring NO and NO_2 in Combustion Systems". Final Report for NSF Grant No. 76-22112, Drexel University, April 1979.

Chen, J. Y., W. J. McLean and F. C. Gouldin: Paper No. 79-17 presented at the Western States Section of the Combustion Institute, Spring Meeting, April 1979.

REFERENCES (Cont'd)

CIAP (Climatic Impact Assessment Program) DOT-TST-75-51, 52 (1975).

Clark, J. A. and A. M. Mellor, Paper presented at the Gas Turbine Conference and Products Show, ASME, Paper No. 80-GT-71, March, 1980.

Cohen, L. S. and R. N. Guile: AIAA Journal, 8, 1053 (1970).

COMESA (Committee on Meterological Effects of Stratospheric Aircraft) U.K. Meterological Office, Bracknell (1975).

Cornelius, W. and W. R. Wade: Transactions of Society of Automotive Engineering, Paper No. 700708, 1970.

COVOS (Comite d'Etudes sur les Consequences des Vols Stratospheriques) Societe Meterologique de France, Boulogne (1976).

Crutzen, P. J.: Quart. J. Royal Met. Soc., 96, p. 320 (1970).

Crutzen, P. J.: Ambio, 1, p. 41 (1972).

Davis, M. G., W. K. McGregor and J. D. Few: Arnold Engineering Development Center Report AEDC-TR-74-124 (AD-A004105), (1976a).

Davis, M. G., J. D. Few and W. K. McGregor: Arnold Engineering Development Center Report AEDC-TR-76-12 (ADA021061), (1976b).

Davis, M. G., W. K. McGregor and J. D. Few: J. Quant. Spectrosc. Radiat. Transfer, 16, p. 1109 (1976).

Dimitriades, B.: Journal of Air Pollution Control Association, 17, p. 238 (1967).

Dodge, L. G., M. B. Colket, M. F. Zabielski, J. Dusek and D. J. Seery: "Nitric Oxide & Measurement Study: Optical Calibration". Report prepared for DOT/FAA Contract No. FA77WA-4081 (1979).

Dodge, L. G., M. F. Zabielski, L. M. Chiappetta and D. J. Seery: United Technologies Research Center, Unpublished report (1979a).

Eckbreth, A. C., P. A. Bonczyk and J. F. Verdieck: "Investigations of CARS and Laser-Induced Saturated Flourescence for Practical Combustion Diagnosis". Final Report under EPA contract 68-02-3105, United Technologies Research Center R79-954403-13, September, 1979.

Eckert, E. R. G. and R. M. Drake: Heat and Mass Transfer (New York; McGraw-Hill, 1959), pp. 154-158.

England, C., J. Houseman and D. P. Teixeira: Combustion and Flame 20, p. 439, (1973).

Falcone, P. K., R. K. Hanson, and C. H. Kruger: Paper No. 79-53 presented at the Western States Section of the Combustion Institute, October 1979.

Falcone, P.: Mechanical Engineering Department, Stanford University, Private Communication, 1979.

Federal Register, Vol. 38, No. 136, July 17, 1973, Vol. 41, No. 181, September 16, 1976.

Few, J. D., R. J. Bryson, W. K. McGregor and M. G. Davis: in Proc. Intl. Conf. Environmental Sensing and Assessment, Las Vegas, Nev. (Sept. 1975).

Few, J. D., R. J. Bryson, and W. K. McGregor: Arnold Engineering Development Center Report AEDC-TR-76-180 (1977).

Flower, W., R. K. Hanson, C. H. Kruger: Fifteenth Symposium (Int'l) on Combustion. The Combustion Institute, p. 823 (1975).

Folsom, B. A. and C. W. Courtney: Proceedings of the Third Stationary Source Combustion Symposium Volume II Advanced Processes and Special Topics. EPA 60017-79-050b, Feb., 1979.

Friedman, R. and J. A. Cyphers: Journal of Chemical Physics, 23, p. 1875, (1955).

Fristrom, R. M. and A. A. Westenberg: Flame Structure, McGraw-Hill, New York, 1965.

Glawe, G. E., F. S. Simmons, and T. M. Stickney: NACA TN 3766, 1956.

Gordon, S. and B. J. McBride: "Computer Program for Calculation of Complex Chemical Equilibrium Compositions, Rocket Performance, Incident and Reflected Shocks, and Chapman-Jouquet Detonations". NASA SP-273 (1971).

Gryvnak, D. A., D. E. Burch: AFAPL-TR-75-101, (1976a).

Gryvnak, D. A., D. E. Burch: AIAA Fourteenth Aerospace Meeting, AIAA No. 76-110, Washington, D. C., (1976b).

Halpern, C. and F. W. Ruegg: Journal of Research of the National Bureau of Standards, 60, p. 29 (1958).

REFERENCES (Cont'd)

Halstead, C. J., G. H. Nation, and L. Turner: Analyst 97, p. 55, (1972).

Hanson, R. K., W. F. Flower and C. H. Kruger: Combustion Science and Technology, 9, p. 79, (1974).

Hilliard, J. C. and R. W. Wheeler: Combustion and Flame 29, p. 15. (1977).

Jensen, D. E. and G. A. Jones: Combustion and Flame 32, p.1, (1978).

Johnson, G. M., M. Y. Smith and M. F. R. Mulcahy: Seventeenth Symposium (International) on Combustion, The Combustion Institute, Pittsburgh, p. 647, 1979.

Johnston, H. S.: Science, 173, p. 517.

Kays, W. M.: Numerical Solutions for Laminar-Flow Heat Transfer in Circular tubes, Transactions ASME, p. 1265, November 1955.

Koshi, M. and T. Asaba: International Journal of Chemical Kinetics, 9, p. 305, (1979).

Kramlich, J. C. and P. C. Malte: Combustion Science and Technology, 18, p. 91, (1978).

Land, T. and R. Barber: Transactions of the Society of Instrument Technology 6, p. 112, (1954).

Lengelle G. and C. Verdier: Gas Sampling and Analysis in Combustion Phenomena. AGARD-AG-168, July, 1973.

Lyon, T. F., W. C. Colley, M. J. Kenworthy and D. W. Bahr: Development of Emissions, Measurement Techniques for Afterburning Turbine Engines. AFAPL-TR-75-52, October, 1975.

Matthews, R. D., R. F. Sawyer, and R. W. Shefer: Environmental Science, and Technology, 11, p. 1092, (1977).

McCullough, R. W., R. H. Kruger, and R. K. Hanson: Combustion Science and Technology 15, p. 213, (1977).

McGregor, W. K., J. D. Few and C. D. Litton: Arnold Engineering Development Center Report AEDC-TR-73-182, AD-771 642 (1973).

REFERENCES (Cont'd)

McGregor, W. K., B. L. Seiber and J. D. Few: in Proc. Second Conf. Climatic Impact Assessment Program, Cambridge, Mass. (Nov., 1972).

Meinel, H. and L. Krauss: Combustion and Flame 33, p. 69 (1978).

NAS (National Academy of Science), "Environmental Impact of Stratospheric Flight", Climatic Impact Committee (1975).

Oliver, R. C., E. Baver and Wasylkiwskyj: DOT-FAA-AEE-78-24.

Oliver, R. C., E. Baver, H. Hidalgo, K. A. Gardner and Wasylkiwskyj: DOT-FAA Rpt. FAA-EQ-77-3 (1977).

Rohsenow, W. M. and H. Y. Choi: Heat, Mass and Momentum Transfer, Englewood Cliffs, New Jersey; Prentice-Hall, p. 192, Eq. 8-34, 1961.

Schefer, R. W., R. D. Matthews, N. P. Cernansky, and R. F. Sawyer, Paper presented at the Western States Section of the Combustion Institute. Paper No. WSCI 73-31, 1973 Fall Meeting.

Schlichting, H.: Boundary Layer Theory, Fourth Edition, McGraw-Hill, New York, 1960.

Seery, D. J., R. N. Guile, L. J. Chiappetta: Paper No. 14, Presented at Eastern States Section of the Combustion Institute, Nov. 10-11, 1977.

Seery, D. J. and M. F. Zabielski: Private communication, 1979.

Shapiro, A. H.: The Dynamics and Thermodynamics of Compressible Fluid Flow, Vol. I, (New York; Ronald Press, 1953), p. 228.

Tiné, G.: Gas Sampling and Chemical Analysis in Combustion Processes Pergamon Press, 1961.

Tuttle, J. H., R. A. Shisler, A. M. Mellor: "Nitrogen Dioxide Formation in Gas Turbine Engines: Measurements and Measurement Methods". Report No. PURDU-CL-73-06, The Combustion Laboratory, Purdue University, 1973.

Wilde, K. A.: Combustion and Flame 13, p. 173, (1969).

Vranos, A., B. A. Knight, J. J. Sangiovanni, L. R. Boedeker, and D. J. Seery: Feasibility Testing of Micronized Coal-Oil (MICO) Fuel in a Model Gas Turbine Combustor, UTRC R79-954451-1, May 1979.

*U.S. GOVERNMENT PRINTING OFFICE:1981 O-725-402/1111

LME